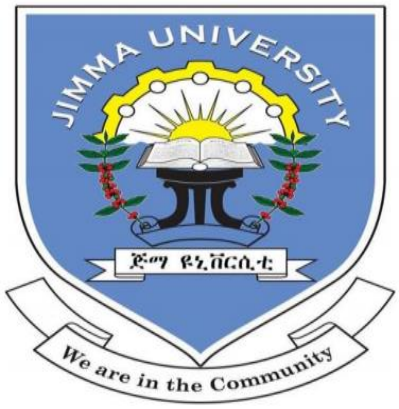

JIMMA UNIVERSITY

JIMMA INSTITUTE OF TECHNOLOGY (JiT)

FACULTY OF MECHANICAL ENGINEERING

"Design and Performance Evaluation of Small-Scale Off grid Solar Thermal Energy Milk Pasteurization System with CFD"

A thesis submitted to the School of Graduate Studies of Jimma University as a partial fulfillment for the requirement of Masters of Science in Mechanical Engineering (Thermal Engineering)

By: Mihretu Woldemichael

Advisor:

Balewgize Amare Zeru (Asst. Prof)

October 2021

Jimma, Ethiopia

JIMMA UNIVERSITY

JIMMA INSTITUTE OF TECHNOLOGY (JiT)

FACULTY OF MECHANICAL ENGINEERING

This is to certify that the thesis is prepared by Mihretu Woldemichael, entitled: **Design and Performance Evaluation of Small-Scale Off grid Solar Thermal Energy Milk Pasteurization System with CFD** and submitted in partial fulfillment of the requirements for the Degree of Master of Science in Thermal Engineering obeys with the regulations of the University and meets the accepted standards.

Submitted by:

Mihretu Woldemichael	_____	_____
Name	Date	Signature

This thesis has been submitted for examination with our approval as a university advisor

Balewgize Amare (Asst. Prof.)		
Advisor	Date	Signature
Nebyou Bogale (Asst. Prof)	_____	_____
Co-Advosor	Date	Signature
External Examiner	_____	_____
Abdulkadir Aman (Dr.)	Date	Signature
Internal Eximiner	_____	_____
Demeke Girma (MSc)	Date	Signature
Ali Seid (MSc)	_____	_____
Chairman	Date	Signature

Declaration

I, the undersigned, declare that this thesis entitled "**Design and Performance Evaluation of Small- Scale Off grid Solar Thermal Energy Milk Pasteurization System with CFD"** is my original work under the School of Mechanical Engineering, JiT, and has not been submitted by any other person for an award of a degree in this or any other University, and that all resources of materials used for this thesis have been duly acknowledged and a list of references is given.

Name

Mihretu Woldemichael _____

Signature

This thesis has been submitted to the Jimma University with my approval as the University Advisor.

Advisor

Balewgize Amare Zeru, (Asst. Professor) _____

Signature

Table of Contents

Declaration II
LIST OF TABLES VII
LIST OF FIGURES VIII
NOMENCLATURE XI
Acknowledgment XIV
Abstract XV
CHAPTER ONE 1
INTRODUCTION 1
1.1. Milk production in Ethiopia 1
1.2. Problem of statement 3
1.3. Objectives 5
1.3.1. General objectives 5
1.3.2. Specific objectives 5
1.4. Scope of the study 5
1.5. Significance of the study 5
1.6. Thesis organization 6
CHAPTER TWO 7
LITERATURE REVIEW 7
2.1 Introduction 7
2.2. Overview of Ethiopia's Dairy Sector Constraints 7
2.3. Purposes of pasteurization 9
2.4. Pasteurization processes 9
2.4.1. Batch or Vat pasteurization processes 10
2.4.2. Continuous pasteurization processes 11
2.5. Types of milk pasteurization 12
2.6. Solar thermal energy 15
2.7. Solar Water Heating System 16
2.7.1. Active Solar Water Heating Systems 17
2.7.2. Passive Solar Water Heating Systems 18
2.9. Solar Thermal Collectors 19
2.9.1. Flat-plate solar collector 20

2.9.2. Compound parabolic collectors 21
2.9.3. Evacuated tube collectors 22
2.10 Selection parameter of Solar Collectors 25
2.10.1 Other considerations when Using Evacuated Tube Collectors 26
2.11. Working principle of U pipe Evacuated Tube Solar Collector 27
2.12. Heat exchanger 28
2.12.1. Geometry of Helical Coil Heat Exchanger 31
2.12. 2. Heat Exchanger Pressure Drop 32
2.12.3. Literature Review Summary 33
CHAPTER THREE 34
METHODOLOGY 34
3.1. Introduction 34
3.1.1. Data collection 34
3.1.2. System Description and Model Design 35
3.2. Location of the study area 35
3.3 Estimation of Solar Radiation 35
3.3.1 Global Solar Radiation 35
3.3.2.Extraterrestrial Radiation on a Horizontal plane 39
3.3.3 Diffuse and Beam Radiation 41
3.3.4 The computing of Hourly Beam and Diffuse Radiation on a horizontal surface 41
3.3.5 The computing of Daily Diffuse and Beam Radiation on a horizontal surface 42
3.3.6 Estimation of Hourly Global Radiation from Daily Data 43
3.3.7 Estimation of Hourly Diffuse Radiation 44
3.3.8 Total Solar Radiation on Tilted Solar Collector 44
3.4 Estimation of Hourly Ambient Temperature 46
3.4.1 For daylight hours 46
3.4.2 For night-time hours 46
3.5 Model system description for applied methodology 47
3.6 Mathematical Model of an Evacuated Tube Solar Collector milk pasteurization system 49
3.6.1 Governing Equations of the Solar Collector 50
3.6.2 Temperature distribution in different sections 51

3.6.3 Formulation of heat transfer coefficient in different sections 52
3.6.4 Overall heat loss coefficients of the ETSCs 54
3.6.5 Useful collected solar energy 54
3.6.6 Absorbed solar energy 55
3.6.6 Collector efficiency 55
3.6.7 Solar Thermal Collector Heat Balance Equations 56
3.6.7 Technical Specification of Evacuated Tube Solar Collector 58
3.6.8 Energy Storage in Solar Thermal Process Systems 59
CHAPTER FOUR 62
4 HELICAL TUBE HEAT EXCHANGER DESIGN 62
4.1. INTRODUCTION 62
4.2. Coil tube Heat Exchanger sizing 62
4.2.1. Analysis of Coil tube Heat Transfer Area 63
4.2.1a. Milk properties 64
4.2.2 Diameter of Stainless-Steel pipe 66
4.2.3 Pitch of the coil tube 67
4.2.4 Required Length of Stainless-Steel Tube 67
4.2.5 The total length of the coil tube 68
4.2.6 Number of coils tube turn 68
4.2.7 The volume occupied by on turn of the coil tube 69
4.2.8 The volume occupied by the whole turn of the coil tube 69
4.2.9 The volume of the Milk Storage Tank 69
4.2.10 Diameter and Height of Milk Storage Tank 69
4.3. Material selection of milk storage tank and its insulation 70
4.4. Coil tube Heat Transfer Analysis 71
4.4.1 Heat gain formulation through coil tube 71
4.4.2 Calculation of Overall Heat Transfer coefficient 72
4.4.3 Inner convection heat transfer coefficient 73
4.4.4 Outer Convection Heat Transfer Coefficient 73
4.5. Energy Balance Equations 74
4.5.1 Logarithmic Mean Temperature Difference (LMTD) 75

4.5.2 Actual Heat Transfer Rate in a Heat Exchanger 75
4.6. Pressure Drop and Selection of Pumping Power 75
4.6.1 Pressure Drop along the Pipe 75
4.6.2 Pressure Drop along in Bending 76
4.6.3 Pressure Drop in the Fittings 78
4.6.4 Total pressure drop in the coil tube, ΔP 78
4.6.5 Pressure Drop in Pipe Lines 78
4.6.6. Total Pressure Drop in the System 81
4.6.7 Determination of Total Dynamic Head 81
4.8. Pumping Power Requirement 82
4.8.1 Volume flow rate 82
4.8.2 Pump selection 82
CHAPTER FIVE RESULTS AND DISCUSSIONS 84
5.1 Design Results of helical coil heat exchanger 84
5. 2. CFD Analysis of Helical Heat Exchanger and Milk Storage Tank 84
5. 2.1. Modeling 84
5.2.2 Name selection and Meshing 86
5.2.3 Problem setup 87
5.2.3 Solution 88
5.2.3a: For steady analysis 88
5.2.3b: For transient analysis 99
CHAPTER SIX 105
CONCLUSION AND RECOMMENDATION 105
6.1 CONCLUSION 105
6.2 RECOMMENDATIONS 105
References 106
APPENDIXES 114
Appendix A: Properties of various materials 114
Appendix B-1: Moody Chart 116
Appendix B-2: Economic Thickness of Insulation 117
Appendix B-3: Solar Water Pump Selection Chart 118

LIST OF TABLES

Table 2. 1: Temperature-time pasteurization requirements for fluid milk..... 12
Table 2.2: Advantages and Disadvantages of Types of Milk Pasteurization 13
Table 3.1: Sunset hour angle of the location..... 38
Table 3.2: Day numbers and standard mean day of the month..... 38
Table 3.3: Metrological data that collected from selected location 40
Table 3.4: Technical Specifications of the Solar Thermal Collector..... 56
Table 3.5: The surface properties and dimensions of evacuated tube solar collector..... 58
Table4.1: Milk properties varies with temperature..... 64
Table 4.2: Inside and Outside diameter of the cylinder 67
Table 5.1: Shows designed coil heat exchanger geometrical values. 84
Table A.1: Evacuated Tube Solar Collector Heat Transfer Coefficients..... 114
Table A.2: Physical properties of manifold header construction materials 114
Table A.3: Properties of Insulation Materials..... 115

LIST OF FIGURES

Figure 2.4: Types of Solar Water Heating System (Jamar, et al., 2016) 17
Figure 2.5: Thermosiphon principle [wiki.lowtechlab.org] 19
Figure 2.6: Flat-Plate Solar Collectors [www.solar-City.net] 20
Figure 2.7: Compound parabolic collectors [researchgate.net] 21
Figure 2.8: Evacuated tube collectors [daviddaring.info/researchgate.net] 22
Figure 2.10: Evacuated Tube with U-type heat extraction system 28
Figure 2.12: Variation of heat exchanger effectiveness with an inlet temperature of hot water (Vishvakarma, et al., 2016). 29
Figure 2.13: The solar fraction and collector efficiency of SWHs (Shuhong, et al., 2014). 30
Figure 2.14: Helical coil tube with its geometrical parameters (Vishvakarma, et al., 2016)] 31
Figure 3.1: Methodology applied for the underlying study. 34
Figure 3.2: Variation of declination angle [powerfromthesun.net] 37
Figure 3.3: Definition of sun's azimuth angle 38
Figure 3.4: Sun-earth relationships[researchgate.net] 39
Figure 3.5: Variation of extraterrestrial solar radiation with a month of year 40
Figure 3.6: Annual Solar Radiation, Doyogena, Ethiopia 41
Figure 3.7: Indication of Beam, Diffuse and Other Solar Radiation [e-education.psu.edu] 41
Figure 3.8: The ratio $\boldsymbol{IdI}$, as a function of hourly clearness index $\boldsymbol{KT}$ (Erbs, et al., 1982). 42
Figure 3.9: Suggested correlation of daily diffuse fraction with $\boldsymbol{KT}$. From (Erbs, et al., 1982). .. 43
Figure 3.10: Diagram of the constructed system for milk pasteurization by solar energy 47
Figure 3.11: Schematic of milk pasteurization by solar energy. 48
Figure 3.12: Schematic of cross-section and illustration U-type ETSC [link.springer.com] 49
Figure 3.13: General description of the collector model (Jean, 2005). 50
Figure 3.14: Thermal Networks of U type Evacuated tube solar collector (Jean, 2005). 51
Figure 4.1: Cross-sectional view of milk Storage tank 63
Figure4.2: Effects of temperature on density of milk 65
Figure4.3: Temperature versus thermal conductivity of milk 65
Figure 4.4: Schematic cut-away view of a helical tube heat exchanger 66
Fig 4.5: Helical tube heat exchanger geometry by ANSYS 67

Figure 5.1: Model of milk storage tank 85
Figure5.2: Model of helical tube heat exchanger..... 85
Figure5.3: Model of HTHx and milk storage tank in one for axial length 187mm and 374mm.. 86
Figure5.4: Name selection of geometry..... 86
Figure 5.5: Meshing of helical tube heat exchanger..... 87
Figure5.6: Temperature contour all domain and wall milk fluid location..... 88
Figure5.7: Temperature contour all domain and plane location..... 89
Figure5.8: Temperature contour milk fluid domain and plane location..... 89
Figure5.9: Temperature distribution in the inlet and outlet area 89
Figure5.10: Temperature distribution at the coil inlet and middle of helical coil 90
Figure5.11: Temperature distribution in the different axial distances..... 91
Figure5.12: Temperature distributions in different plane locations..... 91
Figure5.13: Temperature contour of water fluid domain and plane location HTHx..... 92
Figure5.14: Temperature contour all domain and water fluid location 92
Figure5.15: Velocity streamline all domain and milk fluid domain and starts inlet velocity..... 93
Figure5.16: Velocity streamline water fluid domain start from water inlet velocity..... 93
Figure5.17: Velocity vector all domain and water fluid location 94
Figure5.18: Velocity vector water fluid domain and water fluid and plane location 94
Figure5.19: Pressure contour all domain and wall milk fluid location..... 95
Figure5.20: Pressure contour all domain and plane1 location..... 96
Figure5.21: Velocity contour domain milk fluid and plane location..... 96
Figure5.22: Velocity contour all domain and location plane..... 96
Figure5.23: Residuals for 1200 iteration and residual number $\mathbf{10-6}$..... 97
Figure5.24: Residual graph for1500 iteration and $\mathbf{10-6}$residual number 97
Figure5.25: Residual graph for iteration 500 and 0.001 residual number 97
Figure 5.26a: Output report temperature versus iteration number 1200 and $\mathbf{10-6}$..... 98
Figure5.26 b: Temperature graph for 500 iterations and 0.001 residual number 98
Figure5.27: Transient analysis residual graphs..... 99
Figure5.28a: Transient analysis temp versus iteration graphs..... 99
Figure5.28b: Transient analysis temp versus time graphs..... 99
Figure5.29a: Temperature versus chart count for 187mm axial helical tube length 100

Figure5.29 b: Temperature versus chart count for 374mm axial helical tube length 100
Figure5.30: Temperature versus axial HT length and to show peak pasteurization point..... 101
Figure5.31 a: Velocity versus chart count for 187mm axial helical tube length 102
Figure5.31 b: Velocity versus chart count for 374mm axial helical tube length 102
Figure5.32a: Pressure versus chart count for 187mm axial helical tube length 103
Figure5.32b: Pressure versus chart count for 374mm axial helical tube length 103
Figure5.33: Output temperature versus Axial helical tube length 104
Figure5.34: Output temperature versus Milk fluid inlet velocity 104
Figure B.1: Moody Chart 116
Figure B.3: A graph used to size a pump (from Kyocera Solar) 118

NOMENCLATURE

Notations

A_{at}	The total area of the absorber tube
A_c	Gross area of the collector
A_{coil}	Heat transfer area of coil HX
D_e	Dean number
C_p	Heat capacity of working fluid
d_i	The inner diameter of Helical Coil HX
d_o	The outer diameter of Helical Coil HX
f	Friction Factor
F	Correction factor
F_R	Collector Heat removal factor
g	Gravitational acceleration
G_b	Beam Radiation
G_d	Diffuse Radiation
G_{on}	Extraterrestrial radiation measured on the plane normal to the radiation on the n^{th} day of the year
G_r	Grashof number
G_{SC}	Solar Constant
H	Global Solar Radiation on a Horizontal surface/Total Daily Solar Radiation
H_b	Daily Beam Radiation
H_d	Daily Diffuse Radiation
H_o	Extraterrestrial Solar Radiation on a Horizontal Surface
H_s	Height of storage
H_{sys}	System falling Height, Head
I_T	Total Solar Radiation
I_g	Instantaneous Global Horizontal Radiation
K	Total loss Coefficient
K_T	Clearance index

L_{coil}	Total Length of the Coil
N_{coil}	Number of Coil turns
N_u	Nusselt number
p	Coil Pitch
P	Fluid Pumping Power
ΔP	Total Pressure Drop in the Coil Tube
ΔP_b	Pressure Drop along in Bending
ΔP_f	Pressure in the Fitting
ΔP_{fr}	Frictional Pressure Drop
ΔP_p	Pressure Drop along the Pipe
P_r	Prandtl number
ΔP_t	Total Pressure Drop in the System
Q	Volume flow rate
Q_{th}	Thermal Output of the Collector
R_a	Rayleigh number
R_e	Reynolds number
r_b	Direct or Beam Radiation Factor
$R_{e\ cr}$	Critical Reynolds number
r_d	Diffuse Radiation Factor/ Estimation of Hourly Diffuse Radiation
r_r	Reflected Radiation
r_t	Estimation of Hourly Global Radiation from Daily Data
S	Sunshine hour of the day
S_d	Maximum possible Sunshine duration
S_T	Local Solar Time
ΔT	Temperature Gradient
T (H)	Temperature at any Hour of the Day or Night Period
ΔT_{LMTD}	Change of Logarithmic Mean Temperature Difference
U	Overall Heat Transfer Coefficient
U_L	Overall Heat Loss Coefficient

U_o	Overall Heat Transfer Coefficients from the Environment
V_c	Volume Occupied by the Whole Turn of Coil
V_{st}	The volume of the Milk Storage Tank
W_s	Hour Angle (Sunset Hour Angle)
Z	Elevation of the Sea Level
$\alpha\tau$	Transmittance- Absorbance Product
β	Tilt Angle
γ	Solar Azimuth Angle
δ	Declination Angle
ϵ	Roughness
η	Efficiency of Collector
η_m	Motor Efficiency
η_p	The efficiency of the Pump
θ_i	Angle of Incidence
θ_z	Zenith Angle
μ	Dynamic Viscosity
ν	Kinematic Viscosity
σ	Stefan- Boltzmann Constant
ϕ	Latitude of the Location
ω	Hour Angle

Units

h	Hour
K	Kelvin
℃	Degree Celsius
m	Meter
mm	Millimeter
M	Mega
MW	Mega Watt
Pa	Pascal
W	Watt
KWh	Kilo Watt-hour

Acknowledgment

Foremost, I want to thank the Almighty God help me and strengthened me throughout my work. Next, I would like to express my sincere gratitude to my advisor Mr. Balewgize Amare Zeru (Asst. Prof. and Ph.D. Candidate) for his continuous guidance, intellectual support throughout my thesis work and give me a suggestion on the title.

And, I would like to deepest thanks to my Co-advisor Mr. Nabiyou Bogale (Asst. Professor) for his kind help and support of my idea on my thesis work.

I am also heartily thankful to Wachemo University and the Ethiopian Ministry of Education for financially supporting my Master's Education at Jimma University.

Finally, I must extend my deepest gratitude to my parents, classmates, and close friends for providing me with unwavering support and encouragement throughout the years of study and for the process of researching and writing this thesis work. Thank you for everything.

Abstract

A milk pasteurization system was developed by utilizing solar thermal energy for off-grid periods of rural or urban milk products. This work sited on the warm climate condition of Doyogena. Doyogena is located in Kambata Zone, S.N.N.P.R ., Ethiopia. The milk pasteurization process consumes a huge amount of energy, using solar energy for the pasteurization process decreases the required conventional energy. While milk is a perishable food item and needs careful handling from source to supply. Unreliable handling of milk creates harmful pathogen and spoilage microorganisms and milk-borne diseases in developing countries especially in Ethiopia leads to millions of deaths and billions of illnesses annually. Milk producers in Doyogena, the study area not used any milk preservation systems. Therefore milk pasteurization system is one of several interventions that can improve public health.

The purpose of this work is to analyze the performance of the solar energy-based system for the small-scale milk pasteurization process with a low-cost helical tube heat exchanger immersed in the milk storage tank. The effectiveness of the milk pasteurization system has been studied using CFD (computational fluid dynamics).

The system uses 2.42m^2 the gross area of an inclined evacuated tube solar collector and the solar radiation intensity on the inclined surface of the location has been analyzed from available solar data. The monthly average useful energy received by the collector ranges from 650Wh/m^2 to 10720Wh/m^2 and the maximum hot water temperature exit from the collector ranges from 79℃ to 82.32℃ using water as heat transfer fluid(HTF). Energy loss by convection heat transfer to ambient, the hot water temperature in the thermal storage tank (inlet to the helical tube heat exchanger) found to be 70.0℃ to 78.0℃ which above the required pasteurization temperature ranges from 65.5℃ to 69℃. Overall results indicate that solar-based milk pasteurization system was viable technology in this manner and it achieved the acceptable milk temperature range being heated to kill microorganisms that leads to milk spoilage. I am recommended using an integrated storage system to optimize the system for large-scall milk pasteurization.

Keywords: *CFD, Pasteurization, Helical tube heat exchanger, Thermal storage tank*

CHAPTER ONE

INTRODUCTION

Milk and dairy products are fundamental in humans, consumed by millions of people from all over the world on an everyday basis. According to FAO (Food and Agriculture Organization) in a 2016 statistics study, the world total milk production forecasted was 816 million tons (Yildirim, 2017). It can be used as an important of his diet throughout life. In Ethiopia, milk and dairy products mainly used for home consumption as it has high nutritional value. In addition, it is a source of income for various farm inputs such as feed, fertilizers, and improved crop varieties as well as food and non-food items as educational materials for their children (Melese, et al., 2015). However, the quality of milk produced in Ethiopia is poor and substandard. This is due to poor management practices before milking and after harvesting and the most devastating symptoms of milking (Tsadkan , et al., 2018).

Neglected management and neglect of hygiene measures by milk handling workers can allow undesirable bacteria to come into contact with the milk and in some cases live and increase in quantity and make the milk unsafe for direct use and processing (Chatterjee, et al., 2006).

Milk contains bacteria where improper handles create conditions in which bacteria can increase antibiotic residues in milk due to the widespread use of antibiotics in food-producing animals, which is thought to be a problem for the dairy industry and consumers (Zorraquino, et al., 2008). Many fresh milk bacteria from a healthy animal are harmless or beneficial but rapid changes in the health of the animal, or milk carrier, or contamination from contaminated water, dirt, manure, insects, cuts, and wounds can be harmful milk. Raw milk contains Alkaline phosphate (ALP) is an enzyme naturally present in raw milk that is responsible for bacterial infection in the stomach when milk is used for drinking (Fenoll, et al., 2002). Heating milk at a certain temperature for some time has led to the killing of harmful microorganisms.

1.1. Milk production in Ethiopia

Ethiopia has the largest cattle population in Africa with an estimated 59.5 million head of cattle of which about 98.2% of the total cattle in the country are local bread. Combined and foreign residues accounted for 1.62% and 0.18%, respectively ([CSA], 2017).. As a result, milk production in Ethiopia is highly dependent on traditional breeds, especially cattle, goats, camels, and sheep.

(Tadesse, et al., 2017) reviewed that, Ethiopia is one of the most developed sub-Saharan African countries with the largest livestock population, becoming the first in Africa and the ninth in the world. Estimates of a leading rural farmer show that the country has an estimated 53.9 million head of cattle, 22 million goats, 26 million sheep, and 2.3 million camels. Cattle have the largest share (81.2%) of national milk production, followed by goats (7.9%), camels (6.3%), and sheep (4.6%), although there is a potential for milk production, overall livestock productivity is low, and the direct contribution it makes in the country's economy was limited.

Consequently, Ethiopians have 10.5 million dairy cows which on average produce 1.5 liters of milk per day, and the average annual milk consumption was 19 liters which are below the African country average of 40 liters, contrasted with worldwide consumption of 105 liters and the annual milk production growth rate is 1.2 percent with falls behind the annual human population growth of 3 percent estimated (Steen, et al., 2014).

This is a great gap at the country level which result in a shortage of supply of dairy products and requires the country to spend hard currency to import dairy products from abroad and need to expand of domestic dairy industries for milk producers will have to become more market-oriented (Tegegne, et al., 2013). However, there are many dairy processing firms, individual producers to meet their dairy needs and are unable to satisfy the majority of their diet by providing processed milk and dairy products in Ethiopia (Habtamu, et al., 2015). Way of investing in smallholder farmers. Because it plays a very important role in feeding the rural. In addition, milk and dairy products are very important to the economy and dairy farming is an urban population of Ethiopia.

(Hailemeskel, 2020) Reviewed in a recent study, in Kembata Tembaro, Kadida Gamela, Doyogena, and Kachabira woredas, Southern Province, they examined milk production methods, traditional milk management ,and processing practices and determined the combined quality of dairy and microfuge. A total of 150 families (75 from each woreda) were interviewed individually. Both woredas use traditional Ensira to store and brush milk. A major obstacle to milk production in the study area is the lack of milk collection facilities/market shortages, and low-quality dairy products become a major problem in traditional dairy practices. And some of the problems are shortages of cooling facilities associated with power shortages are major barriers to dairy federations.

(Atia, et al., 2015) pointed that; milk is a perishable foodstuff due to an excellent medium for the growth of microorganisms that cause spoilage. For this reason, milk is heated to a specific temperature for a specific period, to killing harmful microorganisms for making safe milk and one of the best-known heat treatments in milk processing plant was pasteurization which is carried out between 60 - 75℃ according to the processor type to extend the shelf-life and to improve the quality and minimizing the risk of milk poisoning (Yildirim, et al., 2015).

(Modi. , et al., 2014) also explained that thermal processing is an essential step in the milk production process adopted by the dairy industry. Producing fluid milk and milk products through applying thermal treatments such as heating and cooling requires a significant amount of energy. However, energy consumption is a crucial issue in the dairy industry from both economic and environmental view point.

(Patel, et al., 2016) reviewed that, solar panel or concentrator-based milk pasteurizer systems in the dairy industry can meet the demand of pasteurization. It was observed that the base temperature of solar-heated water reached up to 100˚C and the pasteurizer has easily attained pasteurization temperature ranging from 65 to 75˚C in two to three hours.

However, among some parts of rural and urban areas of Ethiopia, Doyogena was one of the efficient solar energy potential found in SNNPR of Ethiopia, part of Kembata Tembaro Zone. And Ethiopia, still suffers reliable, effective, and sufficient electricity in many parts of the country, in particular, rural and other off-grid areas are suffering the most. Thus, this work aimed to study performance evaluation of the solar energy potential of the location for small-scale milk pasteurization for off-grid peri-urban milk producers in Doyogena, which are the abundant milk producers in the area.

1.2. Problem of statement

Consumption of raw milk and dairy products such as cheese, butter, cream, and yogurt is commonly consumed in sub-Saharan Africa including Ethiopia (Yodit, et al., 2017).

In Ethiopia, in addition, the production and consumption of raw milk and various dairy products often occur under unsanitary conditions mainly due to inadequate milk infrastructures such as refrigeration space, lack of clean water, and limited knowledge of milk and dairy products (Bereda, et al., 2013). In addition, critical distribution factors such as milk collection, cooling, and mobility are poorly regulated in milk production in Ethiopia and market systems are common barriers leading to a low country economy from that source.

However, the national milk consumption rate in Ethiopia is 19kg compared to 27kg in other African countries and 100kg worldwide per person consumption (Tadesse, 2017).

(Makita, et al., 2012) identified that, consumption of dairy products was high and microbial are the common causes of foodborne illnesses in many parts of the world and harmful for the human health. Even, raw milk from a healthy cow may contain a low microbial load, but the microbe may increase, multiply if it is stored at the normal temperature of the atmospheric environment (Ruangwittayanusorna, et al., 2016.).

However, according to (Yilma, et al., 2011) review from earlier research conducted in Ethiopia revealed that the microbial counts of milk and milk products produced and marketed in the country there are generally much higher than the acceptable limits.

(Flores-Flores, et al., 2015) suggested, milk must be free of toxic compounds that can be harmful to humans, especially for children who are more susceptible to the action of toxic compounds, because they are the largest consumers of milk as it is one of the principal foods during their first years of life.

To increase the quantity and quality of milk and dairy products being offered to consumers and to increase the development of the dairy sector in Ethiopia, small-scale livestock enterprises milk producers in different urban, peri-urban and rural areas now a time contributes immensely to poverty mitigation and improve nutrition in the country (Tadesse, 2017).

However, per-urban milk producers (about 100 to 310 lt per day) in Doyogena off-grid areas have a serious problem of milk preservation facility and getting their milk to market. This is especially due to liquid milk being handled traditionally and has a very limited shelf-life. Because unpasteurized milk spoils easily and there is also no nearby milk dairy processing facility as well.

Thus, the purpose of this research study was to utilize solar energy for the milk pasteurization process. Since keeping the quality of raw milk and to increase its healthy life of human being as well as to increase its business sector for economic growth and food security of the country.

1.3. Objectives

1.3.1. General objectives

The general objective of this thesis was the Design and Performance Evaluation of Small Scale off grid Solar Thermal Energy Milk Pasteurization system with CFD.

1.3.2. Specific objectives

- Collect weather data and estimating the solar energy potential of the specified location.
- Design a helical tube heat exchanger and milk storage tank.
- Selection of evacuated tube solar collector.
- Modeling transient analysis of helical tube heat exchanger using CFD.

1.4. Scope of the study

The scope of this study was from solar energy potential estimation of the study location to a solar milk pasteurizer system performance evaluation by using CFD analysis.The main components considered in the milk pasteurization system are an evacuated tube solar collector, milk storage tank, thermal storage tank, and coil heat exchanger (figure 3.12). For this component, a transient governing equation was developed to study the hourly useful heat gained by the collector, the hot water temperature exits from the collector, and the hot water temperature in the thermal storage tank. In addition, milk storage tank and helical tube heat exchanger sizing, as well as pumping power requirements for circulating pump, are done. Finally, the performance evaluation of pasteurized milk temperature was studied. However, the cost analysis, testing & installation of the considered system was not performed.

1.5. Significance of the study

This study comes up with several valuable significances.

- A significant benefit of this research was the utilization of solar energy for milk pasteurization and to provide diary processing facilities for small–scale milk producers.
- To create awareness for other milk producer areas, which have solar energy potential to adopt such technologies
- To increase domestic dairy sector involvement through having raw milk collection centers at different dairy farming areas.
- To reduce Ethiopia dairy sector constraints and hard currency the county spends to import dairy products from abroad.

1.6. Thesis organization

This thesis is organized into six chapters. This is the first chapter that gives the details about the studies introduction with elaborating the problems. In addition, it also lays down the objectives of the thesis and its relevance.

Chapter 2 introduces, previous research studies related to solar energy utilization, milk pasteurization processes, solar water heating systems, and other necessary background information for the current study.

Chapter 3 presents, the methodologies and detail mathematical model design of solar thermal collector.

Chapter 4 focuses on sizing the helical tube heat exchanger parameters and calculation of the total pressure drop in the system and pumping power requirement.

Chapter 5 presents the result and discusses the graphically generated outputs from CFD analysis.

Chapter 6 provides the conclusion and recommendation for future works.

CHAPTER TWO

LITERATURE REVIEW

2.1 Introduction

A review of the literature reveals that different previous work which helps for the guidance of work. These previous related works may be journals, conference papers, design works, and books related to this paper. Selection of appropriate conditions approaches, and methodologies with these journals and other materials will strengthen for the successful accomplishment of the paper.

Milk production capacity of Ethiopia in liters of milk per day produced and the average annual milk consumption relative to Africa and the world, research gaps, and basic milk preservation constraints were introduced. The previous research studies related to sun milk pasteurization system model design, operation, performance analysis, and material selection are reviewed to provide background for the current study, and important and key terms are also defined and explained.

2.2. Overview of Ethiopia's Dairy Sector Constraints

(Tadesse, et al., 2017) Explained that, the dairy production system is a biologically efficient and flexible system that converts cellulose from livestock, which is milk, the most nutritious food to man. Dairy production is a critical issue in Ethiopia, a livestock-based society where livestock and its products are more important sources of food and income. However, dairying has not been fully exploited and promoted.

(Demissu, et al., 2014) pointed to that; there are four major dairy production programs in Ethiopian dairy farming depending on the climate, land conservation, and farming systems. These are a dairy farm, a small mountain milk production system, in towns and cities (small and medium-sized dairy farms in and around the backyards and towns and cities) dairy production system.

The milk production system that takes place in cities, in particular, operating in areas where the population is as high as near major cities as well small towns. In this program, it is estimated that 71% of milk producers sell their milk directly to consumers and an important system that protects against excessive milk diversification of service delivery in Ethiopia.

These market-oriented smallholder urban and peri-urban dairy production systems have immensely contributed towards filling in the large demand-supply gap of fluid milk and milk products in urban centers, where consumption of milk and milk product is remarkably high (Tegegne, et al., 2013).

However, there are major dairy sector constraints that hinder the milk production of Ethiopia despite enormous livestock resources as reviewed and studied by other researchers.

The crucial distribution elements such as milk collection center, chilling or refrigeration facility and transportation, inefficient and inadequate milk processing technologies, access to services and inputs, marketing and absence of clear policy support to the sector the absence of clean water and limited knowledge of the clean handling of milk and milk products are also identified as major constraints that hinder dairy sector development in the country (Steen, et al., 2014) - (Tegegne, et al., 2013)

Co-operatives play a significant role in ensuring the availability of sustainable raw milk in the dairy industry by linking the flow of milk to their members and helping them by providing the necessary inputs for the dairy farm.

(Emana, et al., 2009.) reported that 180 co-operatives involved in milk production and marketing operating in different sectors of the country. However, this number only makes up 0.74% of the total agricultural and agricultural federation and 2% of agricultural-based partnerships country.

According to (Yilma, et al., 2011) reviewed, there is a research gap and a weak link between the differences partners in a series of milk prices (Figure: 2.1) are some of the important factors that participate in small-scale development in the Ethiopian dairy sector.

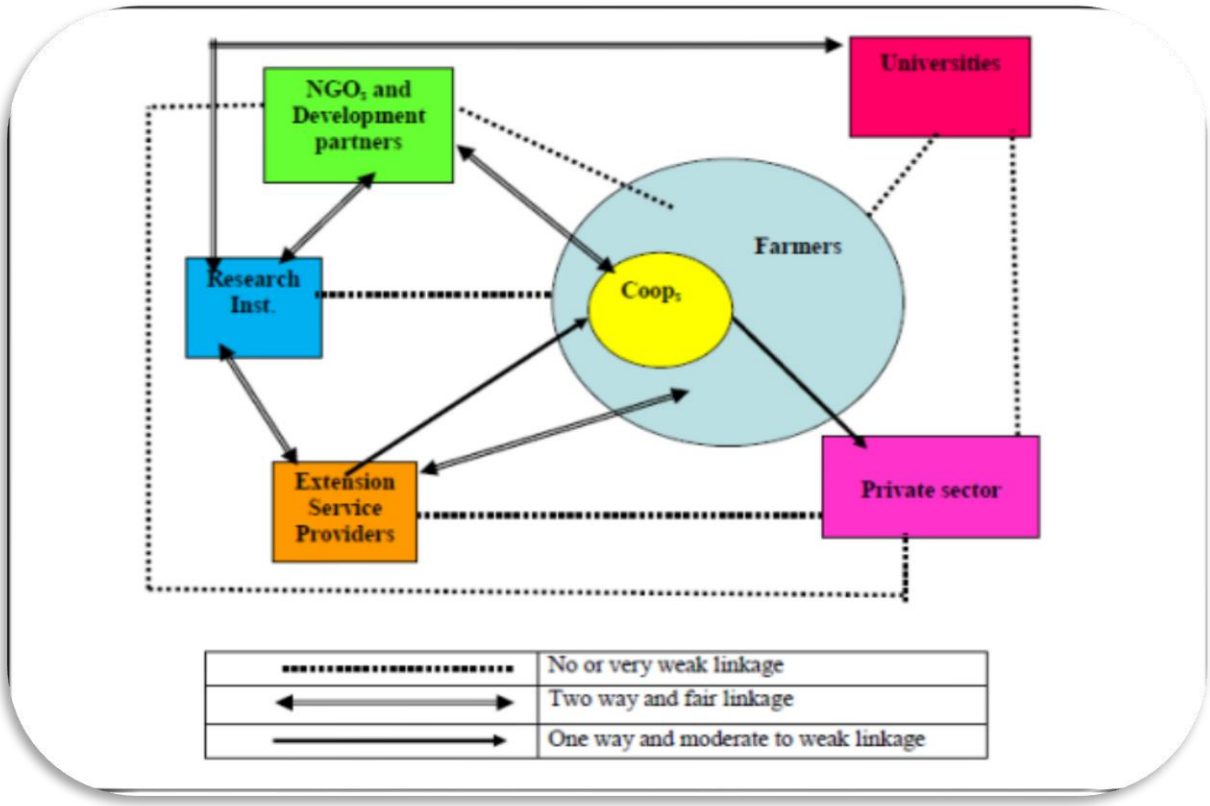

Figure 2.1: Linkages among actors in the Ethiopian dairy value chain [(Yilma, et al., 2011)].

2.3. Purposes of pasteurization

- To make milk safe for human consumption by destroying the pathogenic organisms, this may be present in milk, such as viruses, bacteria, protozoa, molds, and yeasts.
- To improve milk preservation quality by destroying all spoilage microorganisms and enzymes that contribute to reducing the quality and the shelf-life of milk.
- Helps to retain good flavor over a longer period.

As noted in (Modi. , et al., 2014) pasteurized milk is expected to have a shelf life of 14 to 20 days. However, the shelf life time of pasteurized milk stored at ambient temperature depends upon the efficiency of the pasteurization process.

2.4. Pasteurization processes

Pasteurization is the process of heating a product to a pre-determined temperature and holding it up to all or almost all undesirable living things, which may be those who are there, they are killed. This was developed by Louis Pasteur, 1960. Reduced food intake and timely treatment are

a problem between disinfection and the number of other factors such as taste, phosphate inactivity, thinning of the cream line, etc.

The microorganism of milk processing is Mycobacterium tuberculosis (TB virus). (Karunasree, 2016.).

In general, there are two types of milk pasteurization processes. Batch or Vat and Continuous types of pasteurization processes.

2.4.1. Batch or Vat pasteurization processes

This process consists of a coat hanger surrounded by a rotating tap water steam or hot water coil heaters or direct steam.

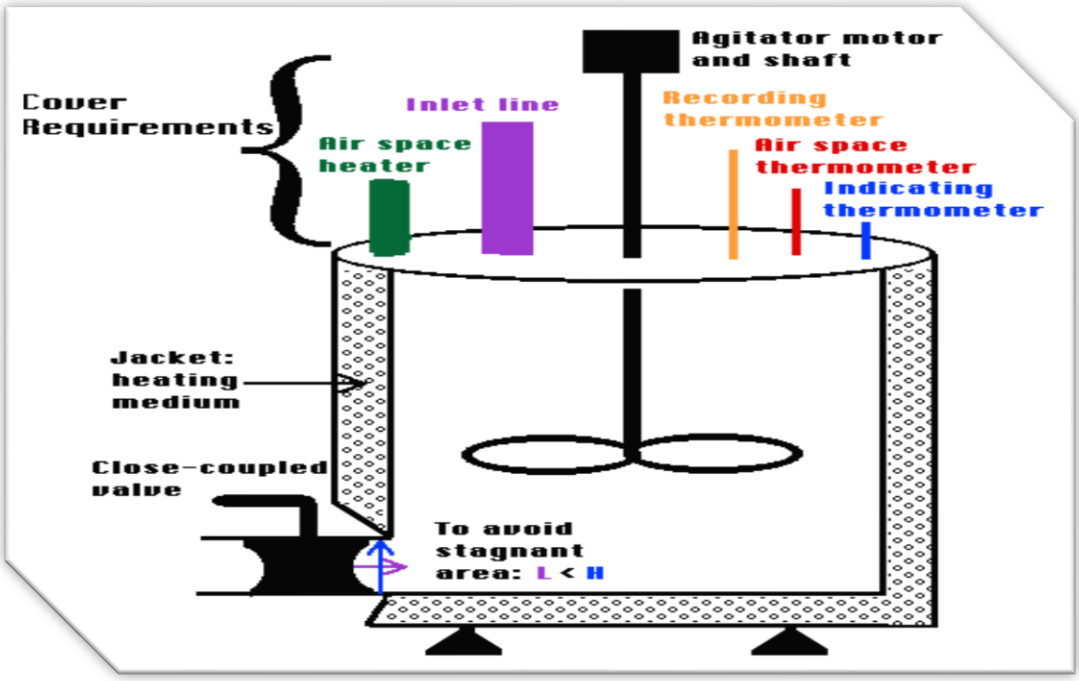

Figure 2.2: Batch or Vat pasteurization processes

In the milk, the milk is heated again caught all the time being caught while turbulent. Milk can cool in the machine or be removed heat after the holding time is completed for all particles. Like conversion, the milk can be heated slightly in a tubular or pre-heated plate to enter the pit. This method does not use much milk but the other is milk products (e.g., creams, chocolates) and special collections. A vat pasteurizer is used especially in the ice cream industry as it allows the melting and mixing of ingredients during the heating section.

2.4.2. Continuous pasteurization processes

The continuous process has several advantages over the vat method; too what is important is time and energy. With continuous processing, high-temperature altitude a short-time heat pasteurizer is used. Heat treatment is achieved using a plate heater. This piece of equipment contains a metal stack. Stainless plates are tied together in a frame. Many flow patterns can be used. Gaskets are used to define channel and protection parameters leakage. In this heat treatment, hot heat is used to heat and cool the food product and a micro-organism or targeted enzyme does not apply to the maximum temperature of the stay provided given to the holding tube.

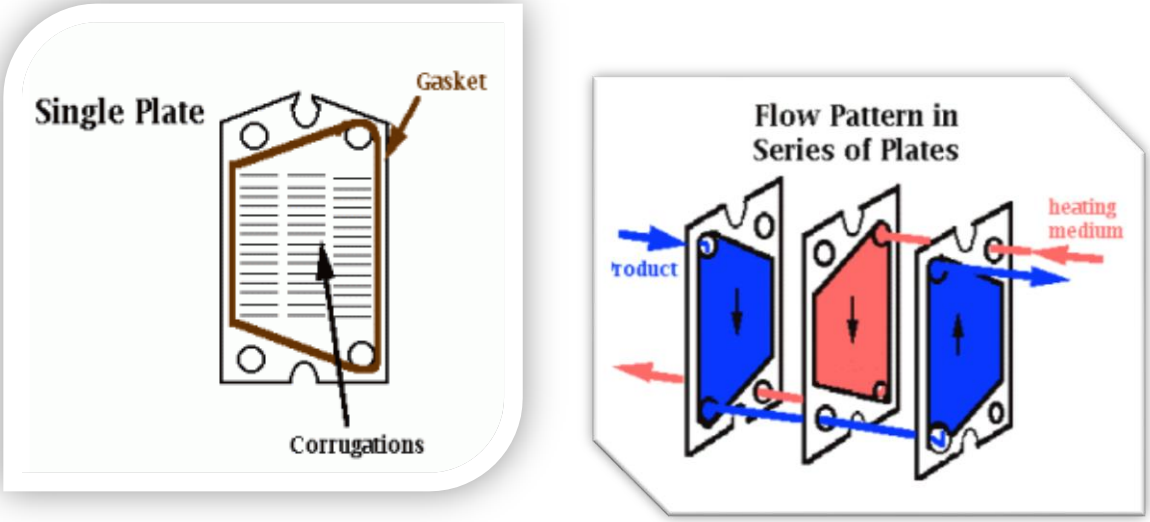

Figure 2.3: Continuous pasteurization processes

(Patel, et al., 2016) Reviewed that, renewable solar energy utilizing in dairy by using solar panels or concentrator-based milk pasteurizer system is developed to meet the demand of pasteurization. It was observed that the base temperature of solar-heated water reached up to 100˚C and the pasteurizer has easily attained pasteurization temperature ranging from 65-75˚C in two-three hours. In this thermal treatment, heat exchangers are used for heating and cooling the food product, while the target micro-organism or enzyme is inactivated at high temperature for a given residence time in a holding tube.

(Yildirim, et al., 2015), Explained that, in the milk processing plant, pasteurization is one of the best-known heat treatment processes. In this process, heat transfer is specially provided by hot water using different types of energy sources such as natural gas, coal, electricity, renewable energies, etc. They also informed that cooling is accomplished by conventional vapor absorption systems with their lower initial and operating costs compared to a cooling tower. However, the refrigerants (chlorofluorocarbons) used in conventional systems are not environmentally friendly.

2.5. Types of milk pasteurization

(Watts, 2016) It is pointed out that four common types of milk pasteurization are different at room temperature and when the milk is handled at that temperature.

- Batch or Vat Pasteurization
- High-Temperature Short Time (HTST)
- Ultra-High Temperature (UHT)
- Uperization (Ultra-Pasteurization)

Table 2. 1: Temperature-time pasteurization requirements for fluid milk

Pasteurization Type	**Time**	**Temperature**
Batch/Vat Pasteurization	30 minutes	63℃
High Temperature Short Time (HTST)	15 seconds	72℃
Higher-Heat Shorter Time (HHST)	1.0 seconds	89℃
"	0.5 seconds	90℃
"	0.1 seconds	94℃
"	0.05 seconds	96℃
"	0.01 seconds	100℃
Uperization (Ultra-Pasteurization)	2.0 seconds	138℃

Vat Pasteurization is a type commonly used by farmers for their use, too is less harmful to dairy nutrients. The milk is heated to 145℉ (63℃) and held e hat a temperature is 30 minutes. Such milk is used to prepare traditional milk (cheese, yogurt, etc.) as it can severely damage milk proteins. The average shelf life is 7-10 days.

In High Temperatures, Short Time (HTST) milk is heated to 161 °F(72℃) and held at their temperature for 15 seconds. This is the most common form of bone marrow transplantation used by local dairies, almost identical to the same shelf life as the vat process.

This method has several advantages over the vat method, which is very important to be time and energy-saving. In the most continuous processing, the shortest period of high temperature (HTST) pasteurizer is used. Heat treatment is achieved using a plate heat body. This piece of equipment contains a large number of stainless steel the plates are fastened together with a frame. Many flow patterns can be used.

In Ultra-Pasteurization (UP) the milk is heated to 280°F (138℃) for 2 seconds. Note this above boiling, which means that high pressure must be applied to the milk to achieve it this is hot, and it will damage its food quality. This method is used because it extends the shelf-life of milk to 60-90 days, and it is a national or regional dairy product choice as it allows for storage and delivery of milk.

In Ultra-High-Temperature (UHT) the milk is heated to 280°F (138℃) to 302°F (150℃) for 1 or 2 seconds followed by packaging in airtight containers. It allows storage without refrigeration for up to 90 days. Again, high pressure is required to reach this temperature.

Table 2.2: Advantages and Disadvantages of Types of Milk Pasteurization

Batch or Vat pasteurization system	
Advantages	**Disadvantages**
✓ Well suited for small plants, low volume products ✓ A variety of products can be handled ✓ Well suited for cultured products such as bottled milk, sour cream, etc. ✓ Simple control ✓ Low installation cost	✓ Batch type ✓ Slow products ✓ As the controls are mostly manual, it requires constant attention ✓ Both heating and cooling are relatively expensive as we do not have heat regeneration
HTST Pasteurization system	
Advantages	**Disadvantages**
✓ Uniform treatment	✓ The system is complicated

✓ Temperature is regulated at close limits and overheating is prevented ✓ Economical than batch system (due to regenerative heating)	✓ Not portable ✓ Installation cost is more

Ultra-High temperature pasteurization system	
Advantages	**Disadvantages**
✓ The better texture of milk due to short holding time ✓ Greater bacterial destruction is possible ✓ Kept for several months without refrigeration, advantageous in warm summers. ✓ Manpower costs are saved ✓ It extends the refrigerated shelf-life of the milk up to 90 days.	✓ The flavor of UHT milk is dissimilar to pasteurized milk ✓ Sometimes fat separation and sedimentation of insoluble particles may occur during storage ✓ Above boiling, this means that high pressure must be applied to the milk to achieve this temperature, and is destructive to its nutritional quality.
❖ The advantages and disadvantages of an ultra-pasteurization system are almost the same as that of an ultra-high temperature pasteurization system.	

NOTE: For my study, the High-temperature short time (HTST) milk pasteurization system is preferable because of the following reasons:

- ❖ Milk is heated uniformly to the required temperature.
- ❖ Temperature is required at close limits and overheating is prevented.
- ❖ Regeneration occurs, this greatly reduces the cost of heating and cooling.
- ❖ Utilizes a heat exchange unit to transfer the thermal energy to the milk.
- ❖ Economic and environmentally friendly.
- ❖ Energy-efficient minimizes the damage of milk being treated and is a very effective process concerning destroying microorganisms.

Key components used to investigate the performance of the milk pasteurization system

- Solar radiation
- Solar collector absorber
- Heat exchanger
- Evacuated tube solar collector
- Flexible tubes
- Valves
- Raw milk storage tank
- Temperature controller
- Solenoid valve
- Positive displacement timing pump

The abundance of solar energy in Ethiopia paired with the concept of milk pasteurization may be a good alternative to achieve environmental conservation, ensure healthy milk, and address the problem of energy and reduce the cost of energy.

2.6. Solar thermal energy

There are two essential types of solar energy technologies; those are Photovoltaic and Solar thermal. Photovoltaic is electricity from the sun and Solar thermal is heat from the sun. These two technologies are technically feasible and cost-effective, and some commercially available plants can produce up to 350MW, these systems are highly dependent on the local climate and energy needs; this is a big limitation because only in certain regions these systems can be efficient enough to be implemented.

(Zekai Sen, 2008), reviewed the growing demand for solar thermal energy has many causes, including depletion of the traditional sources of fuel and energy such as oil, higher availability of the sun which is the source of this renewable energy, low-cost operation, and easy maintenance of these plants. A concentrated solar thermal power plant works nearly in the principle of a conventional steam power plant. However, there is an important difference that there is no harm to the environment as in the case of burning coal, oil, natural gas, or by splitting uranium to produce steam. Steam is produced only by the energy that comes from the sun. (Farjana, et al., 2017) reviewed in simple terms solar thermal energy we find it in the conversion of heat received by the sun's rays and called as the heat of the sun power. Like other renewable energy systems, solar thermal energy can replace residues fuel for industrial systems.

This solar source of energy is sustainable; it does not provide any greenhouse gas emissions and environmentally friendly sources of energy. It is free and maintainable as the sun is here to stay.

(Werner, et al., 2010) Reviewed that, the solar power can be collected by the concentrated solar power systems which collect the solar insolation to concentrated insolation beams on the receiver, and then the beams are used to heat some heat transfer fluid (HTF) which will operate steam turbine in the final.

(Jamar, et al., 2016) You have reviewed that; solar water heating system is an effective technology to convert solar energy into thermal energy. Solar thermal efficiency conversion is around 70% compared to the direct conversion of solar gas systems at 17%.

Typically, in solar thermal applications, water heaters are accomplished by solar collectors, and these devices are responsible for the capture of solar radiation and the transfer of thermal energy to liquids (Sharma, et al., 2017).

2.7. Solar Water Heating System

Solar water heaters have a variety of designs, while all contain a collector as well storage. A solar water heater collector is used to collect radium from sunlight heat water. A storage tank is used to store water for later use. Solar water heaters are often defined by the type of collector and circulation system. Different types of solar water heaters have different operating modes.

(Nahar, 2002), Reviewed, Hot water is important for industries and households. Icon toiletries, laundry, and other household items in urban and rural areas. Hot water is in great demand in hotels, hospitals, hostels, and industries such as textiles, paper, food processing, milk, and edible oils. The hot water was like that much needed for hygiene and bathing in the home

(Wang, et al., 2015) stated that, a solar water heating system can be categorized into direct and indirect systems based on whether or not they require a heat exchanger. In a standard setting, service water is distributed directly between the water tank and collection, during indirect system, heat transfer fluid, frequency anti-freezer, reduced water, or organic fluid is distributed through the solar collector. Temperature switch monitored to affect the transfer of heat from the collector to the service tank in the tank.

They also informed that the heat exchanger could be used inside or outside the hot water tank and the indirect system in most situations performs better than the direct one, which are fewer climates selective and more suitable for use in regions that experience cold temperatures.

(Jamar, et al., 2016), reviewed that, in general, solar water heating systems are classified into two as shown in Figure 2.4. The active system consists of the direct flow (open loop) system and indirect flow (closed-loop) system; whereas the passive system contains thermosiphon and integrated collector storage.

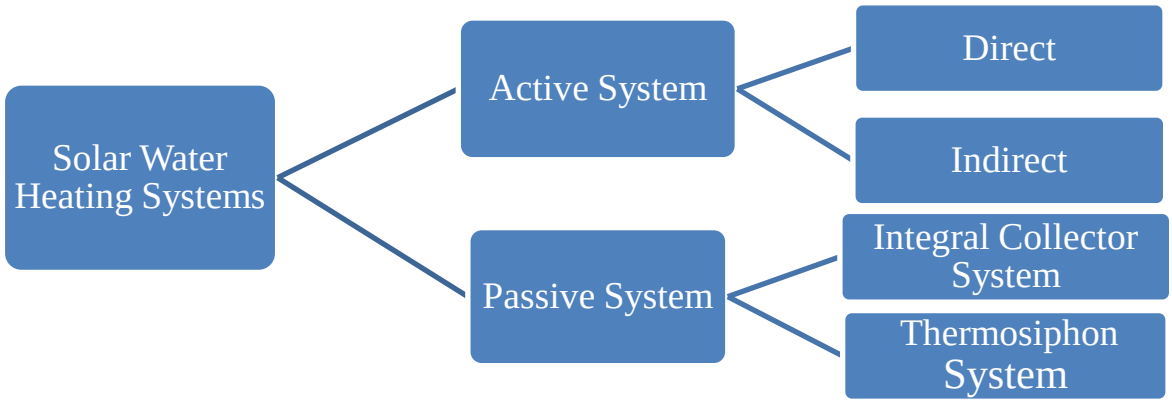

Figure 2.4: Types of Solar Water Heating System (Jamar, et al., 2016)

2.7.1. Active Solar Water Heating Systems

ASWHSs or forced circulation systems use electric pumps, valves, and regulators to transport water from collectors to storage tanks.

(Wang, et al., 2015) defined that, active water heating system is the one that uses electrical pumps to transfer thermal energy, valves, and regulators to distribute water or other heat transfer fluids through the collectors. This system is also known as a forced circulation system and it can be an open-loop (direct) active system or a closed-loop (indirect) active system (Jamar, et al., 2016).

Open-loop (direct) active system heats the actual household water in the solar collectors. Once heated, the water is diffused into a storage tank and then piped to spout for use at home. Whereas closed-loop (indirect) active system uses heat to transfer fluids that are usually a water-antifreeze mixture.

After the heat-transfer fluid was heated in the solar collectors, it was diffused into a storage tank where a heat-exchanger transfers the heat from the fluid to the raw water. This system has an

advantage over the passive system, ranges from 30 – 50% its efficiency is usually between 35% and 80% (Wang, et al., 2015).

2.7.2. Passive Solar Water Heating Systems

Passive systems do not require pumps. Natural convection heats water from the collector in the storage tank.

PSWHS usually transmit heat through environmental broadcasts due to the height due to the temperature difference between the two kingdoms; that's why it does not require the pumps to work. They are the most widely used solar water home heaters are also designed and investigated separately researchers [(R.S Soin, et al., 1979.)- (W. Chun, et al., 1999)]. The flow rate of the natural cycle is usually controlled by the entry-level.

(Jamar, et al., 2016), stated that, the passive system utilized natural convection heat transfer due to density differences. This system is based on a simple mechanism, where the heated fluid loses density and becomes lighter and thus flows up toward the collector and then into the storage tank, while the cold fluid flows down toward the tank floor and enters the collector without using mechanical devices (Wang, et al., 2015).

There are two basic types of passive systems: thermo siphon system and integrated collector storage system.

2.7. 2.1.The thermo syphon solar hot water systems

(J. Razavi, et al., 2003),reviewed that, the facility harvesting solar energy solar collector and the hot water storage tank are separate components, with the hot water tank usually placed at a level higher than the solar collector. Figure 2.5, shows a schematic diagram of this type of SWHS. It can be classified into two, viz., thermo syphon SHWS using phase change materials two-phase systems and thermo syphon SWHS without phase change materials single-phase system. Figure 2.5: Schematic diagram of a typical thermo syphon solar water heater.

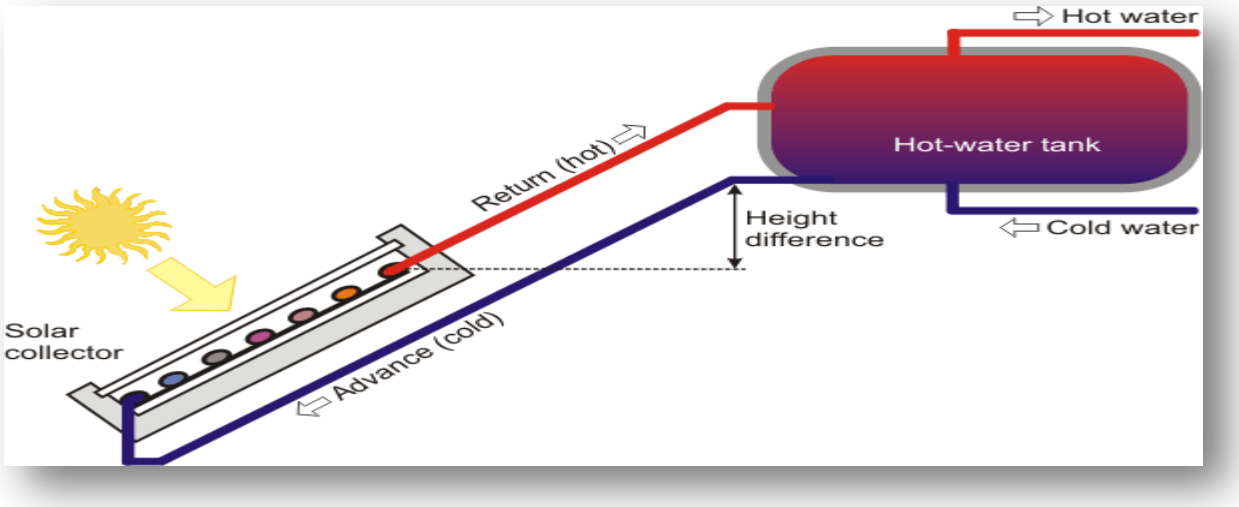

Figure 2.5: Thermosiphon principle [wiki.lowtechlab.org]

2.7. 2. 2. The integrated collector storage system

The system falls under the category of water heating that operates in the sun and is reflected in its having a collector and storage tank for service water as one component, thus introducing an integrated unit. It is the first recorded SWHS record for commercial use (M. Smyth, et al., 2006) and adds in a variety of ways. The progress in its development, from when the ICS type was at its early stages to the present, are presented in Ref (M. Smyth, et al., 2006).

This system integrates, the solar collector and the thermal storage tank components function as a single unit. It is the simplest form of solar water heater on the market and becoming a very popular choice of solar water heater, it also reduced the cost, as they integrate the collector and the thermal storage tank in the same construction (Jamar, et al., 2016).

2.9. Solar Thermal Collectors

(Kalogiroun S, 2000), reviewed that; solar collectors are a special type of heat exchangers that convert solar energy into internal transport power average. A large part of any solar system is a solar collector. This is a tool that absorbs incoming sunlight, converts it into heat, and transmits this heat in a liquid (usually air, water, or oil) that flows to the collector. The power of the sun through it the collection is carried from a circulating liquid directly into hot water or space repair equipment or thermal energy storage tank from which to draw night use and/or cloudy days.

(Kalogiroun S, 2000), reviewed, there are two types of solar collectors: no focus(no concentrating) or standing(stationary) and focused(concentrating). A professional collector with a similar location to meet and receive sunlight, while focusing on following the sun the collector of the sun usually has a concave area that shows restraint and focuses on the solar radiation to a small reception area, thus increasing the flow of radiation.

Currently, three types of solar collector's namely flat plate, Compound parabolic collectors, and evacuated tube solar collectors are commonly used in a solar water heating system (Gao, et al., 2014).

2.9.1. Flat-plate solar collector

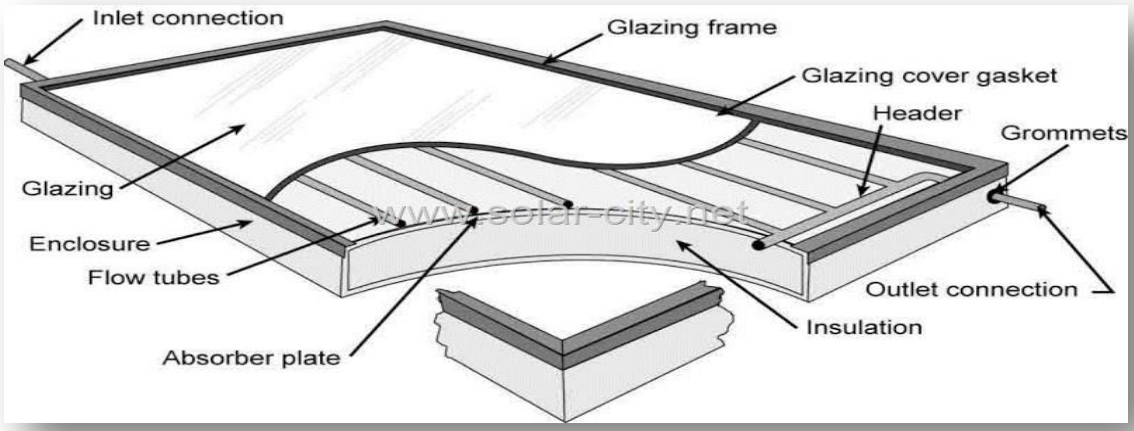

Figure 2.6: Flat-Plate Solar Collectors [www.solar-City.net]

A flat plate collector (FPC) is the heart of the SWH system. Still, work hard at lower temperatures, which reduces their demand for domestic and local water heating Heat (Gao, et al., 2014). When the sun's rays pass through the transparent cover again enters the surface of the black moisture of high absorption, a large part of this energy is absorbed by the plate and then transferred to the transfer area in fluid tubes to be taken for storage or use. The bottom of the reduction plate and the boat, side is well fitted to minimize loss of steering. An exposed cover is used to reduce convection loss from the suction plate by blocking the air layer standing between the suction plate and the glass. It also reduces radiation loss from the collector as glass is exposed to the rays of short waves received by the sun but almost equal to the heat wave-wave radiation emissions from the suction plate (heat effect)

(Fathima,, et al., 2016) argue that, ordinary flat plate collectors are eligible for warm weather and times when the sun's rays intensify too high. In addition, their benefits are reduced when they are exposed to cold, cloudy, and windy days. Furthermore, when exposed to weathering conditions, the tubes and the insulation tend to deteriorate thereby causing loss of performance.

2.9.2. Compound parabolic collectors

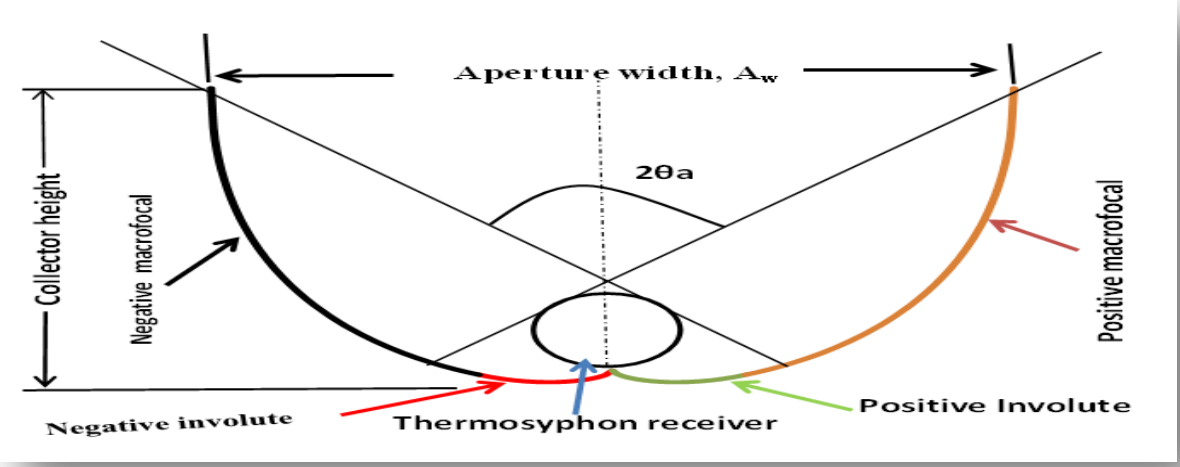

Figure 2.7: Compound parabolic collectors [researchgate.net]

(Winston , 1974), reviewed that, CPC are non-imaging concentrators. These are the ability to display the absorption of all event radiation within broad boundaries. The need to move the focus to accept the change of sun the turn can be reduced by using a two-point parabola facing boat one another, as shown in Figure 2.7. Complex parabolic concentrators can receive inputs radiation at a very wide range. Through a lot of internal thinking, any radiation that enters the hole, inside collector acceptance angle, finds the path to the reduction point found in the area under the collector.

2.9.3. Evacuated tube collectors

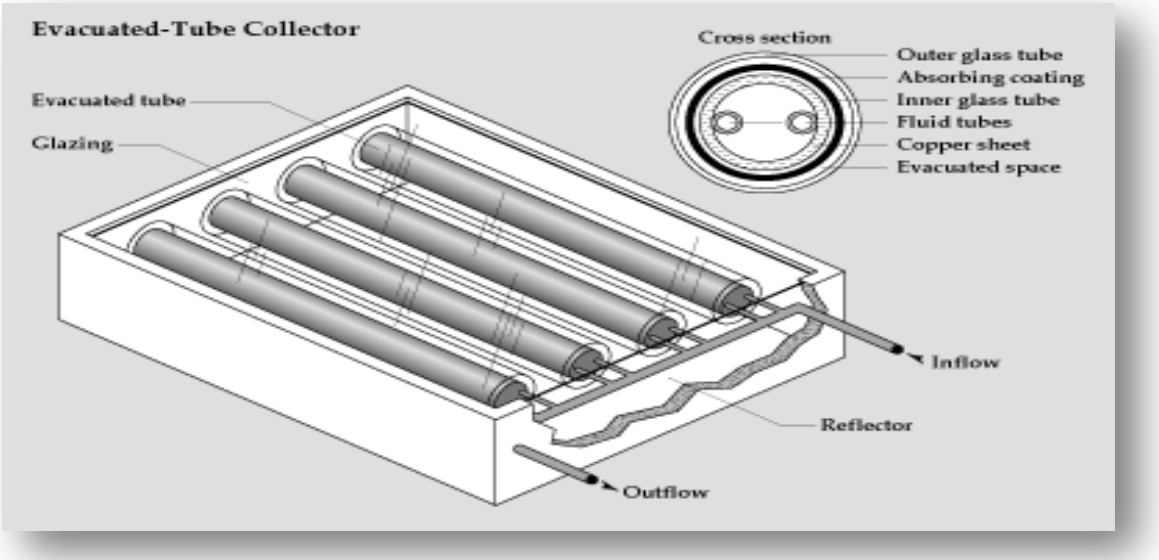

Figure 2.8: Evacuated tube collectors [daviddaring.info/researchgate.net]

The evacuated tube solar collectors are common and can achieve higher temperatures than flat-plate collectors ranging from 50-130 ℃. They are made up of vacuum glass tubes. The absence of air highly reduces convection and conduction thermal losses (Kalogiroun, et al., 2004).

Evacuated–tube collectors can get very hot, exceeding the boiling point of water, and can cause significant issues in an existing domestic solar water system. You need to use your hot water every day to ensure the temperature does not overheat in the tank or end usage. The mixer is easily installed just after the last hot water tank and mixes your regular(cool) water supply with the hot water, to ensure the temperature never exceeds a set limit.

(Sabiha, et al., 2015), explained that, ETSC is used to capture solar radiation, which is then turned to thermal energy and transferred to a working fluid. It is made of parallel evacuated glass pipes. Each evacuated pipe consisting of two tubes, one is inner, and the other is outer tube. Also reviewed, Heat extraction from a long thin absorber is the main problem with evacuated tube solar collectors.

(Kalogiroun, et al., 2004) Reviewed that, solar evacuated tube collectors (ETCs) contain a heat pipe inside a closed tube, as shown in Figure 2.8, ETC has a combination of the selected location

and the active delivery that leads to the top performance. ETCs work on the principle of using vacuum as the best protection obstacle, to prevent heat loss mainly due to convection and conduction.

Using a selective absorbing surface substantially reduces the radiative losses from a collector. To obtain larger temperature differences, it is necessary to reduce the convective losses as well. A method that offers better performance but is more difficult legally to get out of the space between the plate and its glass cover. This requires a very strong structure suspension to prevent the maximum force of the wind from breaking the glass cover; like this, the suspension is the outer tube of the circular cross-section. Inside this removed tube is there he placed a suction tube.

Evacuated tube devices have been proposed as efficient solar energy collectors since the early twentieth century.
(Yadav, et al., 2017), stated that, these two glass tubes are made from extremely strong borosilicate glass. The outer tube allows light rays to pass through its Minor reflection and the inner tube is coated with a selected coating (Al-Nickel/Al) which features excellent solar radiation absorption and minimum reflective characteristics.

ETCs are a relative newcomer to the solar hot water scene and are a serious departure from conventional flat plate collectors. These solar collectors consist of numerous (20 to 30) long, parallel glass or plastic tubes. Inside each tube is a copper pipe as an absorber tube coated with selective surface material. It runs down the center of an absorber plate, which increases the surface area for absorption. Air is diffused out of the glass or plastic tube, creating a vacuum, hence the name evacuated tube collectors (vacuums are poor conductors of heat and therefore great insulators).

Inside each black copper pipe is a heat transfer fluid (methane). It sucks heat created when sunlight hits the selected dark area of the absorber plate. Methanol flows naturally by transferring heat to the heat exchanger above the unit. Here, heat is transferred to another heat transfer fluid, usually a higher temperature non-toxic antifreeze (propylene glycol). It transfers heat to the solar water tank where it is transferred to water and stored for later use. Cooled methanol returns to a continuous cycle.

Water in glass Evacuated tube solar collector (WGETSC) or all-glass evacuated tube solar collector (AgETSC) is a direct liquid contact type and now in China widely used for sanitary water heating, because of its low price and excellent low heat loss features (Gao, et al., 2014)

.According to (Gao Y, et al., 2013) stated that the U-pipe Evacuated tube solar collector (UpETSC) was developed based on improving the WGETSC. U-shaped pipe (usually piercing copper with a diameter of 8-10 mm) and aluminum fins installed in the inner tube of the tube.

The fluid flows into the U-pipe to absorb and transfer useful energy. The key difference is that each extracted or evacuated WGETSC tube is full of active fluid but the liquid is only available in the UET pipe of UpETSC.

(Gao, et al., 2014) also informed that the advantages of UpETSC lay in the tube attaining higher temperatures, long service life, and the ability to bear more intense pressure than those of the water in glass collector. The UpETSC has a well-developed type of collector and rapidly expanded in the market even the costs are higher than the water in glass collector types.

(Sabiha, et al., 2015), reviewed from experimental works; the U pipe evacuated collectors have 25–35% higher energy storage capacity than water in the glass. In addition, the energy storage and also pump operations are influenced by the flow rate and fluid thermal mass. However, the heat pipe is thermal energy absorbing and transferring system with no moving parts which can transfer more energy than copper, where the heat pipes are the best-known conductor and can operate with a temperature up to 300℃ with 50% to 60% efficiency (Siva Kumara, et al., 2017).

(Jafarkazemi, et al., 2016), identified from the experimental comparison between flat plate and heat pipe evacuated solar collector at similar weather conditions within one year. The flat plate and evacuated collector generated 496 KWh/m^2 and 681 KWh/m^2 energies per unit area, respectively. Also, annual averages of thermal efficiencies were 46.1% and 60.7%, respectively. ETSC is strong and durable in the event of a broken tube; simply inserted, which is considered to be a cheaper option compared to a flat plate collector (FPC) that requires the replacement of the whole collector (Ghoneim A, et al., 2017).

2.10 Selection parameter of Solar Collectors

(Jamar, et al., 2016) pointed out that, there is more to consider choosing the right solar collector according to temperature, environmental requirements conditions, collection features, how collectors are organized (static or flexible to follow the rays of the sun's rays), angle of inclination and temperature types transfer liquid (water, aqueous solution ethylene glycol, and air). Collecting the sun the feature can be non-focus collectors and focus collectors.

By not focusing, it can be a flat type with no way to concentrate incoming solar radiation, while concentrating, has the focus of focusing on the force that falls on the opening enters the heat exchanger with a small surface area beyond the hole. This type of collector is called an evacuated tube solar collector.

(Suresh, et al., 2017)suggest a selection of solar collectors depends on several parameters, such as:

- Operating temperature

As the thermal processes required solar collectors categorized as low temperature collectors (LTCs), medium- (MTCs) and high-temperature collectors (HTCs) with operating temperatures of < 800C, 800C - 2500C, and >250 0C, respectively. LTCs are mainly used for water heating and space heating applications.

MTCs are used for the production of hot water, steam, and hot air in heating and cooling processes applications, while HTC is widely used for power generation and thermal supply water/smoke.

- Sun tracking position

Most LTCs and MTCs are stand-alone collectors that do not track the sun, and HTCs collect a variety of collectors and track the position of the sun over the day.

- Cost or capital investment

FPCs and Evacuated Tube Collectors (ETCs) are economical to generate heat up to 150 ℃ for process heating. While HTCs (dish collectors) can generate heat greater than 150 ℃ but require high capital investment.

- Lifetime

ETCs type collectors are made of glass and are fragile, whereas FPCs contain metallic components and have longer lives. In general, plant life for an FPC, an ETC, and a Dish is 15,

20, and 25 years, respectively. Therefore, for my works the evacuated tube solar collector is preferable because of the following reasons:

Many researchers have suggested that the solar evacuated tube collector is superior more profitable than other types of a collector; can be used in any weather, from extremely hot to extremely cold weather and its high humidity ensures working under cold conditions.

A flat plat collector requires wide space to install, were as ETSCs require lesser space and it is very easy to install. Also, ETSCs absorb solar radiation from multiple angles, due to their tubular design and less effect of wind and low temperature.

FPCs stop working in the event of a tube injury, but ETSCs stop working or recovering disclosed but continues to operate at low efficiency in the event of damage to the tube . Since there is no water flow through collecting tubes and tubes closed with a will mark does not suffer from corrosion problems as in the case with other types of solar collectors

The peak energy output by FPC is gained only at mid day when the sun is perpendicular to the the surface of the collector, whereas the evacuated solar tube area can track the sun passively throughout the day as for the cylindrical shape of evacuated tubes. This average output energy from ETSC over an entire year is 25 – 40% higher than FPC per netm^2.

(Pluta, 2011) reviewed that; ETCs are much more sensitive than flat plate collectors in terms of optimal tilt angle. For solar domestic hot water systems where the required temperature of warm water, there is no clear advantage of evacuated solar collectors over the much cheaper flat plate collectors.

2.10.1 Other considerations when Using Evacuated Tube Collectors

- Due to the sealed vacuum within their design, ETCs can get very hot, exceeding the boiling point of water during the hot summer months. These high temperatures can cause significant issues in an existing domestic solar hot water system such as overheating and cracking of the evacuated glass tubes.
- To help prevent this from happening in hot summer climates, bypass valves and large heat exchangers are used to "dump" the excess heat as well as mixer valves which mix regular (cool) water with the hot water, to ensure the temperature and pressure levels never a preset limit.

- Also, heat pipe collectors should never be exposed to direct sunlight without heat transfer fluid flowing through the heat exchanger. Doing so will cause the empty heat exchanger to become extremely hot and which may crack due to the sudden shock once cold water begins to flow through it.
- Even though evacuated tube collectors are capable of heating water to 150degree Celsius in the winter, the outer glass tube of an evacuated tube does not heat like a normal flat plate solar collector when in use. This is due to the inherent insulation properties of the vacuum inside the tube which prevents the outer heat tube from being cooled by the outside ambient temperature which can be well below freezing.
- Thus, in the colder winter months, these types of collectors cannot melt away the large quantity of snow that falls on them at any one time which means clearing the snow and ice from the glass tubes daily can be a problem without breaking them.
- Even if it is very snow or very cold, enough sunlight will get through to keep the tubes well above freezing and still be able to preheat the water which can then be heated further by a standard electrical immersion heater or gas burner reducing the costs of heating the water in winter.
- ETCs are a very efficient way of heating much of your hot water use just using the power of the sun. They can achieve very high temperatures but are more fragile than other types of solar collectors and are much more expensive to install. They can be used in either an active open-loop (without heat exchanger) or an active closed-loop (with heat exchanger) solar hot water system but a pump is required to circulate the heat transfer fluid from collectors to storage to stop it from overheating.

The limitation of ETSCs is the initial cost is high as compared to other collectors and the construction of an evacuated U-tube collector is a little bit complicated as compared to other collectors and thus proper handling is required. Occasionally due to improper handling and maintenance of temperatures, they become very high due to lack of water in the gut and therefore cause hot shock so the tube may rupture and result in machine loss.

2.11. Working principle of U pipe Evacuated Tube Solar Collector

Illustrated in figure 2.10, the Evacuated tube collector receiver consists of a copper U tube inside a glass vacuumed tube. The copper tube is surrounded by a cylindrical aluminum fin pressed on it. The fin improves the heat transfer space inside the inner glass absorber surface and U-tube.

The active fluid enters the collection pipe, then is evenly distributed in the U-tubes, retains heat, and finally, is returned to the bulky outdoor pipe.

The outer cylindrical glass transmits radiation to the inner glass tube, which conducts power on the reduction or absorber line. The energy converted into heat is driven by the fin to the U-brass tube and eventually absorb the active liquid in this case (Aboulmagd, et al., 2014) (Ghoneim A, et al., 2017)]

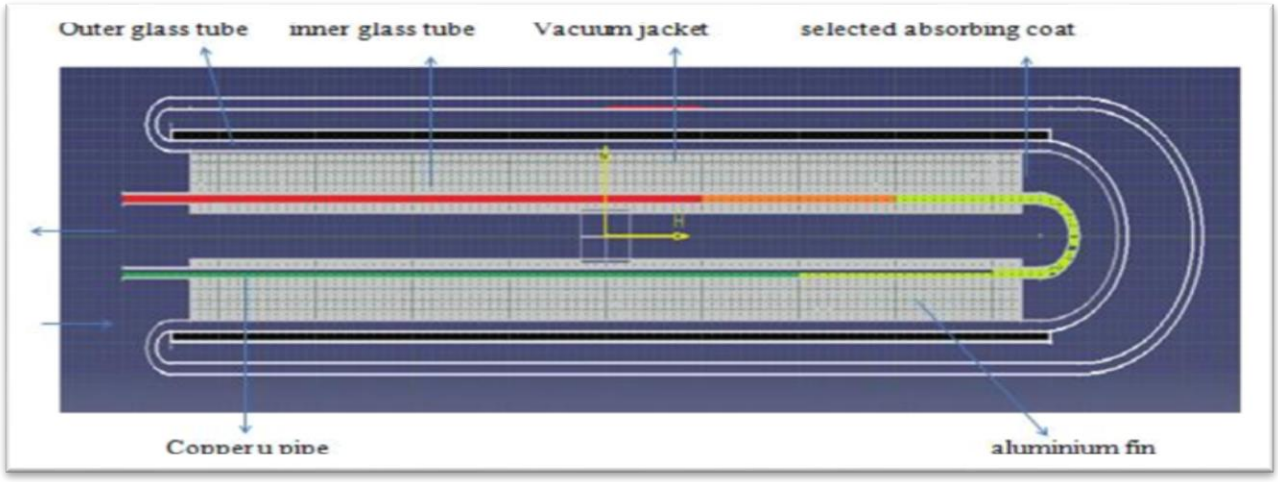

Figure 2.10: Evacuated Tube with U-type heat extraction system

2.12. Heat exchanger

A heat exchanger is a special device used to transfer heat from one fluid to another at different temperatures. The exchange can take place between a process stream and a utility stream (cold water, pressurized steam, etc.), a process stream and a power source (electric heat), or between two process streams resulting in energy integration and reduction of external heat sources.

The selection of a heat exchanger depends on many factors including capital and operating costs, fouling, corrosion tendency, pressure drop, temperature ranges, and safety issues (tolerance to leakage).

(Ramachandra K, et al., 1982) reviewed that, among the different types of heat exchangers, the shell and tube heat exchanger would normally be used for many continuous systems having small to medium heat duties.

(Panchal H, et al., 2018) reviewed that, heat exchangers are multifaceted and widely used in industrial and domestic applications due to the increase in heat transfer applications nowadays. They also point out that, HEs shell and tube types are widely used in the dairy and food industries.

However, under conditions of laminar flow or low flow rates, where a shell-and-tube heat exchanger would become uneconomical because of the resulting low heat-transfer coefficients.

(Vishvakarma, et al., 2016) and (Sadic, et al., 2002) review that, helical coils in the cross-section have been widely used in the preparation and storage of food, milk, refrigerator, storage tanks, heat recovery systems, air conditioning, etc.,

(Purandare, et al., 2015) argued that the helical tube heat exchanger is more than a straight coil in the heat transfer application due to the second flow made by the bending of tubes with centrifugal force detected in the flowing fluid which improves heat transfer in the combined heat tube. In addition, from the test results of a small coil and tube width the size of the secondary development is high. This increase in the power of the secondaries allows for proper mixing of the liquid, which improves the balance of heat transfer of the same flow rate. In contrast, the expansion of the tube and the diameter of the coil tube reduce the improved secondary caries reducing the amount of heat transfer (Purandare, et al., 2015).

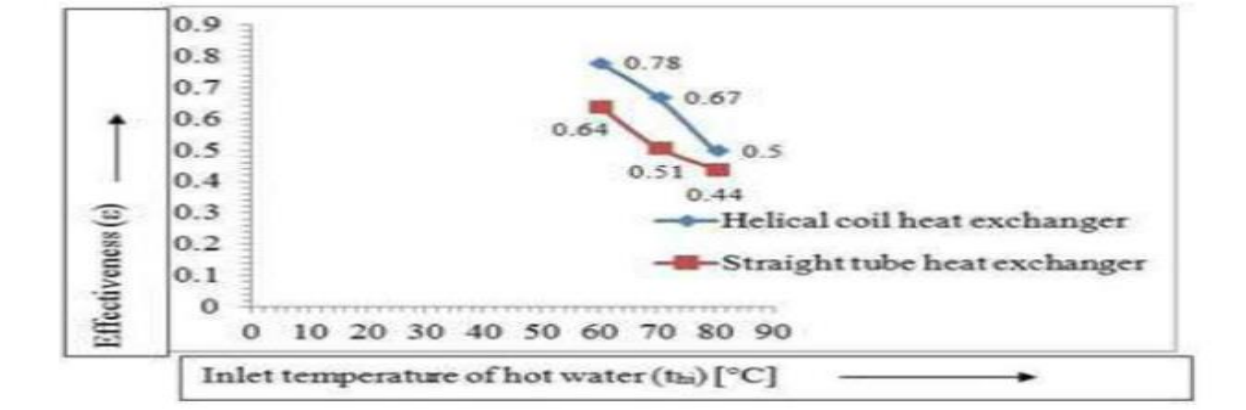

Figure 2.12: Variation of heat exchanger effectiveness with an inlet temperature of hot water (Vishvakarma, et al., 2016).

(Huang, et al., 2015) argued that, heat exchanges were widely used to lubricate or pasteurize liquid food products such as milk. However, the accumulation of pollutants in hot plates of heat exchangers reduces running time, reduces efficiency, and may increase the risk of bacterial contamination.

(Shuhong, et al., 2014) investigated experimental study, on the influence of the position of helical tube heat exchanger in SWHs thermal performance. From efficiency analysis, the maximum annual solar fraction and maximum collector efficiency are 42.2% and 31.4%. And, they concluded that from experimental and annual simulation for long-term performance of SWHs it's better to have the heat exchanger at the under of hot water tank (Shuhong, et al., 2014).

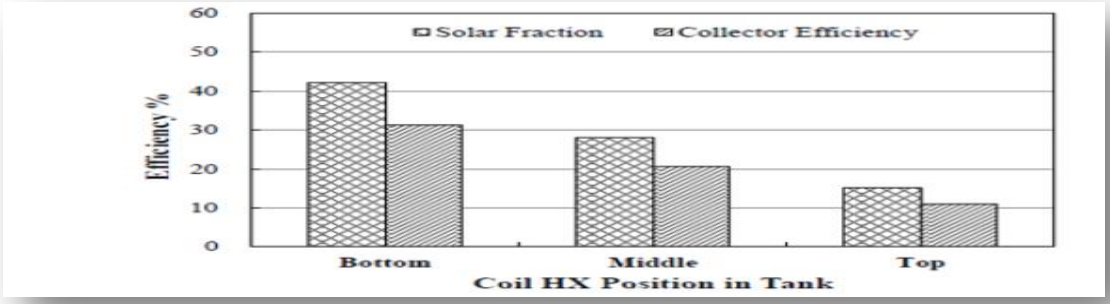

Figure 2.13: The solar fraction and collector efficiency of SWHs (Shuhong, et al., 2014).

As reviewed by many heat exchange researchers, they are designed to be unique applications. Among the various types of heat exchangers, shell and tube heat exchanger is rarely used in many continuous systems with minimal heating functions. However, in this present study, a helical tube heat exchanger was selected. Because of its higher heat transfer rates as compared to a straight tube heat exchanger and following advantages [(Vishvakarma, et al., 2016)] [(Purandare, et al., 2015)] and (Lazova, et al., 2016).

We select helical tube heat exchangers depends on the following reasons (Purandare, et al., 2015):

- Enhanced heat transfer and compactness in structure
- Accommodate large heat transfer surface area in a small space
- Easy to integrate with the system, simple design, and manufacturing, operation at high pressure, suitable under conditions of laminar flow or low flow rates

- Cost-effectiveness, ease of maintenance, and improved thermal efficiency.
- True counter-current flow fully utilizes available LMTD (logarithmic mean temperature difference). Helical geometry allows for the handling of high temperatures and extreme variations in temperatures without too much pressure or expensive expansion joints.
- A coil can provide a large surface area in a relatively small reactor volume and is Suitable for high heat duty application.
- A self-cleaning effect, in which contaminated areas cause a localized increase in fluid velocity, thus increasing water turbulence in the polluted environment, thus helping to eliminate blocking and keeping the heating system clean.
- Another advantage of using more helical coils, the tubes that the duration of stay spread is reduced, allowing helical coils to be used to reduce axial distribution in tubular reactors.

2.12.1. Geometry of Helical Coil Heat Exchanger

A helical tube can be geometrically described by pipe inner diameter 2r, coil tube diameter (measured between the centers of the pipes) 2R and coil pitch *P*, which is the space between consecutive coil turns (measured from the center to center) as shown in Figure 2.14 and δ is the ratio of pipe inner diameter to coil diameter [(Vishvakarma, et al., 2016)- (Sadic, et al., 2002)].

Think of a coil of gas in a plane passing over a coil axis. An angle, from which a single coil emerges directly from an axis, is called a helix angle, and α and φ are the angles of the bending tube at a level.

However, consider any section on the cross-section made by a plane passing through the coil axis. The side of the pipe wall adjacent to the coil is called the inner side of the coil and the far side is referred to as the outer case of the coil pipe [(Vishvakarma, et al., 2016)].

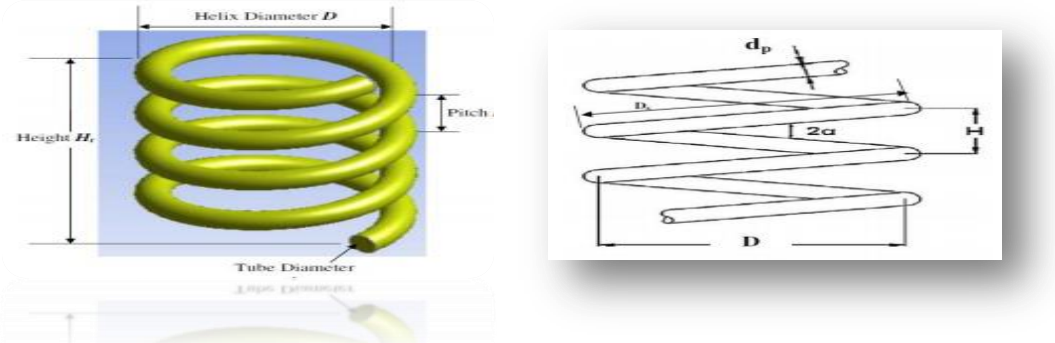

Figure 2.14: Helical coil tube with its geometrical parameters (Vishvakarma, et al., 2016)]

Reynolds number, Re

$$\mathrm{Re} = \frac{2\pi u_{av}\rho}{\mu} \quad (1.1)$$

To fully understand the variables affecting helical coil heat transfer, the Dean number is common is used and defined as seen in Equation (1.2). Dean number represents the viscous ratio of the force acting on the liquid flowing through a curved pipe into centrifugal forces. Dean's number will do never be greater than Reynolds' number of the same flow. The Dean number will never be larger than the Reynolds number for the same flow. As the Dean number approaches that of the Reynolds number, the effects of centrifugal force dominate the flow. This phenomenon and its effects on heat transfer have been studied extensively (Kalb, et al., 1974).

$$\mathrm{De} = \frac{\rho v d}{\mu}\sqrt{\frac{d}{D}} = R_e\sqrt{\frac{d}{D}} = \mathrm{Re}\sqrt{\frac{r}{Rc}} \quad (1.2)$$

(Seban, et al., 1963) studied heat transfer through a helical tube using two different curvature diameter ratios, *d/D*. The curvature diameter ratio is defined as the ratio of the inner diameter of the pipe, *d*, to the curvature diameter of the helix, *D*.

2.12. 2. Heat Exchanger Pressure Drop

(Kuppan, et al., 2000)explained that, the pressure drop inside the heat exchanger is the pressure loss that was not recoverable in the circuit. It also states the determination of pressure drop in a heat exchange is essential for many applications for at least two reasons.

- To identify the primary cost of the power to run fluid moving devices such as pumps, fans, and blowers which is the operating cost of a heat exchanger. This is due to the fluid pumping power; P is proportional to the exchanger pressure drop and given by (Sadic, et al., 2002)].

$$\mathrm{P} = \frac{\dot{m}\Delta P}{\rho n_p} \quad (1.3)$$

Where, P is the fluid pumping power, Watt, $\dot{m}$ is the mass flow rate, Kg/s, ΔP is a total pressure drop, ρ is the fluid density, and n_p is the efficiency of the pump.

- To study the significant heat-transfer rate influenced by the saturation temperature change for a condensing/evaporating fluid for a large pressure drop.

2.12.3. Literature Review Summary

Some previous researchers' studies are discovered related to Ethiopian dairy sector research gaps, solar water heating systems, and some background information about milk pasteurization. However, some experimental investigations are also performed to pasteurize fluid milk using solar energy in different mechanisms as follows to destroy microorganisms that easily spoils milk.

2.12.3.1. Research Gap

(Atia, et al., 2015) conduct experiment with flat plate solar collector and using milk itself, as a working fluid heated by the collector in Egypt. They obtained for the selected month of the year 63℃ and 72℃ pasteurization temperature for 73.9 lt /day and 37.3 lt/day respectively.

(Zahira, et al., 2009) reviewed that, the manufacture of solar adhesive from standard shipping cardboard with multiple layers of standard aluminum adhesive cardboard mounted on a large cardboard box with a rectangular and removable box using a glass window. Inside box with volume (52.5 × 24 × 36) cm covered on both sides with aluminum foil. The metal tray is painted black. And the tests were performed at a temperature of 65 to 75 ℃ (Zahira, et al., 2009).

(Wayua, et al., 2012) studied, on performance analysis of hot water jacketed solar-assisted milk pasteurization in Kenya. They investigate the experiment by varying the volume of milk between 20 to 70 lit and the maximum milk temperature obtained inversely varied from 81.4℃ to 41.7℃ respectively. And the hot water temperature also between 40℃ to 73℃ heated by a flat plate solar collector with the available solar energy of an area from 700 to 1,000 W/m^2.

2.12.3.2.Findings

- To pasteurize one hundred twenty litre milk at one it took fitty seconds.
- To increase the pitch axial length (pitch length) of helical tube heat exchanger and the diameter of the milk outflow to smooth the fluid flow.
- Decreasing the velocity, the flowing fluid gets more heating time and to achieve the required outputs.

In summary, this thesis aims to study the system described in Figure 3.12, in which a coil heat exchanger is directly immersed into the milk storage tank that used as the main heat transfer medium between the hot water inlet through the coil and the raw milk in the tank to study the performance analysis of milk temperature without varying the daily quantity of milk being heated for each month of the year.

CHAPTER THREE

METHODOLOGY

3.1. Introduction

This chapter analyzes the method applied and details numerical expressions of the overall modeled solar milk pasteurization system considered, to achieve the research objectives mentioned in Chapter one. Figure: 3.1 show the schematic diagram of the conceptual framework of the applied methodologies, which was separated into three main parts:

(1) Data collection and clustering

(2) System description and modeling of the main components and,

(3) Analysis of the performance evaluation of the system by applying CFD.

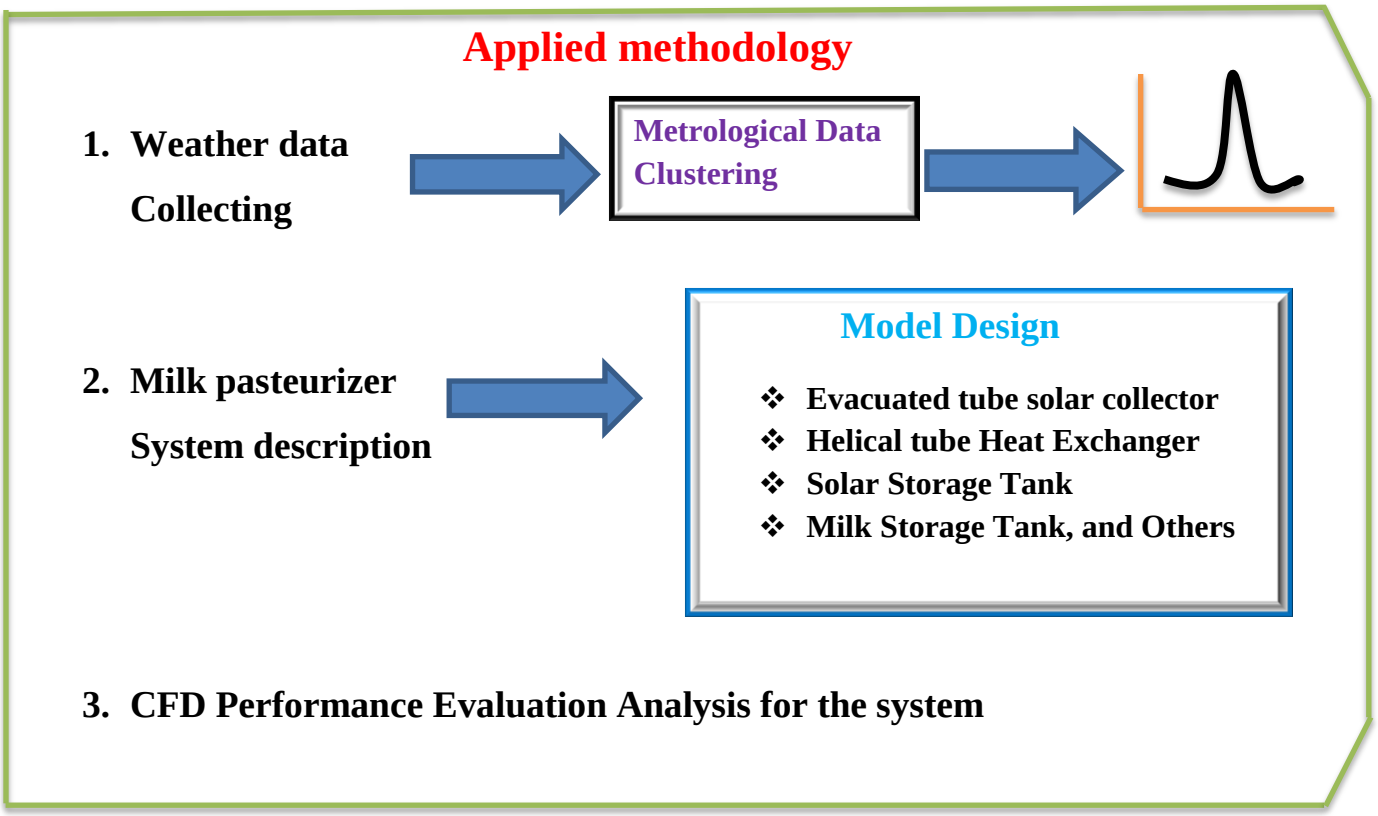

Figure 3.1: Methodology applied for the underlying study.

3.1.1. Data collection

This section refers to the first part of the applying methodology on my work, weather data gathering such as ambient temperature, sunshine hours and geographical site location, etc. Then, clustering the meteorological data to estimate the available solar radiation in KWh/m^2on a

horizontal surface, average monthly solar radiation on an inclined surface, and the useful energy gained by the collector for the study location.

3.1.2. System Description and Model Design

In this section, the milk pasteurizer working principle was described. Next, mathematical model design of main components such as solar thermal collector, helical tube heat exchanger sizing (in chapter four) and milk storage tank analysis is performed. Finally, CFD Performance Evaluation Analysis of the system.

3.2. Location of the study area

The study was conducted for off-grid per urban milk producer in Doyogena Woreda, fund in SNNNPR in Kambata Zone. The area was located at 7.3235°N, latitude, 37.7663°E, longitude, and an elevation of 2100m above sea level. The study area has a warm climatic zone. But we can not get recorded methorological data for steady area doyogena, we take the nearest area hosanna. The minimum and maximum monthly ambient temperature range between 10.38℃ to 28.04℃. However, the potential of solar energy in this location was high, but the precise information on global solar radiation on horizontal and inclined surfaces is not recorded previously.

3.3 Estimation of Solar Radiation

Solar thermal energy (STE) is a form of solar energy and technology to generate energy for use in the industry, as well as in the residential and commercial sectors. Solar radiation is a term used to describe the visible and almost visible rays (ultraviolet and infrared) emitted by the sun.

Solar radiation data is useful for any solar conversion device design and to determine the boundary of solar radiation at the specified location and the amount of energy available at various orientations of the collector.

(Duffie, et al., 2013) The most common measurements of solar radiation are total solar eclipses, commonly referred to as earth or global radiation. However, there are various ways to predict the amount of sunlight reaching the earth's surface in a given area. Efforts have been made to develop strong radioactive relationships from weather data: temperature, humidity, an hour of sunlight, clouds, and rain, which are it is easy to measure and is available in many places.

3.3.1 Global Solar Radiation

Global radiation is the perfect rays of short waves from the sky that fall to the horizontal surface of the earth. It includes direct sunlight and radiation from bright or scattered sunlight.

The most widely used combination of daily solar eclipses is proposed by (Angstrom , 924),, which has found a correlation between the average daily solar radiation at the corresponding day value of the exact$\frac{H}{H_c}$ area and the average daily solar radiation for a possible long daylight period.

The equation is given by:

$$\frac{H}{H_c} = a+b\left(\frac{S}{S_d}\right) \quad (3.1)$$

(Prescott , 1940)and the others have modified the method to base it on extraterrestrial radiation on a horizontal surface rather than on clear day radiation and therefore proposed the following relation:

$$\frac{H}{H_o} = a+b\left(\frac{S}{S_d}\right) \quad (3.2)$$

In addition, a and b are regression coefficients that depend on the location and are expressed as a function of latitude and sunshine hours respectively as follows.

3.3.1.1 Regression coefficients

$$a = -0.309 + 0.539\cos\emptyset - 0.0693*Z + 0.290\frac{S}{S_d} \quad (3.3)$$

$$b = 1.449 - 0.553\cos\emptyset - 0.694\frac{S}{S_d} \quad (3.4)$$

Where: H = global solar radiation on a horizontal surface (KWh/m^2)

Ho = extraterrestrial solar radiation on a horizontal surface (KWh/m^2)

S = sunshine hour of the day

S_d = maximum possible sunshine duration

Z = elevation above sea level (2100m)

$\emptyset$ = latitude of the location (7.3235°)

3.3.1.2 Sunshine Duration

The maximum possible sunshine duration S_d was calculated using the following equation [5]:

$$S_d = \frac{2}{15}W_s \quad (3.5)$$

3.3.1.3 Sunset Hour Angle

The angle of the W_s , is the minimum distance between the viewer meridian and the meridian whose plane contains the sun.

Can be calculated by using equation (3.6) and the values for each month of the year are tabulated in Table 3.1 for the study location.

$W_s = \cos^{-1}(-tan(\emptyset)tan(\delta))$ (3.6)

Where, –180° $< W_s <$ 0° at sunrise and 0° $< W_s <$ +180° at sunset.

$\emptyset$ — The latitude of a specified location on earth in degrees

δ-The Sun declination angle on a specified day in degrees

3.3.1.4 Declination angle (δ)

The descent or declination is a small distance from the sun in the north or south to the equator. As shown in the scheme in Figure 3.2, the maximum and minimum declination angles of the earth's rotation indicate the seasons. Declination distances between 23.45◦ north and 23.45◦ south.

The Declination varies between -23.45°≤δ≤23.45°, and is positive during summer and negative during winter.

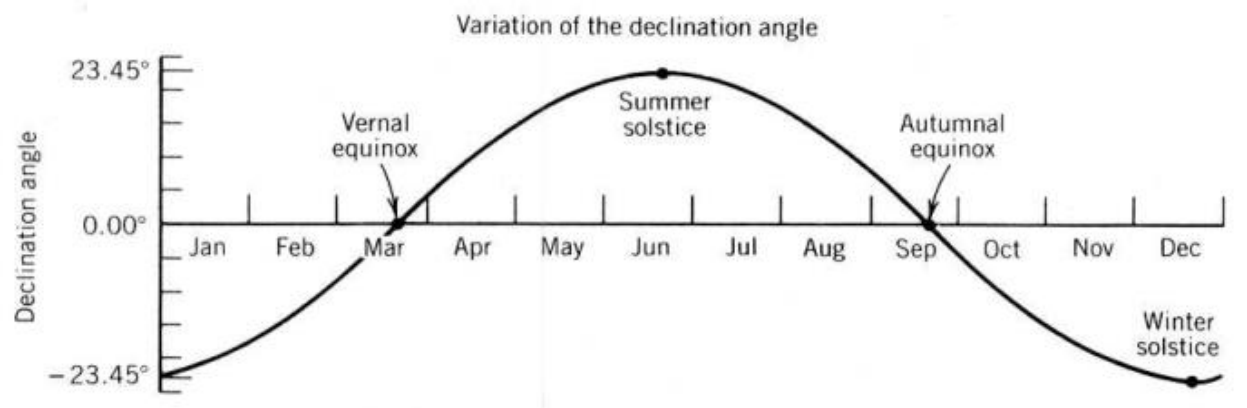

Figure 3.2: Variation of declination angle [powerfromthesun.net]

Its value in degrees for n, the average number of the days in the month (Table 3.2) is given by Cooper's equation:

$\delta = 23.45°[\frac{N+284}{365} * 360°]$ (3.7)

Where, N is the day number of the year, with January 1 equal to 1.

3.3.1.5 Solar Azimuth Angle (γ)

Angular migration from south of the beam radiation level in a horizontal plane is defined as the angle of the solar azimuth. This is schematically illustrated in Figure 3.3.

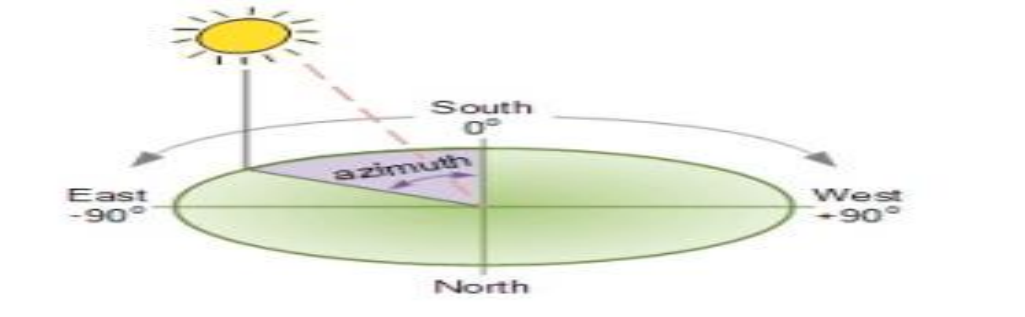

Figure 3.3: Definition of sun's azimuth angle

3.3.1.6 Latitude (∅)

As shown in above figure 3.3, the latitude of an area is the position with relevance north or south of the Equator. The variance of the latitude is from 0° to ±90° (positive for northern and negative for the southern hemisphere), 0°at the Equator and ±90°at the Poles.

Table 3.1: Sunset hour angle of the location

Sunset hour angle (W_s)											
Jan	Feb	Mar	Apr	May	June	July	Aug	Sep	Oct	Nov	Dec
87.09	88.31	89.76	91.31	92.62	93.27	92.98	91.88	90.41	88.86	87.48	86.76

Table 3.2: Day numbers and standard mean day of the month

Months	n for ith Day of Month	For the Average Day of the Month		
		Date	Day of Year(n)	Declination (δ)
January	i	17	17	-20.77°
February	31+i	16	47	-12.39°
March	59+i	16	75	-1.81°
April	90+i	15	105	9.71°
May	120+i	15	135	18.83°
June	151+i	11	162	23.07°
July	181+i	17	198	21.22°
August	212+i	16	228	13.29°

September	243+i	15	258	3.09°
October	273+i	15	288	-8.45°
November	304+i	14	318	-18.18°
December	334+i	10	344	-22.9°

3.3.1.7 Solar constant (G_{sc})

The solar constant(G_{sc}), with the energy from the sun per unit found in the area of the earth unit directly oriented to the direction of radiation in a straight line with the sun outside the atmosphere.

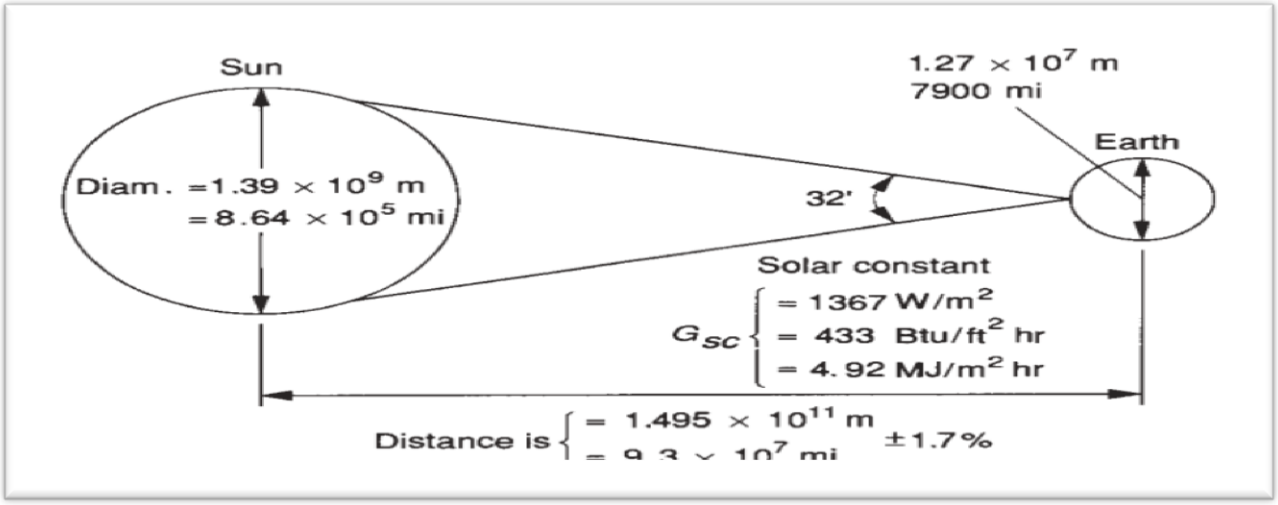

Figure 3.4: Sun-earth relationships[researchgate.net]

3.3.2.Extraterrestrial Radiation on a Horizontal plane

Extra-terrestrial radiation H_o [W/m^2] is the radiation incident on the surface tangent to the outer surface of the atmosphere. Expressed by the following equations by (Duffie, et al., 2013):

$$H_o = G_{sc}\frac{24}{\pi}\left[1+0.033\cos\frac{360*N}{365}\right]\left[\frac{\pi W_s}{180}\sin\emptyset\sin\delta+\cos\emptyset\cos\delta\cos W_s\right] \quad (3.8)$$

$$H_o = G_{0n}\frac{24}{\pi}\left[\frac{\pi W_s}{180}\sin\emptyset\sin\delta+\cos\emptyset\cos\delta\cos W_s\right] \quad (3.9)$$

$$G_{0n} = G_{sc}\left[1+0.033\cos\frac{360*N}{365}\right] \quad (3.10)$$

Where:

G_{0n}- Extraterrestrial radiation measured on the plane normal to the radiation on the nth day of the year (W/m^2).

N- Is the day of the year

0 - the subscript denotes zero air mass (AM_0) and

n – The subscript indicates that the radiation is on a plane normal to the Sun-Earth axis.

Metrological data that collected from selected location for the period 2015 to 2018 : Latitude 7.3235° N, Longitude 37.7663° E and Elivation 2100m above sea level.

Table 3.3: Metrological data that collected from selected location

Month	S(h)	S_d(h)	$\frac{S}{S_d}$	T_{max}(℃)	T_{min}(℃)	H(KWh/m^2)	H_o(KWh/m^2)	$\frac{H}{H_o}$
Jan	9.64	11.61	0.83	29.70	6.98	6. 28	10.72	0.5858
Feb	9.71	11.78	0.82	31.41	9.12	6. 42	10.46	0.6137
Mar	9.62	11.97	0.80	32.54	11.61	6.52	10.05	0.6487
Apr	9.47	12.18	0.78	31.55	12.54	5.95	9.4	0.6287
May	9.41	12.35	0.76	29.17	12.64	5.62	8.09	0.6946
Jun	9.46	12.44	0.76	25.99	12.49	5.09	7.32	0.6953
July	9.57	12.4	0.77	24. 25	12.09	4.51	6.4	0.7047
Aug	9.54	12.25	0.78	24. 29	11.02	4.79	7.1	0.6760
Sep	9.39	12.06	0.78	25.52	11.53	5.52	7.91	0.6977
Oct	9.24	11.85	0.78	26.82	10.09	6.14	10.32	0.5949
Nov	9.21	11.66	0.79	27.12	7.16	5.91	9.97	0.5928
Dec	9.35	11.57	0.80	28.14	7.36	6.19	10.72	0.5774

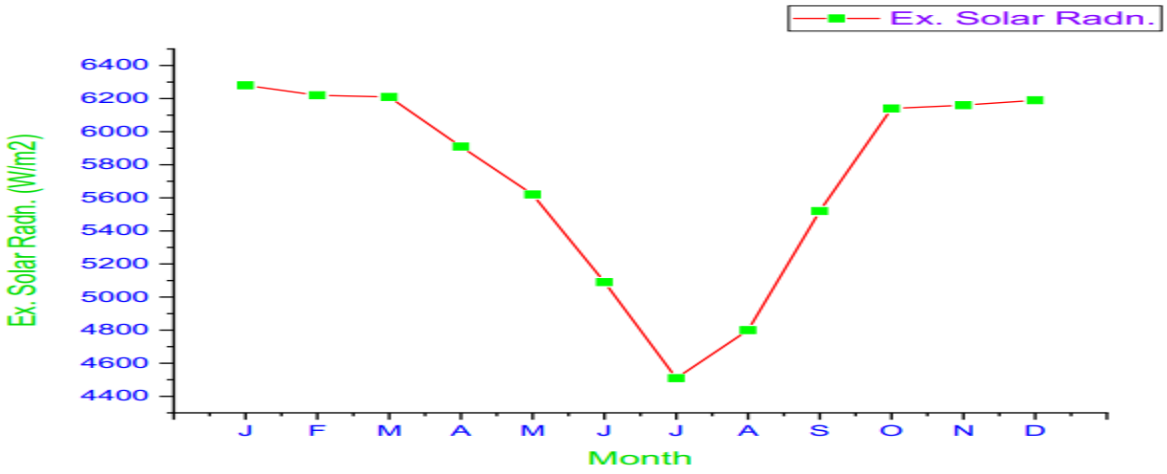

Figure 3.5: Variation of extraterrestrial solar radiation with a month of year

Figure 3.6: Indicates the annual average global or earth solar radiation on the horizontal surface in KWh/m^2, by using sunshine hours, declination angle, and location coordinate data from Ethiopia National Metrology Agency (ENME) for the period 2015 to 2018.

As seen in the figure below the global or earth solar radiation on the horizontal surface is around 0.36 KWh/m^2, which mean that the annual average solar radiation intensity of the location reaches its maximum value 360Wh/m^2 attained at solar noon between 4 hrs to 9 hrs.

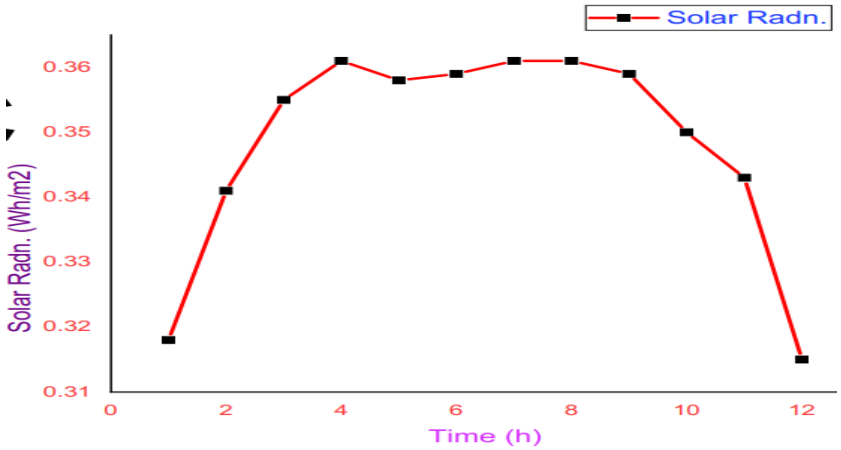

Figure 3.6: Annual Solar Radiation, Doyogena, Ethiopia

3.3.3 Diffuse and Beam Radiation

Beam Radiation Gb, the sun's rays reach the ground without a change in direction.

Diffuse Radiation Gd, the sun's rays reach the ground after a change in the direction of particles in the atmosphere.

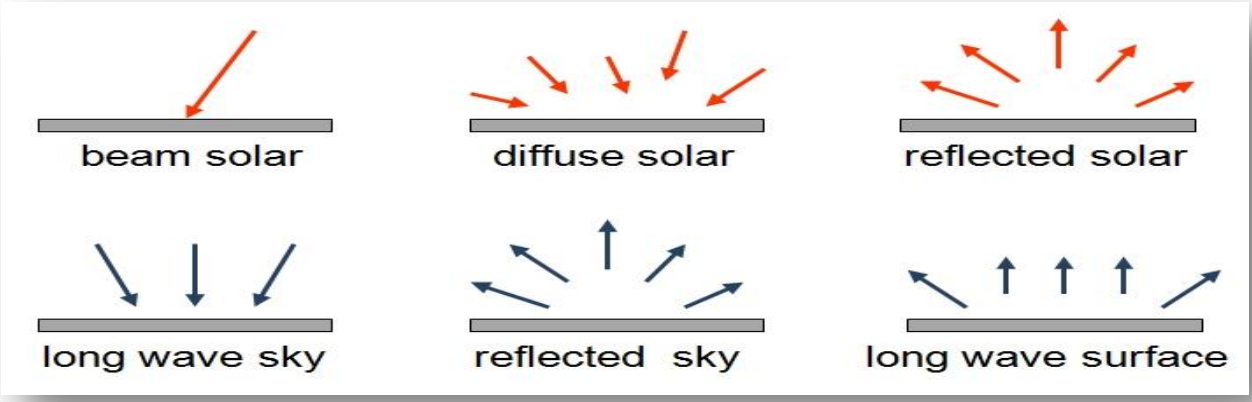

Figure 3.7: Indication of Beam, Diffuse and Other Solar Radiation [e-education.psu.edu]

3.3.4 The computing of Hourly Beam and Diffuse Radiation on a horizontal surface

In these sections, we review methods for estimation of the fractions of total horizontal radiation that are diffuse and beam. To correlate I_d /I, the fraction of the hourly radiation on a

the horizontal plane which is diffuse, with K_T , the hourly clearness index, for (Erbs, et al., 1982).

$$\frac{I_d}{I} = \begin{cases} 1.0 - 0.09K_T & \text{for } K_T \leq 0.22 \\ 0.9511 - 0.1604K_T + 4.388K_T^{\,2} - 16.638K_T^{\,3} + 12.336K_T^{\,4} & \text{for } 0.22 < K_T \leq 0.80 \\ 0.165 & \text{For } K_T > 0.8 \end{cases} \quad (3.11)$$

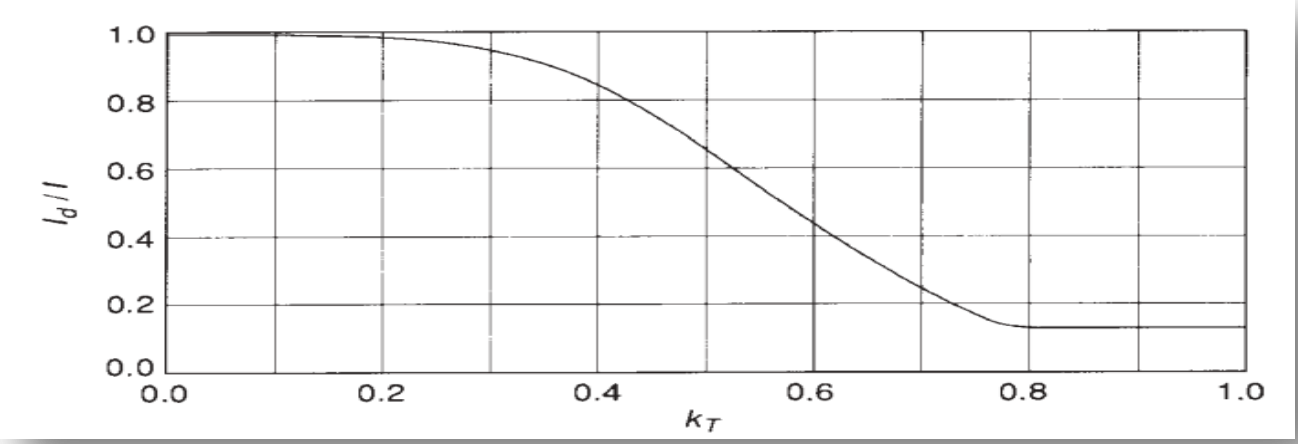

Figure 3.8: The ratio $\frac{I_d}{I}$, as a function of hourly clearness indexK_T (Erbs, et al., 1982).

3.3.5 The computing of Daily Diffuse and Beam Radiation on a horizontal surface

From Table 3.1, the sunset hour angleW_s, is greater than 81.4° because of that the clearness index (K_T) which is the ratio of a particular day's radiation to the extraterrestrial radiation for that day is expressed with Equation (3.8) (Duffie, et al., 2013).

$$K_T = \frac{Daily\ total\ radiation}{Daily\ Extraterrestrial} = \frac{H}{H_o} \quad (3.12)$$

3.3.5.1 Daily Diffuse Radiation (H_d)

For the sunset hour angle greater than 81.4° and $0.3 \leq K_T \leq 0.8$

$$\frac{H_d}{H} = 1.0 - 0.2832K_T - 25557K_T^{\,2} + 0.8448K_T^{\,3} \quad (3.13)$$

$$H_d = H\,[1.0 - 0.2832K_T - 25557K_T^{\,2} + 0.8448K_T^{\,3}] \quad (3.14)$$

3.3.5.2 Daily Beam Radiation (H_b)

Calculated from the total daily solar radiation as follows:

3.3.5.3 Total daily solar radiation (H)

H= H_b + H_d (3.15)

H_b = H - H_d (3.16)

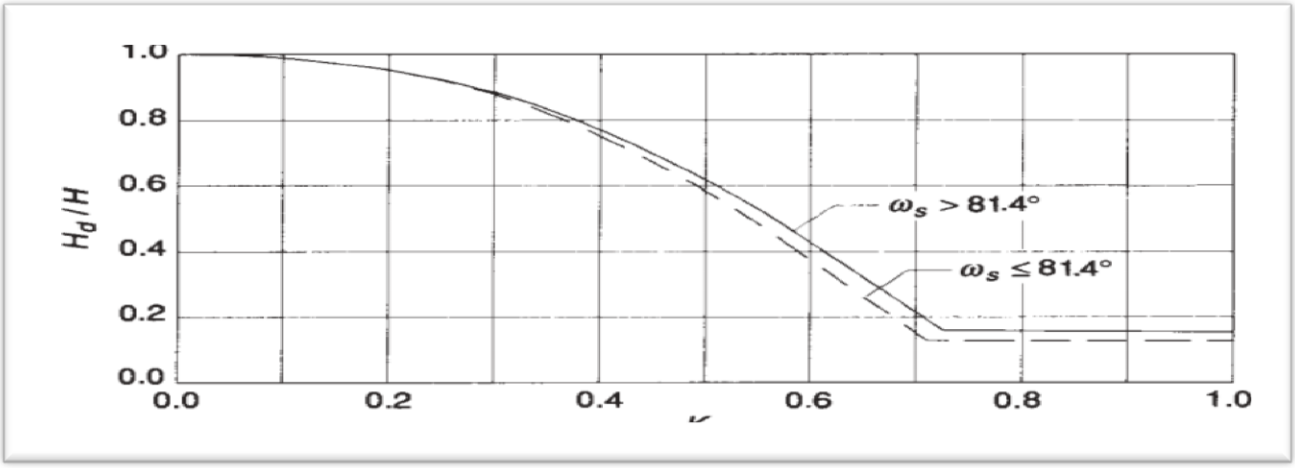

Figure 3.9: Suggested correlation of daily diffuse fraction with K_T. From (Erbs, et al., 1982).

3.3.6 Estimation of Hourly Global Radiation from Daily Data

Estimation of hourly radiation from daily data on horizontal surfaces r_t is the ratio of hourly total to daily total radiation, as a function of day length and the hour in applying the following equations.

$$r_t = \frac{Hourly\ total\ Radiation}{Daily\ total\ radiation} = \frac{I}{H} \quad (3.17)$$

Where: r_t are represented by the following equations from (Collares – Pereira, et al., 1979a)

$$r_t = \frac{\pi}{24}(a + b\cos\omega)\frac{cos\omega - cosw_s}{sinw_s - \frac{\pi w_s}{180}cosw_s} \quad (3.18)$$

Where: ω is the hour angle in degrees expressed by equation (3.21) and w_s is the sunset hour angle.

The coefficients a and b is given by the following equations:

a= 0.409+0.5016sin (w_s - 60) (3.19)

b= 0.6609 – 0.4767sin (w_s - 60) (3.20)

3.3.6.1 Hour Angle (ω)

The hour angle is expressed by the following equation:

ω = (ST- 12) * 15 (3.21)

Where: **ST** is local solar time

3.3.7 Estimation of Hourly Diffuse Radiation

The estimation of the hourly average diffuse radiation from the ratio of hourly diffuse I_d, to daily diffuse radiation H_d, as a function of hour angle and day length. Then apply the following equations:

$$r_d = \frac{Hourly\ Diffuse\ Radiation}{Daily\ Diffuse\ Radiation} = \frac{I_d}{H_d} \quad (3.22)$$

According to Liu and Jordan (1960), apply the following equation:

$$r_d = \frac{\pi}{24}\left(\frac{cos\omega - cosw_s}{sinw_s - \frac{\pi w_s}{180}cosw_s}\right) \quad (3.23)$$

Where: ω is the hour angle in degrees expressed by equation 3.21 and w_s is the sunset hour angle.

3.3.8 Total Solar Radiation on Tilted Solar Collector

In practice, the solar collectors are installed tilted for better energy collection.

The solar radiation falling on a tilted surface will be the sum of:

- Direct or Beam Radiation
- Diffuse Radiation and
- Reflected Radiation

It will be given by (Chetan)

$$I_T = I_b\, r_b + I_d r_d + (I_b + I_d)\, \rho_g r_r \quad (3.24)$$

Where,I_b, I_d and I_r are the instantaneous values of the beam, diffuse, and reflected radiations, respectively. Andr_b, r_d and r_r are the tilt factor for the beam, diffuse, and reflected radiations, respectively. And ρ_g is the reflection coefficient of the ground equal to 0.6.

3.3.8.1 Instantaneous global horizontal radiation (I_g)

$$I_g = I_b + I_d \quad (3.25)$$

3.3.8.2 Direct or Beam Radiation Factor (r_b)

The ratio of the direct solar radiation falling on a tilted surface to that falling on a horizontal surface is called the tilt factor r_b for the beam or direct radiation in equation e. The r_b for the collector surface facing south (γ=0˚) expressed by (Chetan).

$$r_b = \frac{cos\theta_i}{cos\theta_Z} = \frac{sin\delta sin(\emptyset - \beta) + cos\delta cos(\emptyset - \beta) cos\omega}{sin\delta sin\emptyset + cos\delta cos\emptyset cos\omega} \quad (3.26)$$

Similarly, the r_b can be written for a situation where the collection is not facing the south direction, i.e., γ ≠0˚. The beam radiation falling on a tilted surface will be given by$I_b * r_b$, where I_b is the instantaneous value of beam radiation.

3.3.8.3 The angle of Incidence (θ_i)

It is the angle between the beam radiation on a surface and normal to that surface and in the simplified form given by the following equation (Adisu, et al., 2013).

$\text{Cos}\theta_i$ = (Cos$\emptyset cos\beta + sin\emptyset sin\,\beta cos\gamma$) Cos$\delta$ cosω + cosδ sinωsinβsinγ

+ Sinδ (sin$\emptyset$cosβ - cos$\emptyset$ sinβ cosγ) (3.27)

3.3.8.4 Zenith Angle (θ_Z)

The angle between the vertical and the line to the sun, that is, the angle of incidence of beam radiation on a horizontal surface.

$\text{Cos}\theta_Z$ = cos$\emptyset$ cosδ cosω + sin$\emptyset$ sinδ (3.28)

Where, $0 \leq \theta_Z \leq 90°$

3.3.8.5. Diffuse Radiation Factor (r_d)

M.Chikh 1* al. et, stated that the diffuse part of solar radiation is one of the elements necessary for the design and evaluation of energy production of a solar system. And tilt factor for the diffuse radiation $\boldsymbol{r_d}$ is defined as the ratio of the radiation flux falling on the tilted surface to the diffuse radiation falling on the horizontal surface.

The $\boldsymbol{r_d}$ can be written as (M, 2012).

$$r_d = \frac{1+cos\beta}{2} \quad (3.29)$$

3.3.8.6. Reflected Radiation (r_r)

The reflected radiation from the ground and surrounding area can also reach the collector with a tilted surface. The tilt factor for the reflected radiation $\boldsymbol{r_r}$ is given by the following equation (Erbs, et al., 1982)

$$r_r = \rho \frac{1-cos\beta}{2} \quad (3.30)$$

Where ρ is the reflectivity of the surrounding in which the collector is located. Normally, a value of about 0.2 is taken for the reflectivity of grass or concrete. And β is the tilt angle between the plane of the surface and the horizontal.

3.3.8.7 Tilt angle

(Hafez, et al., 2017) States, the optional tilt angle β is calculated by adding 15 degrees to your latitude during winter and subtracting 15 degrees from your latitude during summer.

$\beta = (\emptyset + 15°)$, during winter and (3.31)

$\beta = (\emptyset - 15°)$, during summer (3.32)

Suppose as you have seen Figure 3.2, the solar time of the location is moreover at 1:30 PM or 13:30h,

Therefore, using Equation (3.31) hour angle of the study location and the tilted angle are calculated as follows:

ST from figure 3.2, ST = 13.5

ω = (ST- 12) * 15 = (13.5- 12)$*$ 15 = 22.5

Latitude of the location is $\emptyset$ = 7.3235°

Then tilt angle, β = latitude + 15° = (7.3235° +15°) = 22.3235° $\approx$ 22.3°

Rewriting total solar radiation on an inclined surface in terms of the global radiation (H), beam radiation factor (r_b), diffuse radiation (H_d), and ground reflectivity factor (ρ) as follows (Adisu, et al., 2013).

$I_T = r_b$(H-H_d) +0.5(1+cosβ)H_d +0.5ρ(1- cosβ)H (3.33)

3.4 Estimation of Hourly Ambient Temperature

The performance measure of solar thermal energy is highly dependent on air temperature.

(Parton WJ, et al.) References; a subroutine of the temperature that divides the day into two parts and uses a reduced sine wave during the day and a warming effect at night. Day and night lengths are calculated as DY activity (day of the year) and width. Assume that T_{max} occurs at noon just before sunset and that T_{min} appears a few hours at sunrise. Hour temperatures are given the following statistics

3.4.1 For daylight hours

T (H) = (T_{MAX} -T_{MIN}) sin ($\frac{\pi m}{y+2a}$) + T_{MIN} (3.34)

3.4.2 For night-time hours

T (H) = T_{MIN} + ($T_{sunset} - T_{MIN}$) exp (-$\frac{bn}{z}$) (3.35)

Where T (H) is the temperature at any hour of the day or night period determined from m and n.

y= day length (h)

z= night length (h)

T_{sunset} = temperature at sunset (°C)

m= numbers of hours between the time of T_{MIN} and sunset (h)

n= number of hours from sunset to the time of T_{MIN} (h)

a= lag coefficient for T_{MAX} =1.80 (h)

b= night-time temperature coefficient = 2.20

c= lag time T_{MIN} from time of sunrise = 0.88(h)

The coefficients a, b and c may vary slightly as a function of height and location and be found by parameter optimization for the 1.5-m height (Parton WJ, et al.).

3.5 Model system description for applied methodology

The constructed system consists of four main components; solar concentrator, raw milk tank, helical tube heat exchanger, and heat absorber, shown in the figure. 3.12

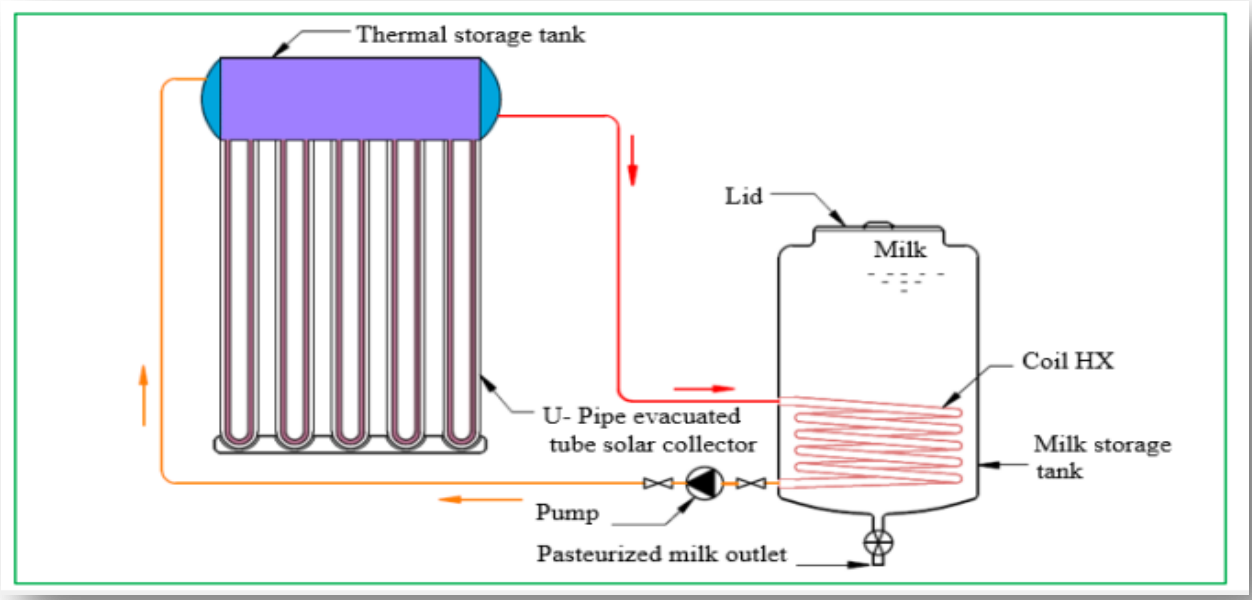

Figure 3.10: Diagram of the constructed system for milk pasteurization by solar energy

In this work, the process of milk pasteurization by solar energy can be partitioned into two separated loops; one of both is a closed-loop system for water heating, the other one is an open-loop system for milk heating. The two loops become in contact inside the helical tube heat exchanger as shown in Figure (3.11).

The cylindrical milk storage tank has a 120-liter milk holding capacity and is well insulated to avoid heat loss to the surrounding.

The evacuated solar collector was inclined at 28.1°, it reflects and concentrates the sun rays on the absorber where transforms it into heat energy, then the heat transfers to the water which slowly flows in the copper serpentine. The water is heated up and flows out to the heat exchanger where the hot water heats the cold milk fluid in storage tank. The resulting water is returned to the absorber for more heating up, and so on. The water flow rate is regulated with valves and a flow meter.

Once the water temperature in the heat exchanger approaches 90 ˚C, the valve is fully opened to let the milk flow from into the inside tube of the heat exchanger. The milk absorbs the heat released by the hot water. When the milk temperature reaches the desired pasteurization temperature of 72 ˚C, a solenoid valve opens to let the milk out to the cooling unit, then use it for different purposes. The solenoid valve is controlled by a temperature controller which senses the temperature of milk in the heat exchanger.

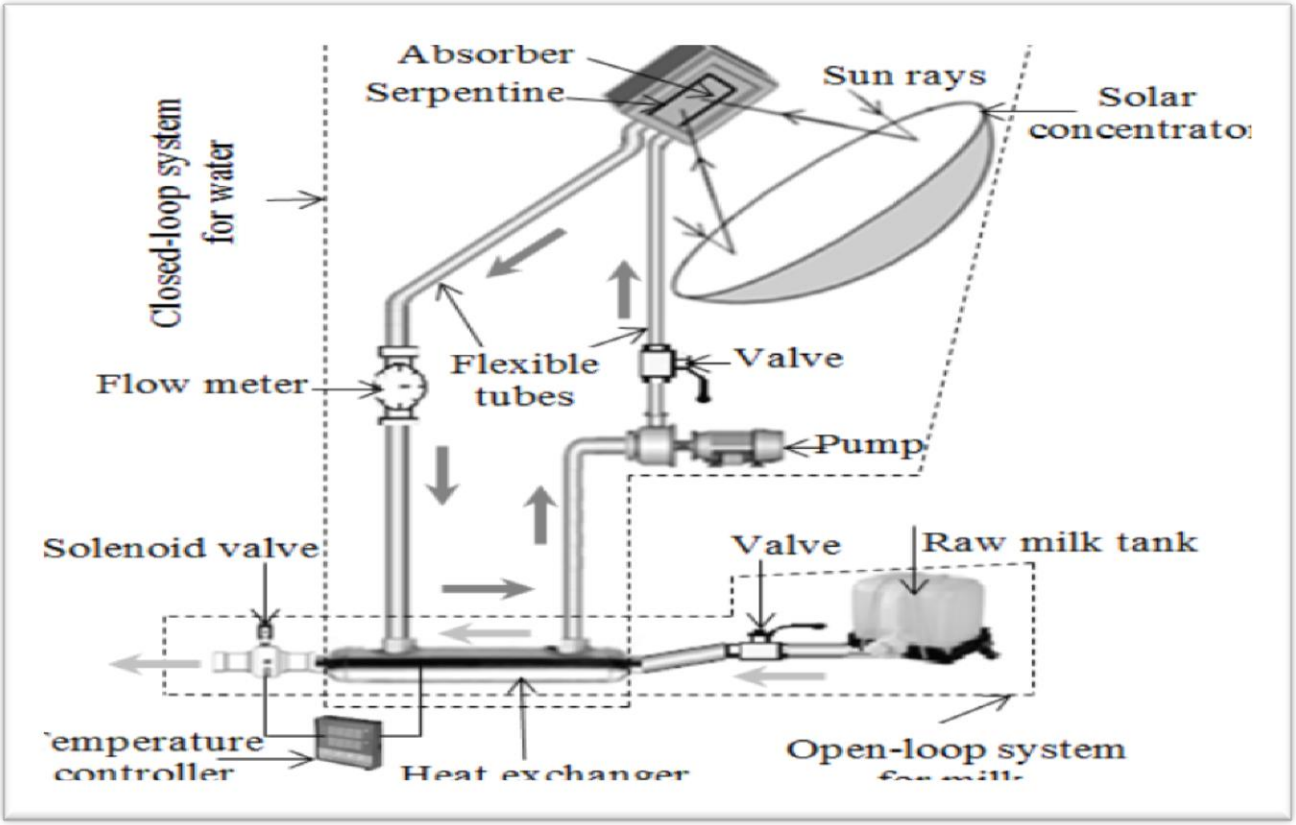

Figure 3.11: Schematic of milk pasteurization by solar energy.

Next, we will discuss mathematical model design and thermal analysis of some components like an evacuated solar collector, helical tube heat exchanger, and milk storage tanks. And performance evaluation with CFD of helical tube heat exchanger and milk storage tank.

3.6 Mathematical Model of an Evacuated Tube Solar Collector milk pasteurization system

A tube that comes out with a solar collector is a device often used to deliver heat to several inputs such as water temperature, air conditioning, etc. This collector can achieve a higher temperature range of above 120 °C, (Harding GL, et al., 1985) due to their combining effects of highly selective surface coating and vacuum insulation.

Many investigators are investigating; the evacuated tube solar collector provides much higher thermal performance than flat plate solar collectors in a different position to accomplish the milking process of pasteurization.

ETCs receiver consists of a copper U-tube inside a glass vacuumed tube. The copper tube is surrounded by a cylindrical aluminum fin pressed on it. This fin enhances the heat transfer area between the inner glass absorber surface and the U-tube. The active fluid enters the collection pipe, is then distributed evenly into the U-tubes, absorbs heat, and, finally, returns to the exhaust pipe. The outer cylindrical glass transmits radiation to the inner glass tube, which transmits energy to the end of the absorber. The energy converted into heat is driven by the fin to a copper U-tube and eventually absorbs the active fluid, which is milk in this case.

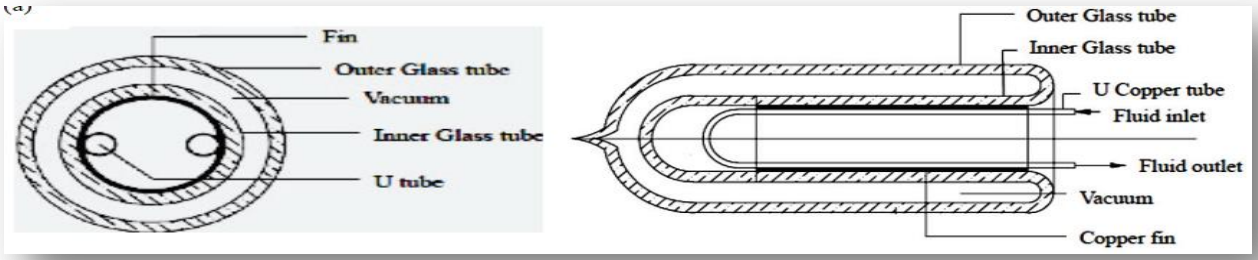

Figure 3.12: Schematic of cross-section and illustration U-type ETSC [link.springer.com]

The following assumptions are made to simplify the analysis:

- ✓ The process of heat transfer is steady.
- ✓ Solar intensity at the collector surface is constant throughout the collector.

- ✓ The specific heat of working fluids remains constant concerning the temperature encountered in the system.
- ✓ The axial mode of heat transfer is negligible.
- ✓ Convective heat transfer between the inner surface of the inner glass tube and the air gap is negligible.
- ✓ Heat loss between the copper tube and the inner glass tube is negligible.
- ✓ Ambient air temperature is from metrology agency
- ✓ The thermos physical properties are constant and the thermal mass is negligible owing to the thin walls of the glass tube, the aluminum fins, and the copper tube.

3.6.1 Governing Equations of the Solar Collector

For predicting the behavior of solar collector at any time step, a thermal network is formed for calculating the heat transforms in any direction of the tube from the solar collector differential equation (Paraene, et al., 2005). Figure 3.13, shows a schematic of heat transfer mechanism in an evacuated solar collector from the absorber tube to glass envelope and from envelope to surroundings and in that of fluid temperature is considered as a function of x. Figure 3.14, gives the mode of the thermal network associated with the heat transfer process of the collector.

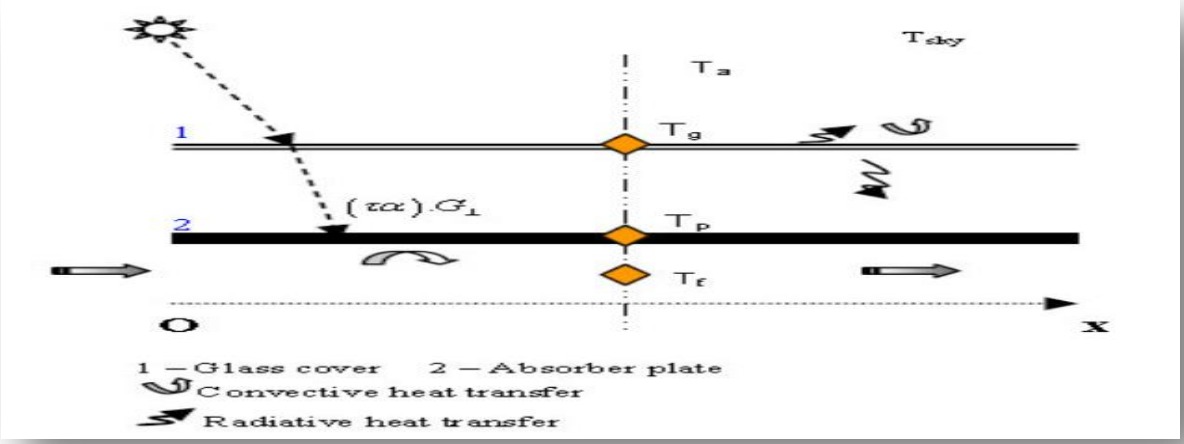

Figure 3.13: General description of the collector model (Jean, 2005).

The governing differential equations for determining the glass temperature,T_g the absorber plate temperature, T_p and the fluid temperature, T_f at any time t steps are as follows: (Siva Kumara, et al., 2017).

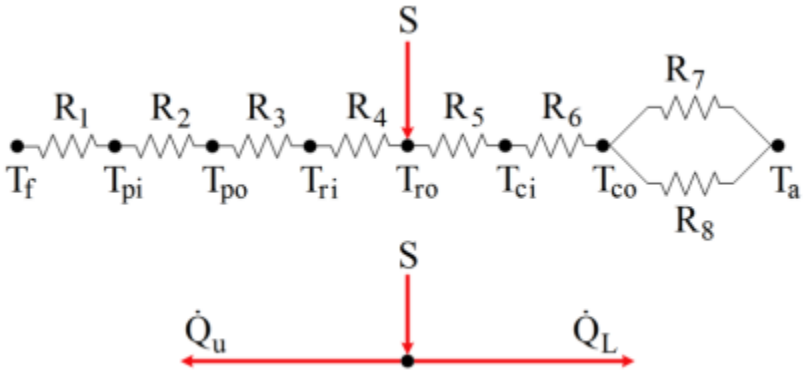

Figure 3.14: Thermal Networks of U type Evacuated tube solar collector (Jean, 2005).

3.6.2 Temperature distribution in different sections

3.6.2.1 The equation for Glass Temperature

$$c_g \frac{\partial T_g}{\partial t} = \varepsilon_g \sigma(T^4{}_{sky} - T^4{}_g) + h_{g-a}(T_a - T_g) + \varepsilon_g \sigma(T^4{}_p - T^4{}_g) \quad (3.36)$$

Where: $T_{sky} = 0.055 T^{1.5}{}_a$

3.6.2.2 The equation for Plate Temperature

$$c_p \frac{\partial T_p}{\partial t} = \tau \alpha I_T + \varepsilon_g \sigma(T^4{}_g - T^4{}_p) + h_{f-p}(T_f - T_p) \quad (3.37)$$

3.6.2.3 The equation for Fluid Temperature

$$c_f \left(\frac{\partial T_f}{\partial t} + u\frac{\partial T_f}{\partial x}\right) = h_{f-p}(T_p - T_f) \quad (3.38)$$

Where,

c_g =heat capacity of glass cover (KJ/m^2K)

C_p = heat capacity of absorber (KJ/m^2K)

ε_g =emissivity of the glass cover

σ = Stefan-Boltzmann constant ($5.64*10^{-8} W.m^{-2}.K^{-4}$)

α = absorptive coefficient

I_T = Global solar irradiance in the plane of the collector (KW/m^2)

h_{g-a} = heat transfer coefficient glass cover-ambient (KW/m^2K)

h_{f-p} = heat transfer coefficient fluid-absorber (KW/m^2K)

T_{sky} = temperature of the sky (℃)

T_g = temperature of glass cover (℃)

T_a = ambient temperature (℃)

3.6.3 Formulation of heat transfer coefficient in different sections

- To examine the radiation heat transfer coefficient between the outer glass tube and the sky, the following equation was formulated by (Kalogiroun SA, 2009).

$$h_{r.co-sky} = \varepsilon_c \sigma (T_{co} + T_{sky})\,(T^2{}_{co} + T^2{}_{sky}) \quad (3.39)$$

Where: σ = Stefan- Boltzmann constant [W.$m^{-2}k^{-4}$]

ε_c = emittance of the glass cover

T_{co} = temperature of the outer glass cover

T_{sky} = sky temperature

The sky temperature can be determined from the following equation below (Patel, et al., 2016).

$$T_{sky} = 0.055 T_a{}^{1.5} \quad (3.40)$$

Where, T_a is the environment temperature in kelvin

Absorber tube temperature,T_A is taken as the average of inlet and outlet fluid temperature

$$T_A = T_m = \frac{T_{fi}+T_{fo}}{2} \quad (3.41)$$

The outer cover of glass temperature, T_{co}

$$T_{co} = T_A - U_L \left(\frac{T_A - T_a}{h_{r.co-sky}}\right) \quad (3.42)$$

Forced convection heat transfer coefficient on the outer tube by the wind, h_{co-sky}

For $0 \leq V_w \leq 5\, m/s$

$$h_{co-sky} = 5.7 + 3.8 V_w \quad (3.43)$$

Where: V_w is ambient air velocity in m/s

- Convection heat transfer coefficient between the outer glass tube and the environment, then the equation given by:

$$h_{c,co-a} = \frac{Nu_a k_a}{D_{co}} \quad (3.44)$$

Where, k_a = thermal conductivity of air $[W/mK]$

Nu_a = Nusselt number of air

D_{co}= outer glass diameter

In the equation (3.44)

Nu_a = 0.4+0.54$Re^{0.52}$ for 0.1<Re<1000 (3.45)

Nu_a = 0.3$Re^{0.6}$ for 1000<Re<50000 (3.46)

Where: Re is the Reynolds number

- The conduction heat transfer coefficient through the outer glass tube is expressed as (Zekai Sen, 2008).

$$h_{d,co-ci} = \frac{k_c}{r_{ci} ln(\frac{r_{co}}{r_{ci}})} \quad (3.47)$$

Where: k_c = thermal conductivity of glass cover

r_{ci} = radius of the inner glass cover

r_{co} = radius of the outer glass cover

Since the place between the inner and outer glass tubes is evacuated, the convection heat transfer is assumed to be zero. Thus, heat transfer occurs only by radiation.

- The radiation heat transfer coefficient between the absorber surface and the outer glass tube is defined as (Incropera FP, et al., 2007).

$$h_{r,ro-ci} = \frac{\delta}{\frac{1}{\varepsilon_r} + \frac{r_{ro}}{r_{co}}(\frac{1}{\varepsilon_c} - 1)} (T_{ro} + T_{ci})(T^2{}_{ro} + T^2{}_{ci}) \quad (3.48)$$

Were: ε_r = emissivity of the selective absorber coating

ε_c = emissivity of the glass cover

Subscripts i and o stand for inner and outer glass tubes.

3.6.3.1 Heat transfer coefficients for inner tubes

- Conduction heat transfer through the absorber wall can be expressed as

$$h_{d,ro-ri} = \frac{k_r}{r_{ri} ln(\frac{r_{ro}}{r_{ri}})} \quad (3.49)$$

Where k_r is the thermal conductivity of absorber coating

- The conduction heat transfer through the aluminum fin. The following equation is given by (Incropera FP, et al., 2007).

$$h_{d,ri-b} = \frac{k_b}{\delta_b} \quad (3.50)$$

Where: k_b = thermal conductivity of Al-fin

δ_b = thickness of U-tube (δ_b= 1mm)

3.6.4 Overall heat loss coefficients of the ETSCs

The overall heat loss coefficients of ETSCs (U_L) are expressed as the summation of top loss coefficients and edge loss coefficients, the equation is given as follows (Aboulmagd, et al., 2014).

$$U_L = U_{TOP} + U_{EDGE} \quad (3.51)$$

$U_L = U_{TOP}$, because the edge loss coefficient was neglected due to the assumption of proper heat insulation at the edges of the solar collector.

Therefore, the top loss coefficient from the absorber tube to the ambient U_{TOP} can be expressed as:

$$U_L = U_{TOP} = [\frac{r_{co}}{h_{r,ro-ci}r_{ro}} + \frac{r_{co}}{h_{d,ci-co}r_{ci}} + \frac{1}{h_{c,co-a}+h_{r,co-sky}}]^{-1} \quad (3.52)$$

Also, the heat loss of the evacuated U-tube can be expressed as:

$$U_L\,(T_{ro} - T_a) = h_{c,co-a}\,(T_{co} - T_a) + h_{r,co-sky}\,(T_{co} - T_{sky}) \quad (3.53)$$

Absorber temperature,T_{ro} can be easily calculated iteratively by using equation [3.53].

- The overall heat transfer coefficients from the environment (U_O) to the fluid inside the U-tube is calculated by using the following equations:

$$U_O = [\frac{1}{U_L} + \frac{r_{co}}{h_{d,ro-ri}r_{ro}} + \frac{r_{co}}{h_{d,pipe}r_{ro}} + \frac{r_{co}}{h_{fi}r_{pipe}}]^{-1} \quad (3.54)$$

3.6.5 Useful collected solar energy

The amount of energy needed to increase the temperature of the active liquid or the energy used is equal to the amount of energy a solar collector can absorb. The amount of energy used per day the collector transferred to the liquid is expressed as follows (Allouhia, et al., 2017).

$$\dot{Q_U} = \dot{m}c_p * (T_{out} - T_{in}) \quad (3.55)$$

In terms of collector heat removal factor (F_R) and the overall heat loss coefficients (U_L), the useful collected rate of solar energy ($\dot{Q_U}$) expressed by the following equations:

$$\dot{Q_U} = F_R A_c * [S\text{-}U_L\,(T_A - T_a)] \quad (3.56)$$

$$S = I_T\,(\tau\alpha) \quad (3.57)$$

$$A_c = D_c * L \quad (3.58)$$

Where: S= solar irradiance

F_R = collector heat removal factor

A_c = collector area

T_{in} And T_{out} = inlet and outlet temperature of the working fluid

T_A = absorber tube temperature

T_a = ambient temperature

I_T = total solar radiation of tilted solar collector

$\tau\alpha$ = the transmittance-absorbance product

D_c = is the mean diameter of the glass envelope and L is the length of tubes.

- The heat removal factor (F_R), is described by (Kalogiroun SA, 2009).

$$F_R = \frac{\dot{m}c_p}{A_c U_L}[1\text{-}\exp(\frac{-A_c U_L F'}{\dot{m}c_p})] \quad (3.59)$$

Where: F'= the collector efficiency factor and defined as, F'= $\frac{U_O}{U_L}$

$\dot{m}$ = mass flow rate of water

c_p = heat capacity of water

3.6.6 Absorbed solar energy

The summed solar energy received by absorber plate in ETSCs is given by the following equation [(Paraene, et al., 2005)][(Rodriguez, et al., 2017)]:

$$\dot{Q_{abs}} = (\tau\alpha)\, I_T A_c \quad (3.60)$$

3.6.6 Collector efficiency

The thermal efficiency test of the solar collector removed or evacuated tube solar collector is calculated using the efficiency of the collector (η) Ref (Rodriguez-Hidgalo MC, et al., 2012). It is defined as the amount of heat detection net for the active fluid in a solar product in the collector and the collector area (A_c).

$$\eta = \frac{\dot{Q_U}}{A_c I_T} = \frac{\dot{m}c_p(T_{out}-T_{in})}{A_c I_T} = \frac{\dot{m}c_p(T_{out}-T_{in})}{SA_c} \quad (3.61)$$

Collector efficiency was also calculated using the following equations [3.62]

$$\eta=\eta_o\text{-}a_1(\frac{T_{avg}-T_a)}{S}\text{-}a_2(\frac{T_{avg}-T_a}{S})^2 \quad (3.62)$$

$$T_{avg}=\frac{T_{in}+T_{out}}{2} \quad (3.63)$$

Where: η_o is collector optical efficiency, attained from the manufacturer's data sheet or official test report, $a_1$and a_2 are the thermal loss parameters. Technical specifications of the solar thermal collectors are listed in Table: 3.3.

Table 3.4: Technical Specifications of the Solar Thermal Collector

Parameter	Value	Unit
η_o	0.64	[-]
a_1	1.25	$[W/m^2\,k]$
a_2	0.009	$[W/m^2k^2]$

3.6.7 Solar Thermal Collector Heat Balance Equations

The thermal model description of heat balance equations analysis for each part of evacuated tube solar collector, based on Ref. [(Gao, et al., 2014)-(Ghoneim A, et al., 2017)]expressed below as follows:

3.6.7.1 Outer Glass Tube

$$h_{in-out}P_{in-out}\,(T_{in}-T_{out})+h_{out-a}P_{out}\,(T_a-T_{out})=0 \quad (3.64)$$

Here, $h_{in-out}=h_{r,in-out}+h_{d,in-out}$ (3.65)

$$h_{out-a}=h_{r,out-a}+h_{c,out-a} \quad 3.66)$$

$$P_{in-out}=\left(\frac{P_{in}+P_{out}}{2}\right) \quad (3.67)$$

Where:

$T_{in} and T_{out}$ = inner and outer glass tube temperature

T_a = ambient temperature

h_{in-out} = heat transfer coefficient between the inner and outer glass tube

h_{out-a} = heat transfer coefficient between the outer glass tube and ambient environment.

$h_{r,in-out}\ and\ h_{d,in-out}$ = radiation and conduction heat transfer coefficients between inner and outer glass tubes, and $h_{d,in-out}$ is treated as zero.

$h_{r,out-a}+h_{c,out-a}$ = radiation and convection heat transfer coefficients between the outer glass tube and ambient temperatures, $h_{c,out-a}$ is a function of the wind velocity.

$P_{in}\ and\ P_{out}$ = perimeters of the inner and outer glass tubes

However, heat conduction can be overlooked due to the very thin layer of vacuum the space between the inner and outer tubes, where the vacuum level is 10^{-4}Pa and the heat conduction coefficient is less than $0.27*10^{-5}$W/m℃

3.6.7.2 Inner Glass Tube

$$h_{in-out}P_{in-out}\ (T_{out} - T_{in}) + h_{in-Al}\ (T_{Al} - T_{in}) + Q_{edge} + \tau_{og}\alpha_i D_o S = 0 \quad (3.68)$$

Here, $h_{in-Al} = h_{r,in-Al} + h_{d,in-Al}$ (3.69)

$$Q_{edge} = h_{in-a}P_{in}\ (T_a - T_{in}) \quad (3.70)$$

$$P_{in-Al} = \left(\frac{P_{in}+P_{Al}}{2}\right) \quad (3.71)$$

Where:

T_{Al} = perimeter of aluminum fin

h_{in-Al} = total heat transfer coefficient between the inner glass tube and aluminum fin.

$h_{r,in-Al}\ and\ h_{d,in-Al}$ = radiation and conduction heat transfer coefficient between the inner glass tube and aluminum fin.

τ_{og} = transmission coefficient of the outer glass tube.

α_i = absorption coefficient of the selective coating on the inner glass tube

D_o = diameter of the outer glass tube

S = total solar irradiance of the collector aperture surface

P_{Al} = perimeter of aluminum fin

Q_{edge} =heat loss of the tube edge to the manifold

h_{in-a} = tube edge heat loss coefficient of the collector approximately equal to $0.61 W/m^2$ K.

3.6.7.3 Aluminum fin

$$h_{in-Al}\ (T_{in} - T_{Al}) + h_{Al-cu}P_{cu}\ (T_{cu} + T_{Al}) = 0 \quad (3.72)$$

$$h_{Al-cu} = h_{r,Al-cu} + h_{d,Al-cu} \quad (3.73)$$

Here; $h_{in-Al} = \frac{k_{Al}}{\delta_t}$ (3.74)

Where:

k_{Al} and δ_t= thermal conductivity coefficients Al-fin and the thickness of U-tube

T_{cu} = temperature of U copper pipe

P_{cu} = perimeter of the copper pipe

h_{Al-cu} = total heat transfer coefficients between the aluminum fin and U copper pipe

$h_{r,Al-cu} + h_{d,Al-cu}$= radiation and conduction of heat transfer coefficients between aluminum fin and U copper pipe respectively.

3.6.7.4 U-Pipe Copper

$h_{Al-cu}P_{cu}\ (T_{Al} - T_{cu}) + h_f P_{cu}\ (T_f - T_{cu}) = 0$ (3.75)

Where: h_f = fluid convective heat transfer coefficient inside the U copper pipe and its coefficient are variable with the flow velocity.

3.6.7.5 Working fluid

$h_f P_{cu}\ (T_{cu} - T_f) * X + \dot{m} c_p\ (T_{wfi} - T_{wfo}) = 0$ (3.74)

Where,

$T_{wfi}\ and\ T_{wfo}$ = inlet and outlet temperatures of working fluid in the U copper pipe

X = the interval of the fluid along the tube axis

$\dot{m}\ and\ c_p$ = mass flow rate and specific heat capacity of the working fluid.

Each heat transfer coefficient value is given in Table C-1.

3.6.7 Technical Specification of Evacuated Tube Solar Collector

Table: 3.4: Shows the surface and dimensions of ETSCs, two glass tubes made of very strong Borosilicate glass. The transparent outer tubes allow light rays to pass through with a small reflection and the inner tube is coated with a specially selected fabric (Al-Nickel / Al), which is an excellent source for absorbing sunlight and small reflective features (Aboulmagd, et al., 2014).

Table 3.5: The surface properties and dimensions of evacuated tube solar collector

S.No.	Parameters	Symbols	Units	Values
1	Gross area of collector	A_c	m^2	2.42
2	The total area of the absorber tube	A_{at}	m^2	1.21
3	Thermal conductivity of the glass	K_g	$W/m.K$	1.21
4	Thermal conductivity of the air	K_a	$W/m.K$	0.03
5	Thermal conductivity of the fin	K_f	$W/m.K$	307
6	Outer glass tube transmittance	τ	-	0.81
7	Inner glass tube inner surface emissivity	ε	-	0.8

8	Selective surface properties of the inner tube	α	-	0.92
9	Diameter of the outer glass tube	D_o	m	0.047
10	The thickness of the outer glass tube	δ_o	m	0.0012
11	Diameter of the inner glass tube	D_i	m	0.037
12	The thickness of the inner glass tube	δ_i	m	0.00012
13	Collector tube length	L_{ct}	m	1.5
14	Tube spacing	s_t	m	0.001
15	Fin thickness	δ_f	m	0.0006
16	Working fluid (water)	c_p	$kJ/kg.K$	4.2
17	Number of tubes			5

3.6.8 Energy Storage in Solar Thermal Process Systems

Energy storage may be in the form of the sensible heat of a liquid or solid medium, as the heat of fusion in chemical systems, or as chemical energy of products in a reversible chemical reaction. The choice of storage media depends on the nature of the process. For water heating, energy storage as sensible heat of stored water is logical. If air heating collectors are used, storage in sensible or latent heat effects in particulate storage units is indicated, such as sensible heat in a pebble bed heat exchanger. In passive heating, storage is provided as sensible heat in building elements. If photovoltaic or photochemical processes are used, storage is in the form of chemical energy.

The major characteristics of a thermal energy storage system are:

- It is capacity per unit volume
- The temperature range over which it operates, that is, the temperature at which heat is applied to and removed from the system
- Easy to add or remove heat and the corresponding temperature variations
- Temperature stratification in the storage unit
- Energy requirements to add or remove heat
- Containers, tanks, or other structural elements associated with the storage system
- Ways to control heat loss from the storage system as well
- Its cost.

The most important thing in any storage system is those things that affect the solar collector's performance. The useful profit for the collector decreases according to its size as the temperature plate increases. The relationship between collector temperature and the temperature at which the heat is delivered can be recorded as:

T (collector) – T (delivery) = ΔT(transport from collector to storage) + ΔT(in to storage) + ΔT(storage loss) + ΔT(out of storage) + ΔT(transport from storage to application) + ΔT(in to application) (3.75)

Thus, the temperature of the collector, which determines the useful gain for the collector, is higher than the temperature at which the heat is finally used by the sum of a series of temperature difference driving forces.

3.6.9.1. Water storage

(Lavan Z, et al., 1977) stated that, for many solar systems water is the ideal material in which to store usable heat. Energy is added to and removed from this type of storage unit by transport of the storage medium itself, thus eliminating the temperature drop between transport fluid and storage medium.

The energy storage capacity of water (or other fluid) storage unit at a uniform temperature (i.e., fully mixed, or unstratified) operating over a finite temperature difference is given by (Lavan Z, et al., 1977):

$$Q_s = (mc_p)_s \Delta T_s = (mc_p)_s (T_{wo} - T_{wi}) \quad (3.76)$$

Where $Q_s$the total heat capacity is for a cycle operating through the temperature range ΔT_s and m is the mass of water in the unit.

The temperature range over which such a unit can operate is limited at the lower extreme for most applications by the requirements of the process. The upper limit may be determined by the process, the vapor pressure of the liquid, or the collector heat loss.

An energy balance on the fully mixed or, unstratified tank shown in Figure 3.15 is

$$(mc_p)_s \frac{dT_s}{dt} = Q_u - \dot{L_s} - Q_{loss,thermal} \quad (3.77)$$

$$m = \rho V_s \quad (3.78)$$

$$Q_{loss,thermal} = (UA)_s (T_s - T_a') \quad (3.79)$$

$$(\rho V_s c_p)_s \frac{dT_s}{dt} = Q_u - \dot{L_s} - (UA)_s (T_s - T_a') \quad (3.80)$$

Where, Q_u and $\dot{L_s}$ = are rates of addition or removal of energy from the collector and to the load.

$T_a{}'$ = is the ambient temperature for the tank, in kelvin

T_s = instantaneous tank temperature, in kelvin

U = overall heat transfer coefficient

A = area of the tank, in m^2

c_p = specific heat transfer coefficient of water, $J/kg.K$

ρ = density of water

V_s = volume water in the storage tank, m^3

CHAPTER FOUR

HELICAL TUBE HEAT EXCHANGER DESIGN

4.1. INTRODUCTION

This section focuses on the design of a helical tube heat exchanger, based on numerical process and the application of a logarithmic mean temperature difference method and parameter determination of the coil size. Next, performance tests of the helical tube heat exchanger using CFD, and using the basic heat transfer that controls the equations are also improved to produce the temperature of the pasteurized milk.

In a hot exchange of shell and a simple tube, heat is transferred from one liquid to another active fluid without informal contact with the partition walls while in the coil heating elements, there is a disturbance due to the coiled helix. This fluid in the liquid causes an air coil to vibrate. However, this vibration is not sufficient for low velocity (mass flow rate).

The helical tube heat exchanger machine design contains design calculations that combine material strength, durability, durability, etc., and the operating conditions in which the system will be installed. In a helical tube heat exchanger, the energy required for an object in the system is an important factor. Therefore, the power to consider the design of the geometry and the size of the object.

4.2. Coil tube Heat Exchanger sizing

Figure: 4.1 shows a cross-sectional schematic drawing of the milk storage tank, which consists of an immersed coil tube heat exchanger placed at the bottom of the tank and fitted on the lateral wall of the tank. The cross-sectional cut way views of helical tube heat exchange dimensional parameters are also shown in Figure: 4.2.

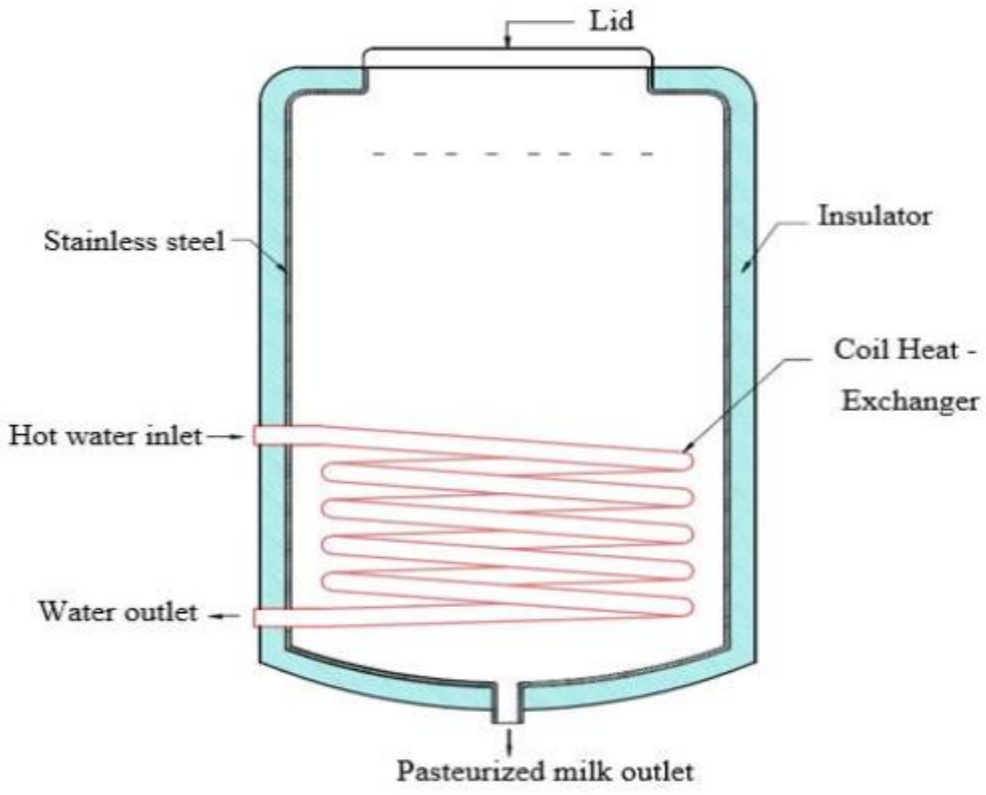

Figure 4.1: Cross-sectional view of milk Storage tank

4.2.1. Analysis of Coil tube Heat Transfer Area

Considering very important input parameters for designing the helical tube heat exchangers. First of all, to calculate the heat transfer area of the coil tube, A_{coil} by applying the equation (4.1). To use equation (4.1), let assume the maximum inlet and outlet or return water temperature of the water from the coil tube to be 80.5℃ and 73℃ respectively, and the inlet and the final temperature of the milk in the storage are 32 ℃and 69℃ respectively as used by (Verechshagin, et al., 2016).

The thermal output of the collector (hot water exits from the collector), transferred through helical tube heat exchanger can be calculated and expressed based on equation (4.1) (Cuiping, et al., 2007).

$Q_{th} = \eta * (A_c Q_{sun})$ (4.1)

Where, η= thermal efficiency of the collector, 51%

A_c = Gross area of the collector, 2.42m^2 (From table 3.4)

Q_{sun} = the quantity of heat obtained by the collector for every square meter, and its nominal value is equal to $798 W/m^2$

From equation (4.1), we get

$$Q_{th} = 0.51 * 2.42 * 798$$
$$= 984.9 W$$

The amount of heat transferred through the coil tube heat exchanger to the raw milk obtained in terms of change of mean temperature difference is as follows:

$$Q_{th} = A_{coil} \varepsilon U_o \frac{\Delta T_m}{C_r} \quad (4.2)$$

$$\Delta T_m = T_{avg,cw} - T_{avg,m} \quad (4.3)$$

Were,

ΔT_m = the difference between the average temperature of circulating water inside the coil, $T_{avg,cw}$ and the average temperature of milk in the tank, $T_{avg,m}$.

ε = the coefficient of furring, which results as an uneven distribution of thermal media effect the efficiency of the heat transfer coefficient, 0.6 to 0.8 normally used 0.7.

C_r = the heat loss coefficient, 1.1 to 1.2

The water comes from some sources with the help of water pump and inter in to collector absorber and the water temperature heated up to 80.5℃ in absorber and after that heated water goes to haet exchanging media , but energy loss by convection heat transfer to ambient and the hot water temperature inlet to the helical tube heat exchanger are 70℃ to 78℃.

$$T_{avg,cw} = \frac{T_{cw,f} + T_{rw,o}}{2} = \frac{80.5+73}{2} = 76.75℃$$

4.2.1a. Milk properties

The properties of milk like density, thermal conductivity, specific heat, and viscosity varies with varies the temperature values. From refering different literature reviews the density of raw milk depends on its composition.

Table4.1: Milk properties varies with temperature

Temperature (℃)	Specific heat (J/kg.K)	Density (kg/m^3)	Themal conductivity (W/m.K)	Viscosity (Pa.s.)
10	3881	1031.146	0.5532	0.0009025
20	3897.8	1028.1	0.5665	0.000858
30	3914.6	1024.562	0.5798	0.0008135
40	3931.4	1020.532	0.5931	0.000769

50	3948.2	1016.01	0.6064	0.0007245
60	3965	1010.996	0.6197	0.00068
70	3981.8	1005.49	0.6330	0.0006355
80	3998.6	999.492	0.6463	0.000591
90	4015.4	993.002	0.6596	0.0005465
100	4032.2	886.02	0.6729	0.000502

The properties of whole milk is found the temperature between 30℃ and 40℃ from refering the literature reviews.

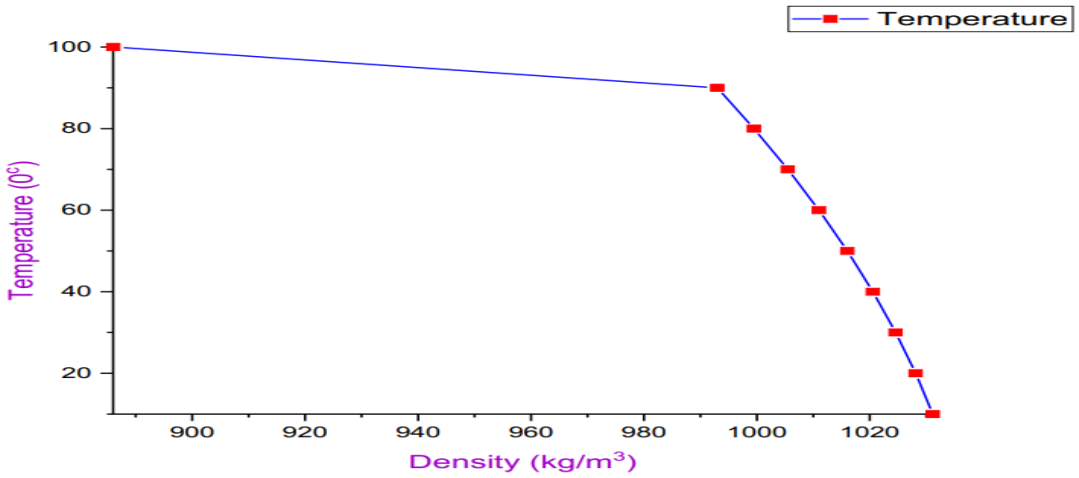

Figure4.2: Effects of temperature on density of milk

The above figure shows the temperature increases the density of milk decreases and visversa.

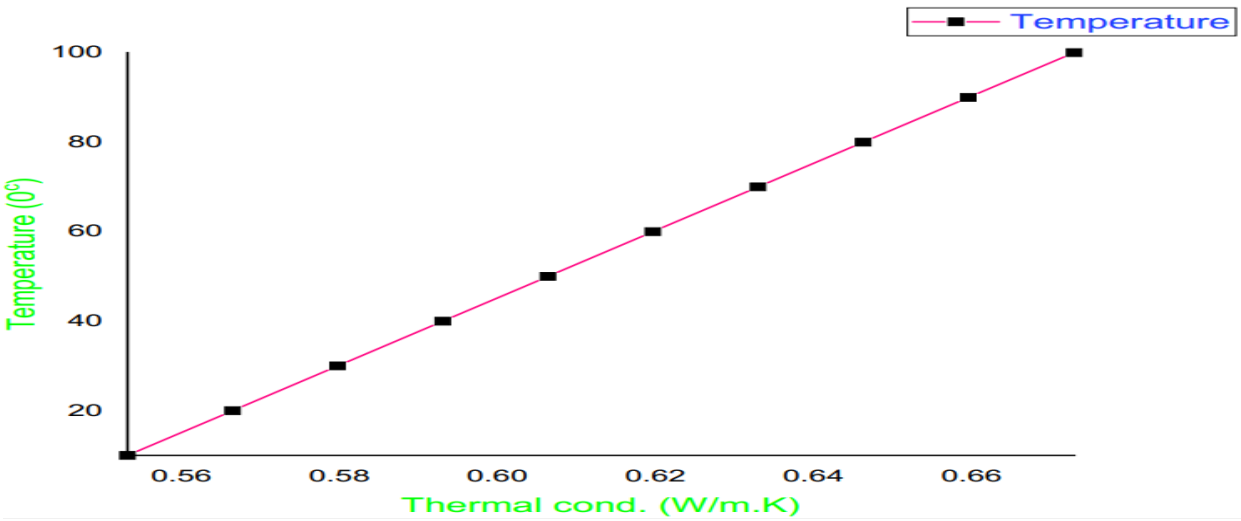

Figure4.3: Temperature versus thermal conductivity of milk

Figure **a** shows the temperature and thermal conductity is directly proportional i.e, the temperature increses the thermal conductivity of milk increases.

$T_{avg,m} = \frac{T_{m,i}+T_{m,f}}{2} = \frac{32+69}{2} = 50.5℃$

Then, ΔT_m = 80.5℃ - 50. 5℃ = 30 ℃

The overall heat transfer coefficient for helical tube heat exchangers was between 200 to 500 $W/m^2℃$ (Sinnott, et Al., 2005). Suppose the overall heat transfer of this kind of heat exchanger to be (460$W/m^2℃$, nominal value) then we can calculate the required heat transfer area of the helical tube heat exchanger by applying the following equation.

Take the value of C_r = 1.1

$$A_{coil} = \frac{C_r Q_{th}}{\varepsilon U_O \Delta T_m} \quad (4.4)$$

$$A_{coil} = \frac{1.1*984.9}{0.8*460*36.5} = \frac{1083.39}{11040} = 0.098m^2$$

4.2.2 Diameter of Stainless-Steel pipe

In our case for helical tube, the tubes are made of stainless steel. The reason for using stainless steel is due to its increased thermal conductivity in addition to the stability and firmness provided to the structure. It is also resistant to corrosion, chemical damage, and heat damage.

Instead of large diameter pipes, using small diameter pipes because will provide a high heat transfer area. For helical tube heat exchanger nominal outer diameter is 8.96 ≈ 9mm and inner diameter is 7mm, and thickness is 1.24mm commercially available copper tube was selected.

d_o = 8.96 ≈9mm

d_i=7mm

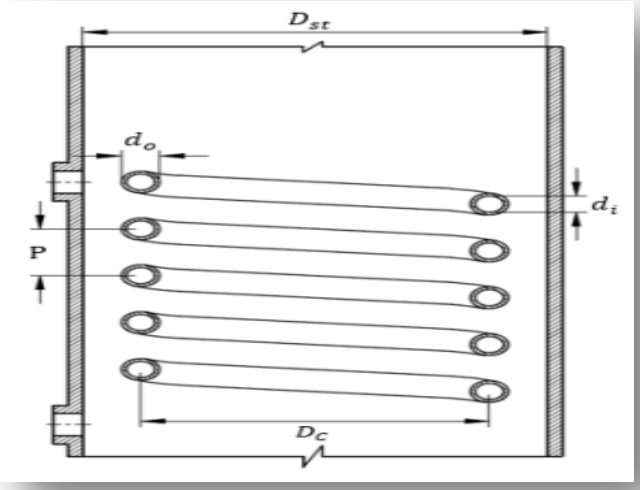

Figure 4.4: Schematic cut-away view of a helical tube heat exchanger

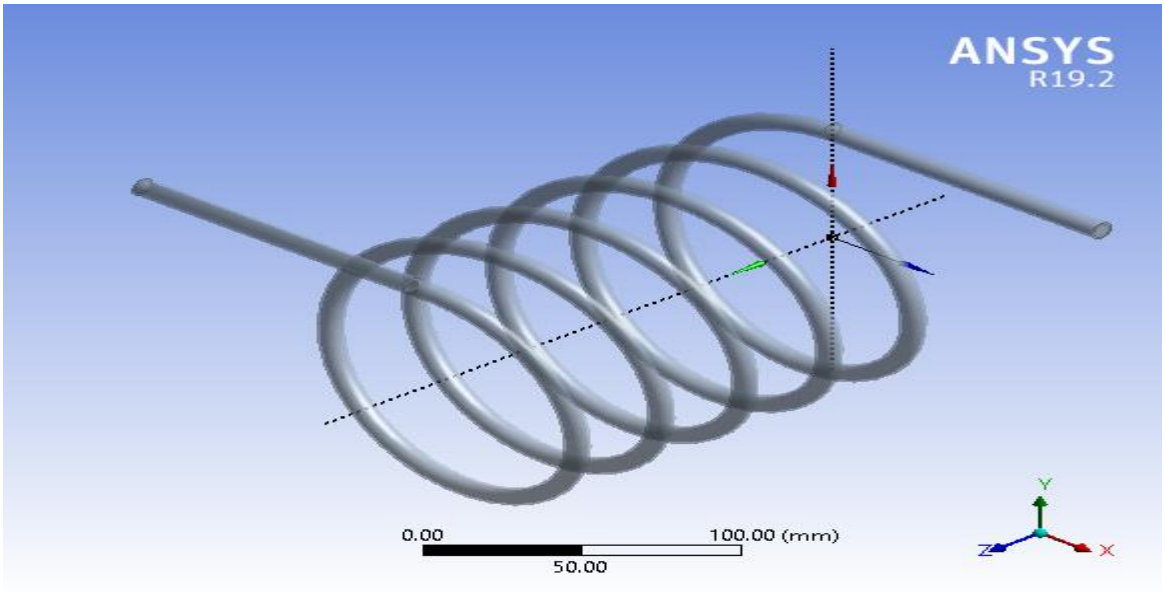

Fig 4.5: Helical tube heat exchanger geometry by ANSYS

4.2.3 Pitch of the coil tube

To calculate the coil tube of pitch applying the following equation,

$p = 1.5 d_o$ (4.5)

Substitute the value of d_o in the above equation,

p= 1.5*0.009m = 0.0135m ≈ 0.014m

4.2.4 Required Length of Stainless-Steel Tube

The required length of coil tube for one turn can be easily calculated by the formula given by:

$L_{1,turn} = p + \sqrt{(2\pi r)^2}$ (4.6)

Where p is the pitch of the coil tube and r is the radius of the helix

Table 4.2: Inside and Outside diameter of the cylinder

Parameters	Values in meter
Inside diameter of cylinder (D_c)	0.127 m
The outside diameter of the cylinder (D_{st})	0.2286m

The average diameter of helix = $D_h = \frac{D_c + D_{st}}{2} = \frac{0.127 + 0.2286}{2} = 0.1778$m

Average radius of helix is calculated as:

Average radius of helix = $r = \frac{D_h}{2} = \frac{0.1778}{2} = 0.0889$m

Inside Diameter of helix:

$D_{h1} = D_h - d_o = 0.1778 - 0.009 = 0.1688$ m

Outside Diameter of helix:

$D_{h2} = D_h + d_o = 0.1778 + 0.009 = 0.1868$ m

Then, substitute the value of r in equation (45), to simply calculate $L_{1,turn}$

$L_{1,turn} = 0.014 + \sqrt{(2 * \pi * 0.0889)^2} = 0.573$m

Approximately the length of coil tube for one turn is 0.6m

4.2.5 The total length of the coil tube

Apply the following formula to calculate the required total length of coil tube:

$$L_{coil} = \frac{A_{coil}}{\pi d_o} \quad (4.7)$$

$L_{coil} = \frac{0.098}{\pi * 0.009} = \frac{0.098}{0.0283} = 3.18$m

Approximately the total length of coil tube needed to make several turns was 3.0m.

4.2.6 Number of coils tube turn

Increases heat transfer performance with a growing number of coils turning.

The number of coils turning on the terminal, N_{coil} coil processes the coil tube length and pitch as provided by (Purandare, et al., 2015) obtained using Equation (4.8).

$$N_{coil} = \frac{L_{coil}}{\sqrt{(\pi D_c)^2 + p^2}} \quad (4.8)$$

Substitute the known value of L_{coil}, D_c and p in equation 4.8 and then we can calculate the value ofN_{coil}:

$N_{coil} = \frac{3.0}{\sqrt{(\pi * 0.127)^2 + 0.014^2}} = 4.95$

However, the actual number of coil tube turns needed N_{coil} is simply rounded to the next highest integer equal to 5 turns.

Note: Number of coil is directly proportional to length of coil, $N_{coil} \sim L_{coil}$. The axial length of helical tube increases, heat tranfer rate also increases. This information graphically described in

chapter five. From equation (4.15), heat transfer rate is directly proportional to heat transfer area and A ~ L_{coil}.

4.2.7 The volume occupied by on turn of the coil tube

$$V_{c,1turn} = \frac{\pi}{4} * {d_o}^2 * L_{1,turn} \quad (4.9)$$

Substitute the values,

$$V_{c,1turn} = \frac{\pi}{4} * (0.009)^2 * 0.573$$

$$= 3.645*10^{-5} m^3$$

4.2.8 The volume occupied by the whole turn of the coil tube

$$V_c = \frac{\pi}{4} * {d_o}^2 * L_{coil} \quad (4.10)$$

Substitute the known values,

$$V_c = \frac{\pi}{4} * (0.009)^2 * 3.0$$

$$= 1.91*10^{-4}\ m^3 = 0.191 \text{litre}$$

4.2.9 The volume of the Milk Storage Tank

Considering the volume occupied by the coil tube and assumes 0.12 m^3 (120 liter)the volume of milk in the tank, the volume of the milk storage tank is calculated by applying the following formula:

$$V_{st} = (V_c + 0.12)\ m^3 \quad (4.11)$$

$$= 1.91*10^{-4} + 0.12$$

$$= 0.12002 m^3 = 120.02 \text{ litre}$$

4.2.10 Diameter and Height of Milk Storage Tank

$0.12m^3$ the volume of milk is occupied in the vertical cylindrical tank shown in Figure 4.1. Let the space between D_{st} and D_c to be X = 50.8mm. The milk storage tank diameter and height is determined as follows:

4.2.10.1 Milk Storage tank Diameter

The value of storage diameter is already tabulated above, but for sure applies the following equation to calculate the storage internal diameter.

$$D_{st} = 2X + D_c \quad (4.12)$$

$$= 2(50.8) + 127 = 228.6\text{mm}$$

4.2.10.2 Height of storage

If you consider 10% more of the total volume and use the standard equation to calculate cylindrical tank volume and D_{st} input equation (4.12) to equation (4.13), the height of the milk storage tank H_s can be found as follows:

$$V_{st} = \frac{\pi D^2{}_{st}}{4} * H_s \quad (4.13)$$

From equation (4.13) we derive H_s,

$$H_s = \frac{4V_{st}}{\pi D^2{}_{st}} \quad (4.14)$$

Substitute the known values of V_{st} and D_{st} in equation (4.14),

$$H_s = \frac{4*(0.01+0.12002)}{\pi*(0.2286^2)} = \frac{0.13002}{0.1642} = 0.782\text{m} \approx 0.8\text{m}$$

Using the above information we can calculate the storage area

$$A_{st} = \frac{V_{st}}{H_s} = \frac{0.12002}{0.8} = 0.15m^2$$

4.3. Material selection of milk storage tank and its insulation

Dairy and food industries are concerned with the reliability of equipment and the purity of the product. This requires the use of cleanable, corrosion-resistant material. Due to the following reasons, stainless steel was recommended for milk storage tank construction.

The major characteristics of stainless steel that are widely used in food and dairy industries are (Dewangan, et al., 2015):

- Durability and corrosion resistance
- Ease for fabrication
- High heat resistance
- Flavor and color protection and clean ability
- Strength and ductility at ambient and service temperature
- Low total cost, including initial cost, installed cost, and the effective life expectancy of the finished product.

Heat losses from the milk storage tank are an irreversible process. Thus, thermal insulation is required to prevent heat losses from a milk storage tank. However, the warm insulator is a poor conductor of heat having low thermal conductivity, but, it does not eliminate heat transfer, it merely reduces it.

So, the optimum thickness of insulation to be installed was recommended based on minimum total cost as shown in figure D.2 (Sinnott, et al., 2005).

In table: C.3: Various thermal insulation material properties are listed. However, glass fiber insulation material is selected for the following reasons.

- Lower thermal conductivity properties
- Low cost per unit cost
- Higher temperature resistance
- Higher durability in the presence of moisture
- Higher resistance of water
- Cost-effective and steady in performance

4.4. Coil tube Heat Transfer Analysis

In the previous class, to analyze the size of helical tube heat exchanger parameters, the hot water temperature flow through the coil was assumed to be uniform. But it changes during the process of any instant of time. The milk pasteurizer tank is carefully insulated to minimize heat losses and such losses are assumed to be negligible.

4.4.1 Heat gain formulation through coil tube

The heat transfer rate can be used in conjunction with the LMTD method through the entire coil given as: (Incropera FP, et al., 2007).

$$\dot{Q} = UA_o\Delta T_{LMTD} \quad (4.15)$$

Equation (4.15) is used when simple or co-current flows exist. If the flows pattern is more complex (such as the case with most shell and tube heat exchangers), then a correction factor (F) term is used and the equations become:

$$\dot{Q} = UA_oF\Delta T_{LMTD} \quad (4.16)$$

Where, $\dot{Q}$ = Heat transfer rate

U = overall heat transfer coefficient

F = correction factor

A_o = outer surface area of the exchanger

ΔT_{LMTD} = change of logarithmic mean temperature difference

Depending on the complexity of the selected model, the required information in Figure (4.16) can vary from negative rating to electrically based calculation geometry.

4.4.2 Calculation of Overall Heat Transfer coefficient

The overall heat transfer coefficient indicates the ease with which heat relief from one medium to another. And described in terms of three thermal resistances and expressed as following [(Amitkumar, et al., 2015) (Mohapatra, et al., 2017)].

First, analyze the heat resistance due to movement and conduction

The thermal resistance of inside coil tube material due to convection

$$R_{in,convcn.} = \frac{1}{h_i A_i} \tag{4.17}$$

Thermal resistance through coil tube material due to conduction

$$R_{condcn.} = \frac{ln\frac{d_o}{d_i}}{2\pi L_{coil} K_c} \tag{4.18}$$

The thermal resistance of outside of coil tube material due to convection

$$R_{out,convcn.} = \frac{1}{h_o A_o} \tag{4.19}$$

Then the total thermal resistance is the result of the sum of individual thermal resistances.

$$R_t = R_{in,convcn.} + R_{condcn.} + R_{out,convcn.} = \frac{1}{h_i A_i} + \frac{ln\frac{d_o}{d_i}}{2\pi L_{coil} K_c} + \frac{1}{h_o A_o} \tag{4.20}$$

Then the overall heat transfer coefficients U, are expressed by total thermal resistances

$$UA_i = UA_o = \frac{1}{R_t} = (R_{in,convcn.} + R_{condcn.} + R_{out,convcn.})^{-1} \tag{4.21}$$

$$UA_i = UA_o = \frac{1}{R_t} = \left(\frac{1}{h_i A_i} + \frac{ln\frac{d_o}{d_i}}{2\pi L_{coil} K_c} + \frac{1}{h_o A_o}\right)^{-1} \tag{4.22}$$

$$A_o = \pi d_o L_{coil} \tag{4.23}$$

$$A_i = \pi d_i L_{coil} \tag{4.24}$$

Were,

A_o = the outer surface area of the heat exchanger

A_i = the inner surface area of the heat exchanger

h_i and h_o = the heat transfer coefficient of the natural and forced convection of coil tube material, respectively.

d_i and d_o = the inner and outer diameter of the coil tube respectively.

K_c = is the thermal conductivity of the copper tube.

R_t = is the total thermal resistance, given by the combination of individual thermal resistances associated with the natural convection outside the coil tube, the conduction across the thickness of the coil tube, and forced convection inside the coil tube.

4.4.3 Inner convection heat transfer coefficient

As per (Prabhanjan, et al., 2004), the inside coil tube heat transfer coefficient $\boldsymbol{h_i}$, can be expressed in terms of Nusult number in equation (4.25):

$$N_{ui} = 0.0397(Re)^{0.784}(Pr)^{0.3} \quad (4.25)$$

$$h_i = \frac{N_{ui} * K_c}{d_i} \quad (4.26)$$

Where Pr is the Prandtl number

$$\text{Pr} = \frac{C_p * \mu}{K_c} \quad (4.27)$$

Where, C_p = specific heat capacity

K_c = thermal conductivity of the used material

μ = the relative values of viscosity

The critical Reynolds number correlation proposed by (Smith E.M, 2005) is used in the present work for the determination of the flow regime:

$$Re_{cr} = 2300[1+8.6(r_i/D_c)^{0.45}] \quad (4.28)$$

Where, r_i and D_c are inner helical tube radius and inside diameter of the cylinder.

The ratio r_i/D_c is called coil tube curvature ratio, δ

$$\delta = r_i/D_c = \frac{0.0035}{0.127} = 0.02913$$

Substitute the value in equation (4.28), the critical Reynolds number is 6329.

$Re_{cr} = 6329 > 4000$, this shows the flow inside the coil tube is turbulent.

4.4.4 Outer Convection Heat Transfer Coefficient

Correlation expressed in Equation (4.29) was established using the tube outer diameter as characteristic length, to calculate the outer natural convection heat transfer coefficient as follows (Cuiping, et al., 2007).

$$Nu_o = \frac{0.36+0.518*Ra^{0.25}}{[1+(\frac{0.559}{Pr})^{9/16}]^{4/9}} \quad (4.29)$$

Or

$$Nu_o = \frac{0.36+0.518*{R_a}^{0.25}}{[1+(\frac{0.559}{P_r})^{0.5625}]^{0.444}} \quad (4.30)$$

Where, R_a is the Rayleigh number,

$$R_a = G_r * P_r \quad (4.31)$$

Where, G_r is the Grashof number

$$G_r = \frac{g\beta {d_o}^3 \Delta T}{\nu^2} \quad (4.32)$$

Where, g = the gravitational acceleration= $9.81 m/s^2$

β = coefficient of volumetric thermal expansion

ΔT = temperature gradient

ν = kinematic viscosity

4.5. Energy Balance Equations

The total energy balance of any two heat areas, using the following equations (4.33), complements the first law of thermodynamics (Kuppan, et al., 2000).

$$Q = UA_o\Delta T_{LMTD} = \dot{m}_w C_p \Delta T \quad (4.33)$$

This implies,

$$Q = \dot{m}_w C_p (T_{cw,f} - T_{wr,o}) \quad (4.34)$$

Where, $T_{cw,f}$ = final inlet hot water temperature to the coil tube.

$T_{wr,o}$ = outlet water temperature from the coil tube.

$\dot{m}_w$= mass flow rate of water

However, the final hot water temperature inlet to the coil tube or storage tank water temperature supplied to the next loop at any time step can be estimated from the initial storage tank temperature as follows:

$$T_{cw,f} = T_{cw,i} + \frac{t_{step}}{\dot{m}C_p}(Q_U - \dot{L}_S - \dot{Q}_{Loss}) \quad (4.35)$$

Equating equation (4.33) and equation(4.34), the return water temperature through coil tube to the solar collector thermal storage, $T_{wr,o}$ is evaluated as:

$$T_{wr,o} = T_{cw,f} - \frac{UA_o\Delta T_{LMTD}}{\dot{m}_w C_p} \quad (4.36)$$

4.5.1 Logarithmic Mean Temperature Difference (LMTD)

Unlike the logarithmic mean temperature, LMTD can be used as a gradient for the temperature range operating between two different liquids. It can be written as follows: (Kuppan, et al., 2000)

$$\Delta T_{LMTD} = \frac{(T_{cw,f} - T_{m,f}) - (T_{rw,o} - T_{m,i})}{ln\frac{(T_{cw,f} - T_{m,f})}{(T_{rw,o} - T_{m,i})}} \quad (4.37)$$

4.5.2 Actual Heat Transfer Rate in a Heat Exchanger

The actual transfer of heat to the heat exchanger, $\dot{Q}_{act}$ from the energy balance in the cold or hot liquid can be determined in the following equation below (Andrzjcryk, et al., 2016).

$$\dot{Q}_{act} = C_h\,(T_{h,i} - T_{h,o}) = C_c\,(T_{m,f} - T_{m,i}) \quad (4.38)$$

This implies,

$$m_m\,C_{p,m}\,(T_{m,f} - T_{m,i}) = \mathrm{U}A_o\Delta T_{LMTD} \quad (4.39)$$

Were,

$T_{h,i}\ and\ T_{h,o}$ = are inlet hot water temperature to the coil and outlet hot water temperature from the coil.

$T_{m,f}\ and\ T_{m,i}$ = final and initial temperature of the milk

C_h and C_c = are the heat capacity rates of the hot and cold fluids respectively

m_m = mass of the milk

$C_{p,m}$ = specific heat capacity of the milk

4.6. Pressure Drop and Selection of Pumping Power

The total pressure drop inside the coil tube is the summation of three resistance considerations, such as resistance along the pipe, resistance along bending, and the resistance along the import and export of connecting tubes fitting [(Sadic, et al., 2002) (Cuiping, et al., 2007)].

4.6.1 Pressure Drop along the Pipe

The resistance along the pipe $\Delta P_{p,}$ is calculated from the applying following equation below:

$$\Delta P_{p,} = \mathrm{f}\,\frac{L_{coil}\rho {V_i}^2}{d_i} \quad (4.40)$$

Where f is the friction factor

The friction factor f is calculated by applying the following expression (Amitkumar, et al., 2015).

$$\mathrm{f} = \frac{7.2}{{Re_i}^{0.5}}\left(\frac{d_i}{D_c}\right)^{0.25} \quad (4.41)$$

Where, d_i = inside diameter of coil (0.007m)

D_c = inside diameter of cylinder (0.127m)

To calculate the internal Reynolds Re_i, number, apply the following formula below:

$$Re_i = \frac{\rho_h d_i V_i}{\mu} \quad (4.42)$$

The terms;

ρ_h = hot water density (990.688kgm^{-3})

d_i = inside diameter of coil (0.007m)

V_i= velocity of hot fluid inside the tube (assumed to 0.5m/s)

μ = dynamic viscosity (0.000612$N - s/m^2$)

Then we can calculate the internal Reynolds number Re_i, substituting the known values in equation (4.42).

$$Re_i = \frac{990.688*0.007*0.5}{0.000612} = \frac{3.4674}{0.000612}$$

Re_i = 5665.7

Substituting the values ofRe_i, d_i and D_c in equation (4.41), we can calculate the friction factor f;

$$f = \frac{7.2}{5665.7^{0.5}}\left(\frac{0.007}{0.127}\right)^{0.25} = \frac{7.2}{75.7} * 0.4845 = 0.0465$$

After that, substituting the values of Re_i and f in equation (4.40), we can calculate the pressure drop along the pipe.

$$\Delta P_p = 0.0465 * \frac{2.83*990.688*0.5^2}{2*0.007} = \frac{32.592}{0.014}$$

ΔP_p = 2328 Pa

4.6.2 Pressure Drop along in Bending

A complete drop in pressure in the bent area is the amount of pressure drop in head loss due to bending, conflicting head loss due to the length of the bend, and the head loss due to excessive pressure drop in the lower pipe due to velocity profile deviation.

$$\Delta P_b = \frac{K\rho {V_i}^2}{2} \quad (4.43)$$

Where, K is the total loss coefficient, expressed by the following equation:

$$K = \frac{4fL_{coil}}{D_h} + K^* \quad (4.44)$$

Where, K^* is the loss coefficient for turbulent flow the recommended value is given as follows:

K^* = B (∅) [0.051+0.38($\frac{R}{d_i}$)$^{-1}$] (4.45)

Where:

$$B(\emptyset) = \begin{cases} 1 & for\ \emptyset = 90° \\ 0.9sin\theta & for\ \ \emptyset \leq 70° \\ 0.7 + 0.35sin\left(\frac{\emptyset}{90}\right) & for\ \emptyset \geq 70° \end{cases} \quad (4.46)$$

Where: f = is a frictional factor for a straight pipe at the Reynolds numberR_e, in the bend.

K^* = combined loss coefficient other than loss coefficient

D_h = hydraulic diameters for pressure drop and circular tube its value equal coil tube inner diameter, ($D_{h=d_i}$)

R = radius of curvature, ($\frac{D_c}{2}$)

r= coil tube inside radius in (m)

∅ = bending angle of the tube in degree

Using the bending angle of tube ∅ = 360°

B (∅) =$0.7 + 0.35sin\left(\frac{\emptyset}{90}\right)$ $for\ \emptyset \geq 70°$

B (∅) = 0.7+0.35sin ($\frac{360}{90}$)

B (∅) = 0.724

Substituting the value of B (∅) in equation (4.45), we can get K^*

K^* = 0.724 [0.051+0.38($\frac{0.0635}{0.007}$)$^{-1}$] = 0.724+0.099

K^* = 0.099

Then, total loss coefficient K is

K= $\frac{4fL_{coil}}{D_h}$ +K^*= $\frac{4*0.0465*2.83}{0.007}$ +0.099 = 75.197+0.099

K = 75.29

Substituting the values of K, ρ and V_i in equation (4.43), we get ΔP_b

$\Delta P_b = \frac{K\rho {V_i}^2}{2} = \frac{75.29*990.688*0.5^2}{2} = \frac{18647.22}{2}$

ΔP_b = 9323.6 Pa

4.6.3 Pressure Drop in the Fittings

The pressure drops at the import and export connecting tube fitting are calculated as a total loss coefficient, given in the equation below. (Cuiping, et al., 2007).

$$\Delta P_f = 1.5\frac{\rho {V_i}^2}{2} \quad (4.47)$$

$$\Delta P_f = 1.5* \frac{990.688*0.5^2}{2} = \frac{371.508}{2}$$

$$= 185.75\text{Pa}$$

4.6.4 Total pressure drop in the coil tube, ΔP

The total pressure drops in the coil, ΔP is calculated from the achievement of the pressure drop along the pipe, the decrease in bending pressure, and the drop in pressure of the fittings.

$$\Delta P = \Delta P_p + \Delta P_b + \Delta P_f \quad (4.48)$$

$$\Delta P = 2328+9323.6+185.75$$

$$= 11837.35\text{Pa} = 0.1184* 10^5\text{Pa}$$

This value is less than the total allowable value of $0.3* 10^5$Pa for helical, so this value is acceptable.

4.6.5 Pressure Drop in Pipe Lines

Pressure drop or loss of head occurs in all plumbing systems due to changes in height, turbulence caused by sudden changes in direction, and conflicts within the piping and installation. The most common methods used to determine head loss on a fiber glass pipe are described by Hazen-Williams, Manning, and Darcy-Weisbach equations.

The system is briefly shown in figure 3.12, there are connecting pipelines from thermal storage outlet to coil inlet and return pipelines from coil outlet to solar water storage tank.

Thermal storage outlet → Pipelines → Coil outlet → RPL → Solar water storage tank

For fully developed flow in a pipe, a pressure drop occurs due to friction as a function of (fluid flow rate, fluid density, viscosity, pipe diameter, pipe length, and pipe surface roughness)

It can be calculated from using the Darcy-Weisbach equation:

$$\Delta P_{fr} = \rho f \frac{L_p}{d}\frac{V^2}{2} \quad (4.49)$$

Where: ΔP_{fr} = frictional pressure drops, N/m^2

f = the friction factor

L_p and d= the pipe length and diameter respectively, m

ρ = density of fluid

v = is the flow velocity in m/s

The friction factor f is related to the flow regime, Reynolds number is a good criterion for prediction of flow regime. (Michael g, et al.)

$$\text{Re} = \frac{\rho V d}{\mu} \quad (4.50)$$

Where μ is the kinematic viscosity of the fluid

For Laminar flows, where Re <2300, f is calculated as:

$$f = \frac{64}{Re} \quad (4.51a)$$

For Turbulent flows, where Re >2300, f is a function of Reynolds number and pipe roughness or absolute roughness, **k**.

Relative roughness, **k** = absolute roughness/pipe inside diameter

For hydraulically smooth pipes, Re < 65d/k, and a Reynolds number in the range of $2300<Re<10^5$, the pipe frictional coefficient is calculated using the Blasius formula:

$$f = \frac{0.3164}{\sqrt[4]{Re}} \quad (4.51b)$$

For rough pipes, the pipe friction coefficient is read from Moody diagram or evaluated using Colebrook formula: Fig D.1 in appendix part

$$f = [2log(\frac{2.51}{Re\sqrt{f}} + \frac{0.27k}{d})]^{-2} \quad (4.52c)$$

Flow resistance in the pipeline network causes a loss of flow head pressure. Complete head loss in the pipeline network contains the following:

- Major losses (h_{maj}), and
- Minor losses (h_{mnr})

4.6.5.1 Major losses (h_{maj})

This loss refers to the loss of flow head pressure due to the effects of the collision. Such losses can be assessed using Darcy-Weisbach statistics:

$$h_{maj} = f\frac{L_p}{d}\frac{v^2}{2g} \quad (4.53)$$

The equation above is valid for any fully developed, steady, and incompressible flow.

4.6.5.2 Minor losses (h_{mnr})

In a plumbing network, the availability of plumbing fixtures such as bends, elbows, valves, sudden expansion or contraction causes losses to the compression head. Such losses are referred to as minor losses. Minor losses are shown using the following equation.

$$h_{mnr} = \mathrm{K}\frac{v^2}{2g} \tag{4.54}$$

Where: K is called the Loss Coefficient of the pipe fitting under consideration.

The summation of equations (4.53) and (4.54) gives total head loss, h_{tot} obtained as follows:

$$h_{tot} = h_{maj} + h_{mnr} \tag{4.55}$$

$$= \mathrm{f}\frac{L_p}{d}\frac{v^2}{2g} + \mathrm{K}\frac{v^2}{2g}$$

$$= \frac{v^2}{2g}\left(\mathrm{f}\frac{L_p}{d} + K\right)$$

Suppose the total closed-loop pipe length of supply and return pipelines to be, L_p = 4.5m and as shown in fig: 3.3 there is four (4) bend.

For 90° standard curved elbow ($^{R}/_{D} = 1$), K value is 0.75.

Properties of water at 50℃ (suppose average temperature of the water inside the pipelines), ρ=998kg/m^3, and μ= 1.003$*$ 10^{-3} kg/m.s.

Whereas, V≤ 1m/s for domestic applications

V≤ $2m/s$ for other applications

V≤ $5m/s$ for wastewater applications

For was recommended value for pump selection, using V= 1.9m/s and 32mm diameter galvanized steel pipe. By using the above procedure, we can calculate the internal area of the pipe and the Reynolds number.

The internal area of the pipe and Reynolds number can be calculated applying the following equation:

$$A_i = \frac{\pi d^2}{4} = \frac{\pi * 0.032^2}{4} = 8.0425 * 10^{-4} m^2$$

$$\mathrm{Re} = \frac{\rho V d}{\mu} = \frac{998 * 1.9 * 0.032}{1.003 * 10^{-3}} = 60496.9$$

For galvanized steel, the equivalent roughness is ($\in = 0.15mm$)

$$\frac{\in}{d} = \frac{0.15}{32} = 0.0046875$$

Enter the Moody chart on the right at $\epsilon/d \approx 0.0047$ (with interpolate), and move to the left to intersect with Re ≈ 60496

From Moody chart reading f≈0.0397 at the bottom. Then we can calculate the total head lossh_{tot}, by substituting known values in equation (4.55)

$$h_{tot}\ \text{loss} = \frac{v^2}{2g}\left(f\frac{L_p}{d} + K\right) = \frac{1.9^2}{2*9.81}\left(0.0397* \frac{4.5}{0.032} + 4 * 0.75\right)$$

$$= 0.184(5.583+3)$$

$$= 1.58\text{m}$$

Finally, substituting the above-known values into Equation (4.49)

$$\Delta P_{fr} = \rho f \frac{L_p}{d}\frac{V^2}{2} = 998*0.033* \frac{4.5}{0.032} * \frac{1.9^2}{2}$$

$$= 32.934*140.625*1.805$$

$$= 8359.6\text{Pa}$$

4.6.6. Total Pressure Drop in the System

The total pressure drop in the system is the summation of results found in equations (4.48) and (4.49):

$$\Delta P_t = \Delta P + \Delta P_{fr} \qquad (4.56)$$

$$= 11837.35+8359.6$$

$$= 20196.95\text{Pa}$$

Total pressure drop in the system is 20196.95Pa.

4.6.7 Determination of Total Dynamic Head

4.6.7.1 Total specific work of water pump

Total pressure drops, ΔP_t=20196.95Pa

Then, total specific work (W_{sp}) is calculated by applying the following formula:

$$W_{sp} = \frac{\Delta P_t}{\rho} = \frac{20196.95}{998}$$

$$= 20.24 m^2/s^2$$

4.6.7.2 Total Head

Total specific work, W_{sp}= $20.24 m^2/s^2$. Then, the total head, H is:

$$\text{H} = \frac{W_{sp}}{g} = \frac{20.24 m^2/s^2}{9.81 m/s^2} = 2.06\text{m} \approx 2.1m$$

4.8. Pumping Power Requirement

The fluid pumping power P, in considering the total system head loss, H_{sys}. The input fluid pumping power can be calculated by applying the following equation. (4.57) (Frank, et al.)

$$P = \frac{\rho g Q H_{sys}}{\eta_p \eta_m} \quad (4.57)$$

Here, $H_{sys} = h_{tot} + h_z$ (4.58)

Where:

P= fluid pumping power

ρ = density of fluid (kg/m^3)

g= gravitational acceleration (9.81m/s^2)

Q=volume flow rate (m^3/s)

H_{sys} = system falling height, Head (m)

h_z = head loss of pump due to elevation (up to 1.3- 1.6), let's take 1.4m

η_p = pump efficiency (0.80-0.85), using 0.80

η_m = motor efficiency (allowable motor eff. 0.95)

Substituting the known value in equation (4.58), we get H_{sys}

$H_{sys} = h_{tot} + h_z$= 1.58+1.4=2.98$m \approx 3m$

4.8.1 Volume flow rate

Q = A_iV= 8.0425$*$ 10^{-4} $*$1.9

= 0.001528075=1.53$*$ $10^{-3} m^3/s$

Then we can calculate fluid pump power, by substituting the values of Q,ρ, g, H_{sys}, η_p and η_m in equation (4.57):

$$P = \frac{\rho g Q H_{sys}}{\eta_p \eta_m} = \frac{998*9.81*1.53*10^{-3}*3}{0.8*0.95} = \frac{44.9378}{0.76}$$

= 59.94W$\approx$ 60W

Therefore, the power requirement for PV is ≈60W

4.8.2 Pump selection

The active water circulation system is festinated to complete the solar milk pasteurizer system. Solar-powered water pumps are designed to use the direct current (DC) provided by a

photovoltaic (PV) array. However, the determination of specific pump size and PV array is based on the performance charts provided by the manufacturer's referring to pumping power, total dynamic head, and desired to pump flow rate as shown in FigureD.3 (Kyocera Solar pump manufacturer, Inc. catalog). The PV array will be specified in terms of wattage and voltage. It is standard procedure to increase the specified wattage by 25% (multiply by 1.25) to compensate for power losses due to high heat, dust, aging, etc. Therefore, the total amount of power needed for pumping by the solar panel was approximately 60 Watt. Which is multiplied by 1.25 and equal to 60*1.25 = 75watt.

4.8.2.1 Brief description, advantages, and uses of pump

- Proper selection and application of pumping technology can greatly improve the reliability of a pumping system.
- Pumps are the prime movers of liquids in process applications. Pumps are used to increase the static, or inlet pressure of the liquid and deliver the liquid at the specified discharge pressure and flow rate in a process application. Part of the increase in static pressure is required to overcome frictional resistance in the process.
- Pumps are available in a variety of types, models, and sizes, each of which is designed for specific applications. The selection should represent the best available configuration by a prescribed set of requirements.
- Mechanical integrity, process safety, maintainability, and environmental protection are important considerations for pump applications. Pumps shall be manufactured from materials acceptable to the process. Materials shall be corrosion and erosion-resistant.
- Provide the head and flow required for all flow paths, plumbing adjustments, process flow features, and other product structures. Product features to be considered for specific gravity, viscosity, vapor pressure, specific temperature, and temperature range.
- Pumps used in the same service will be the same in design and size, will operate at the same speed, and will be installed by the same impellers. It is the customer's responsibility to ensure that the plumbing fixtures of the pumps work in parallel with the geometric shape to achieve equitable sharing between the pumps.

CHAPTER FIVE

RESULTS AND DISCUSSIONS

In this chapter, briefly describe the design results in tabular form and CFD analysis graphically and discuss the performance analysis of the system, mentioned in chapter one.

5.1 Design Results of helical coil heat exchanger

Table 5.1: Shows designed coil heat exchanger geometrical values.

Parameters	Values	Units
Thermal ouput of the collector (hot water exit from the collector)	984.9	W
Outer tube diameter of the coil, d_o	9	mm
Inner tube diameter of the coil, d_i	7	mm
The thickness of the tube, t	1.24	mm
Coil diameter, D_c	127	mm
Pitch of the coil tube,p	0.014	m
The total length of the coil tube, L_{coil}	3	m
Number of coils turns, N_{coil}	5	-
Total heat transfer area, A_o	0.098	m^2
The volume occupied by the whole turn of the coil, V_c	$1.91 * 10^{-4}$	m^3
The volume of the Milk Storage Tank	0.12002	m^3

5. 2. CFD Analysis of Helical Heat Exchanger and Milk Storage Tank

5. 2.1. Modeling

The standard modeling process is performed by the ANSYS 19.2 workbench. We use the design modeler workbench to model any geometry in ANSYS 19.2.

There are two separate sections in the assembly where the milk storage tank can enter and open the milk and one has copper pump coils where hot water flows.

The total height of the milk storage tank is kept at 324mm and the outer diameter of the container is 210mm and the diameter of the inlet and outlet of milk is 12mm. The height of the helical coil is 187mm and 374mm.

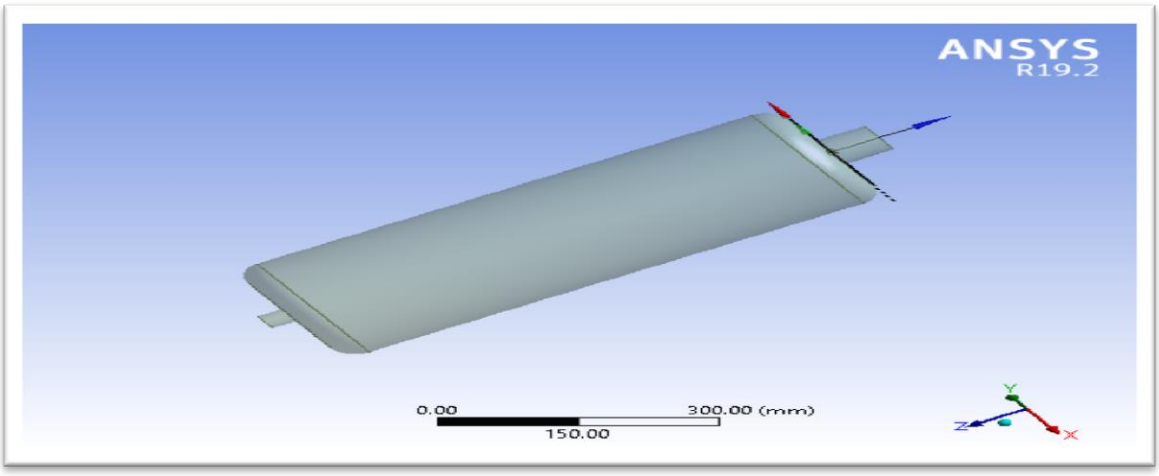

Figure 5.1: Model of milk storage tank

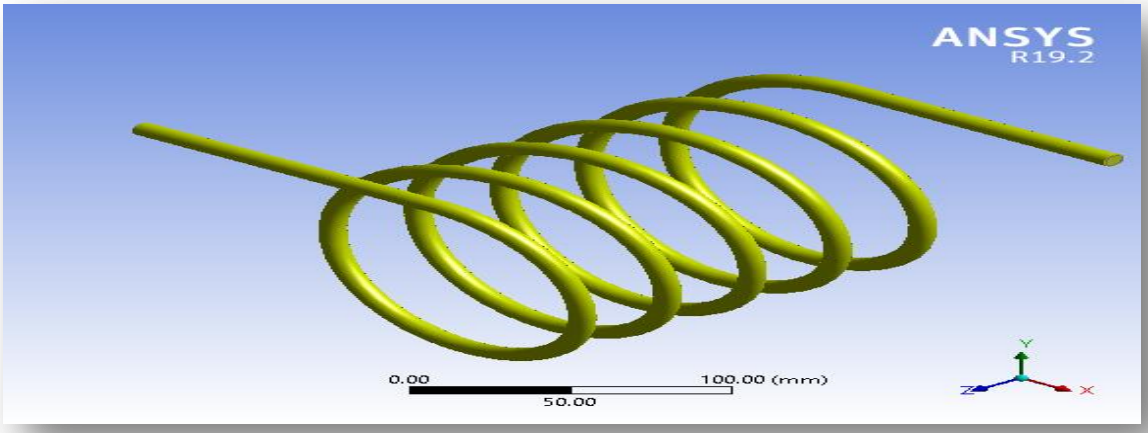

Figure5.2: Model of helical tube heat exchanger

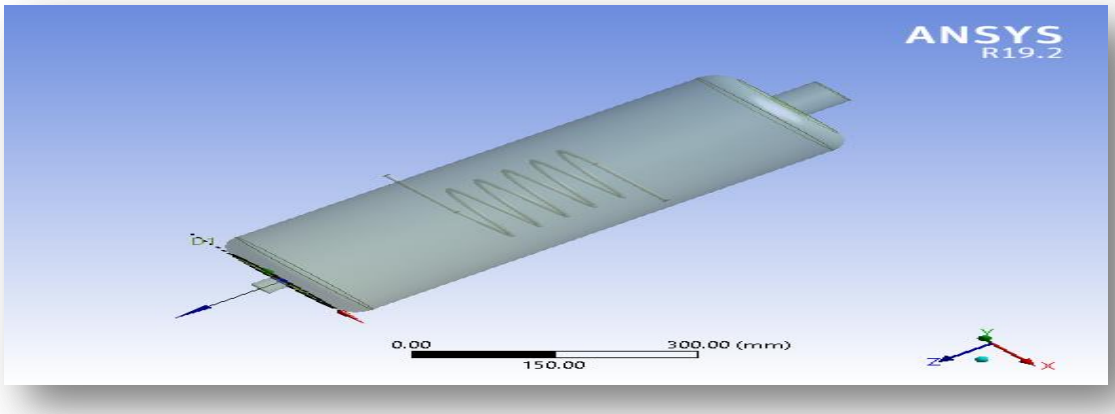

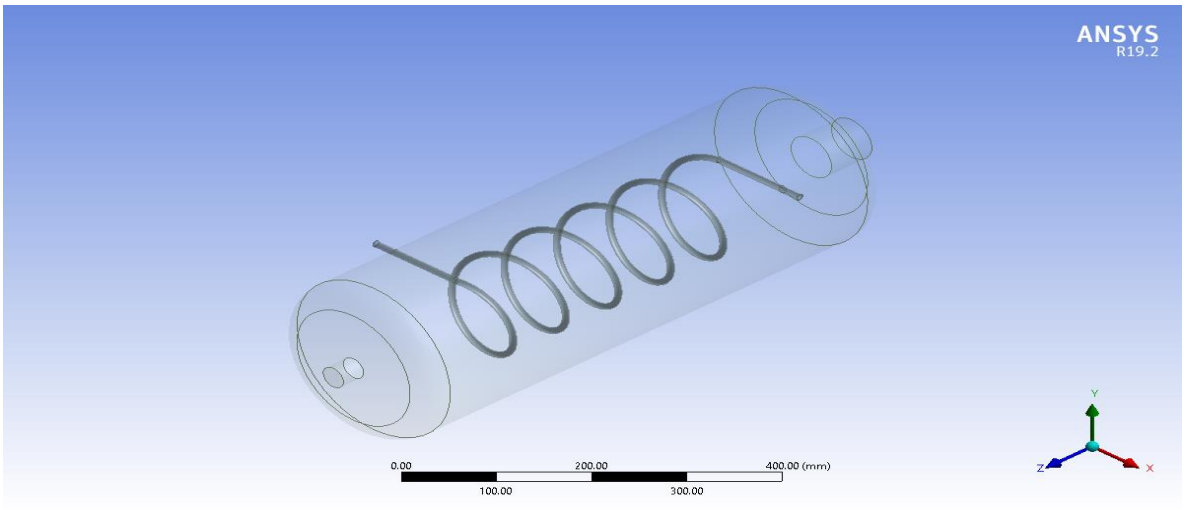

Figure5.3: Model of HTHx and milk storage tank in one for axial length 187mm and 374mm

5.2.2 Name selection and Meshing

5.2.2.1 Name selection

The different faces and bodies are properly named. The outer cover is used as insulation.

Save the project again at this point and close the window. Refresh and update the project on the workbench.

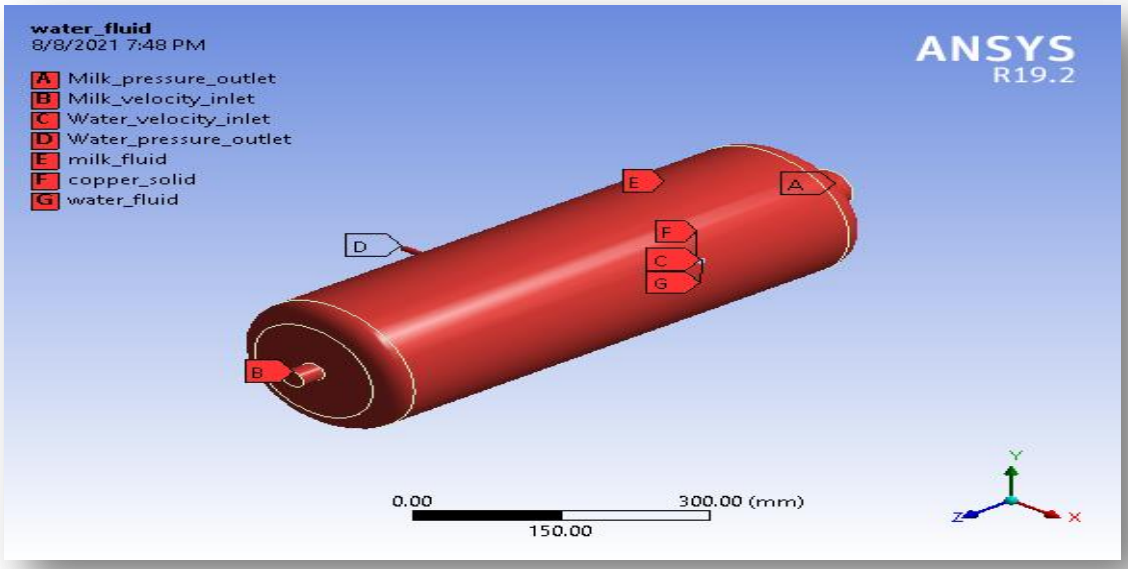

Figure5.4: Name selection of geometry

Now open the setup. The ANSYS Fluent Launcher will open in a window. Set dimension as 3D, option as Double Precision, processing as Serial type, and hit OK. The Fluent window will open.

5.2.2.2 Meshing

Initially, a mesh course is produced. This mesh consists of interlocking cells (Tetra and hexahedral cells) with both triangular and square sides at the borders. Care should be taken to use as well-organized hexahedral cells as possible. This will reduce the spread of prices as much as possible by building the mesh properly, especially near the wall circuit. Later, a fine mesh was made. In this beautiful mesh, the edges and regions with high temperatures and pressures have good messages

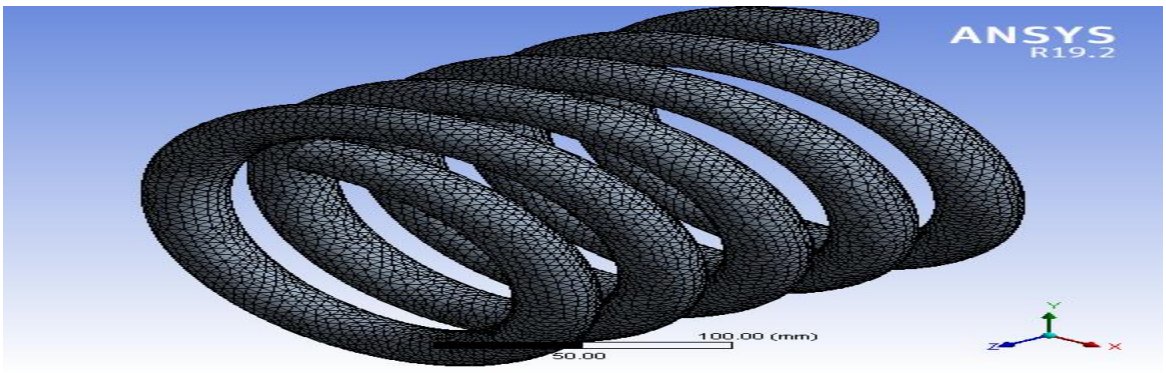

Figure 5.5: Meshing of helical tube heat exchanger

5.2.3 Problem setup

The mesh is checked and quality is obtained. The analysis type is changed to Pressure Based type. The velocity formulation is changed to absolute and time to steady-state.

5.2.3.1 Models

Energy is set to ON position. Viscous model is selected as "k-ε model (2 equation).

5.2.3.2 Materials

The create/edit option is clicked to add water-liquid and copper to the list of fluid and solid respectively from the fluent database. But milk fluid is not found in the fluid database, create a new fluid that is fluid milk and give the properties of milk properly.

5.2.3.3 Cell zone conditions

The parts are assigned as water, milk, and copper as per fluid/solid parts.

5.2.3.4 Boundary conditions

Boundary conditions need to be specified for obtaining the output results. Proper selection of boundary conditions leads to giving proper results and their improper selection of boundary conditions to give false results.

Inlet and outlet of different fluids	Boundary condition type	Temperature(K)	Velocity magnitude(m/s)	Pressure magnitude (pa)
Water inlet	Velocity inlet	373	2	-
Water outlet	Pressure outlet	346	-	-
Milk inlet	Velocity inlet	305	1	-
Milk outlet	Pressure outlet	341	-	-

5.2.3 Solution

The CFD gives the solution of different fluid flow based on the given boundary condition. We can perform the solution by applying different input and output parameters. The input parameters like inlet milk fluid velocity and length of the helical coil heat exchanger and output parameters like temperature and mass flow rate of milk.

5.2.3a: For steady analysis

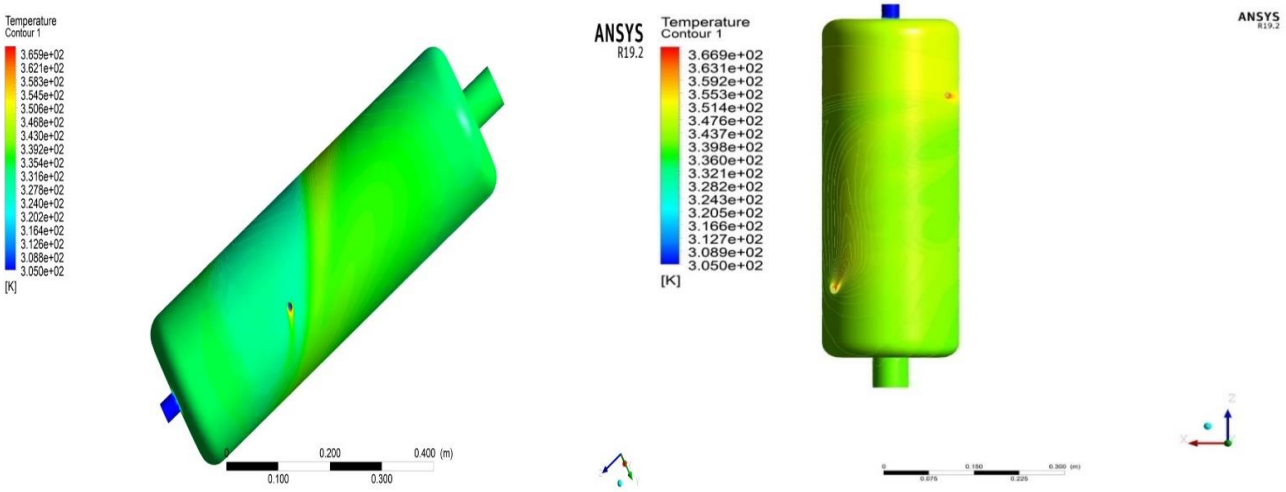

a. For helical tube axial length 187mm b. For helical tube axial length 374mm

Figure5.6: Temperature contour all domain and wall milk fluid location

The temperature of the milk storage tank exit is higher than the temperature of the milk storage tank intake, as seen in this figure. The minimum and maximum temperatures are 305K and 366K, respectively. This gives me the desired output pasteurization temperature. From the above figures we memorize, increasing the pitch length of the helical tube we get the smooth flow and desired output.

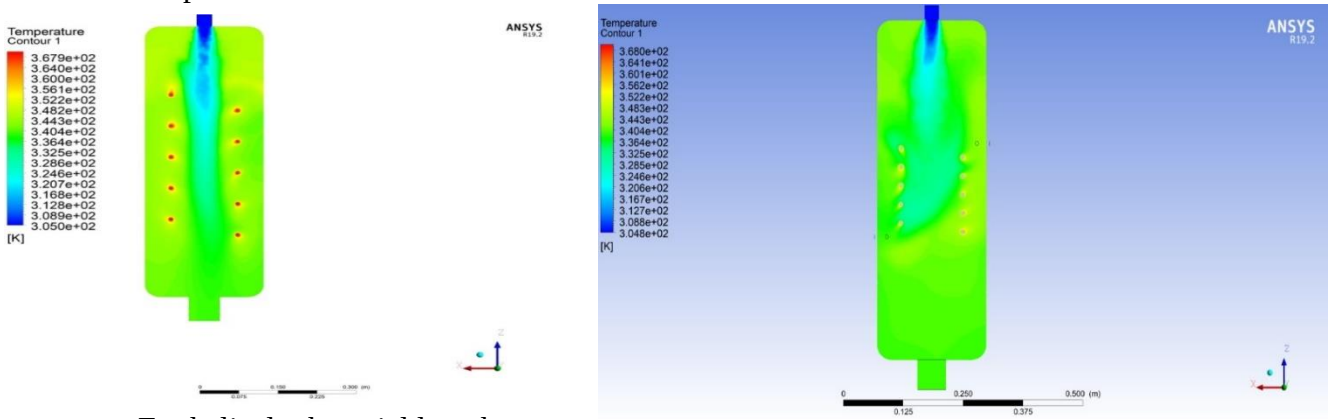

a. For helical tube axial length 374mm

b. For helical tube axial length 187mm

Figure5.7: Temperature contour all domain and plane location

The temperature contour for all domain and selected plane locations is shown in this figure. We can see that the heat in the center area is high due to the heat exchange between the hot water in the helical tube and the cold milk fluid. The smoothness of the flow is important when comparing different figures. Because the axial helical tube length of figure (a) is greater than that of figure (b), figure (a) is smoother than the figure (b). As a result, increasing the axial helical tube length improves fluid flow smoothness and heat transfer rate.

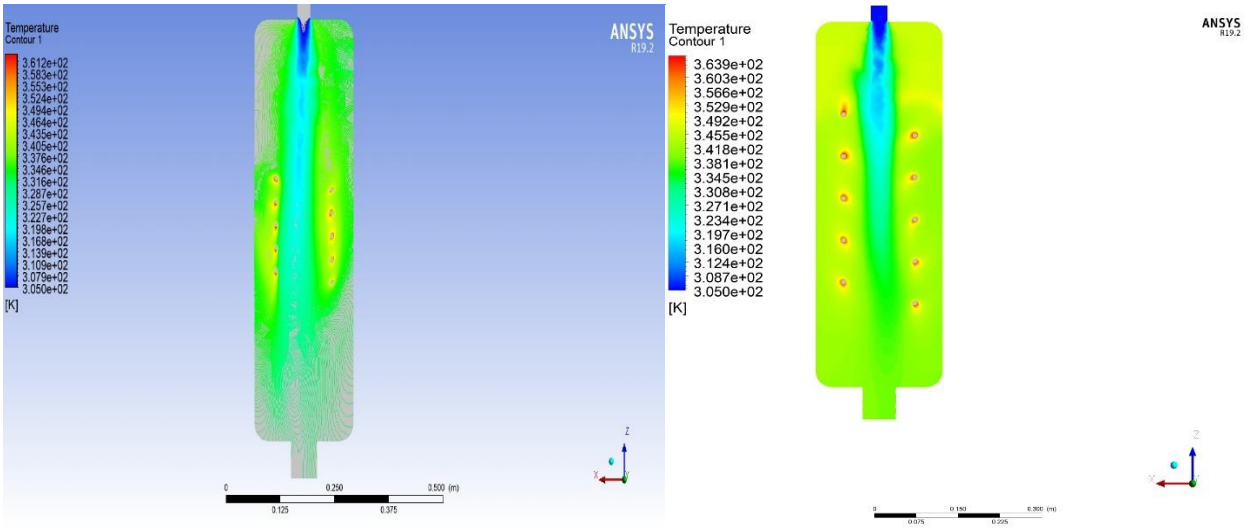

a. For helical axial length 187mm b. For helical axial length 374mm

Figure5.8: Temperature contour milk fluid domain and plane location

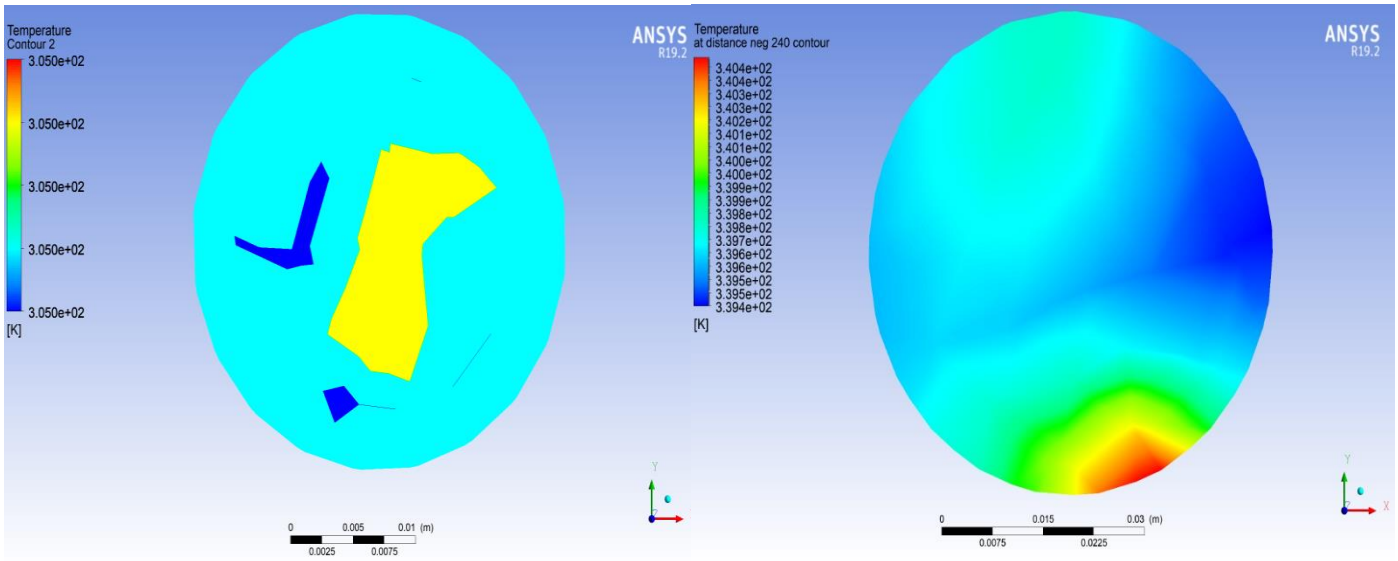

a. Temp. distrbn at inlet b. Temp. distrbn at exit

Figure5.9: Temperature distribution in the inlet and outlet area

The temperature distribution in the fluid input is shown in figure a, and the temperature distribution in the exit area is shown in figure b. We may deduce from these statistics that the temperature in the inlet area is constant because the fluid is at 305K in its initial state. And the temperature distribution in the exit area is uniform; the minimum and maximum are 339.5K and 340K, this number shows small variation because the milk fluid goes to coiling media . This value informs uniform distribution at the exit and nearly equal to my wanted pasteurization temperature.

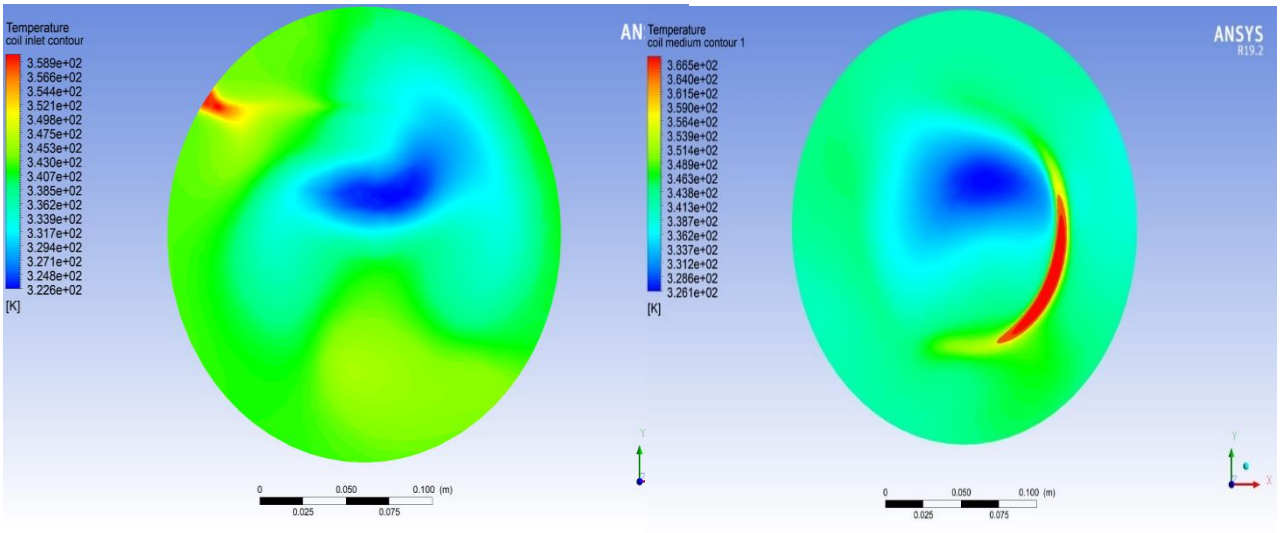

a. Temp distrbn at fluid meets coil tube inlet tube

b. Temp distrbn at the middle of helical

Figure5.10: Temperature distribution at the coil inlet and middle of helical coil

Heat exchange between the two locations begins when the milk fluid approaches the heated helical tube, and the cold fluid temperature climbs above its original value. According to figure a, the minimum and maximum temperatures are 322.6K and 359.9K, respectively. Figure b demonstrates that the rate of heatin increases as the temperature rises transfer this place. The lowest and highest temperatures are 326.1K and 369.8K, respectively, as shown in Figure a.

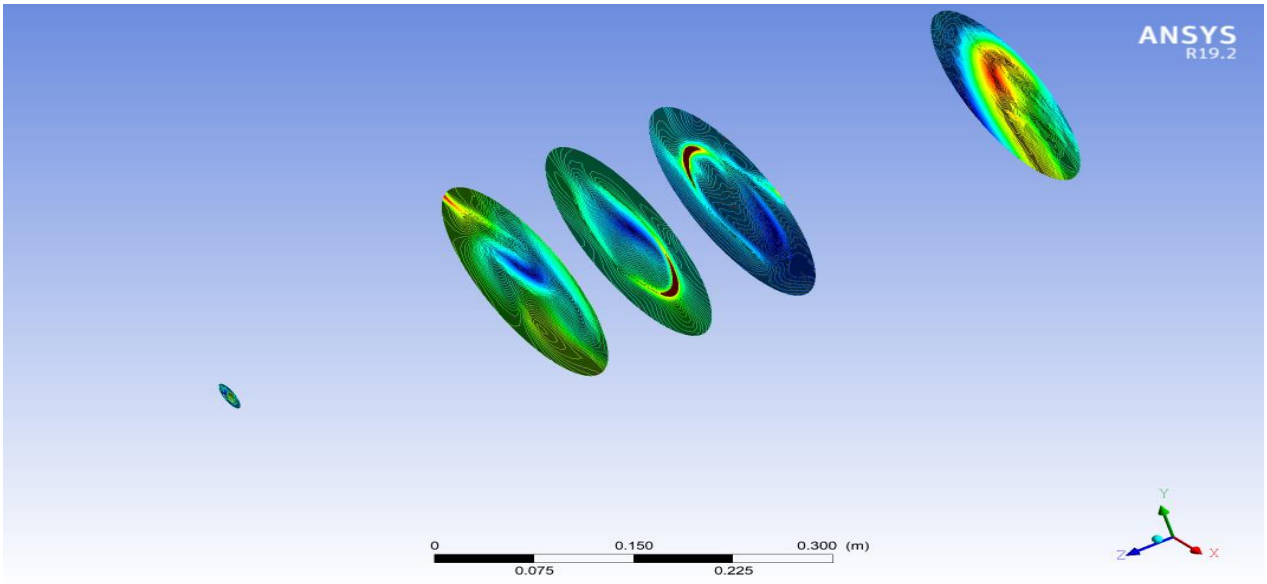

Figure5.11: Temperature distribution in the different axial distances

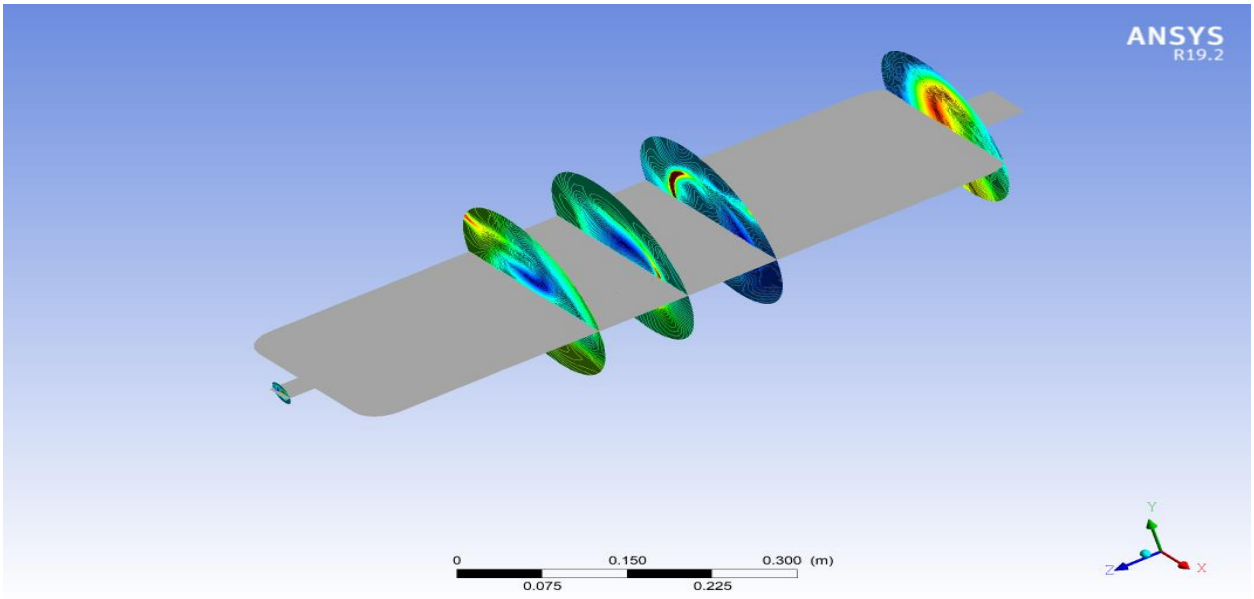

Figure5.12: Temperature distributions in different plane locations

The temperature distributions at the different plane positions are represented in the figures above. The temperature rises until pasteurization occurs, after which it is evenly distributed.

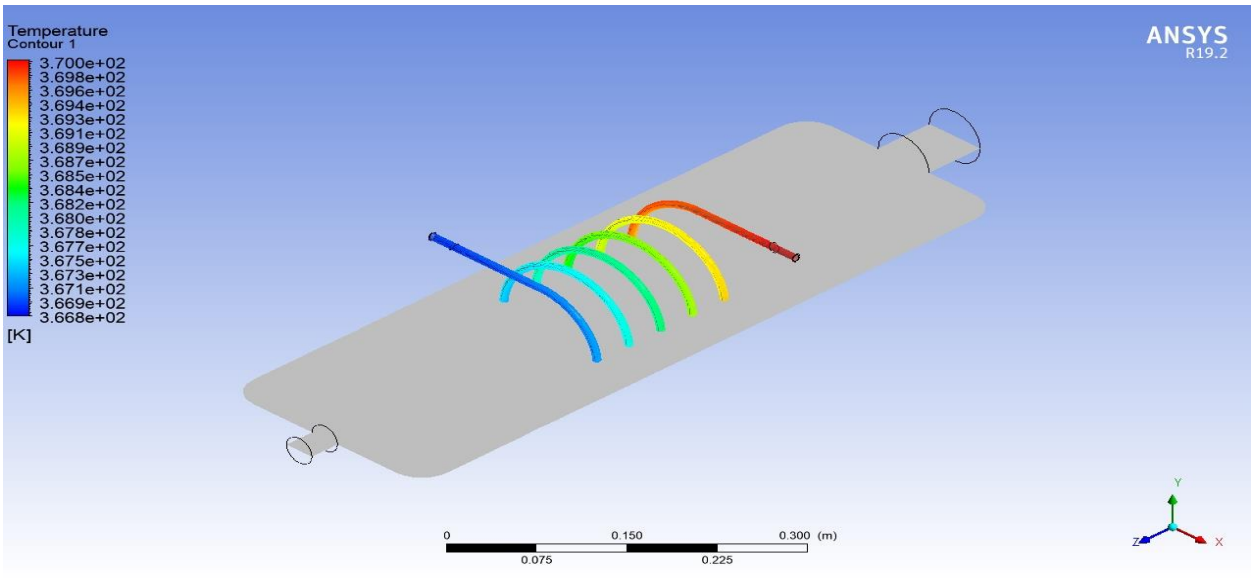

Figure5.13: Temperature contour of water fluid domain and plane location HTHx

Because of heat exchanges between hot water fluid in the helical tube and cold milk fluid, the temperature of the coil falls while the temperature of the milk increases, as seen in the graph above. The water in the helical tube's input is hotter than the water in the helical coil's outlet. Because the temperature at the output is after the milk has been pasteurized.

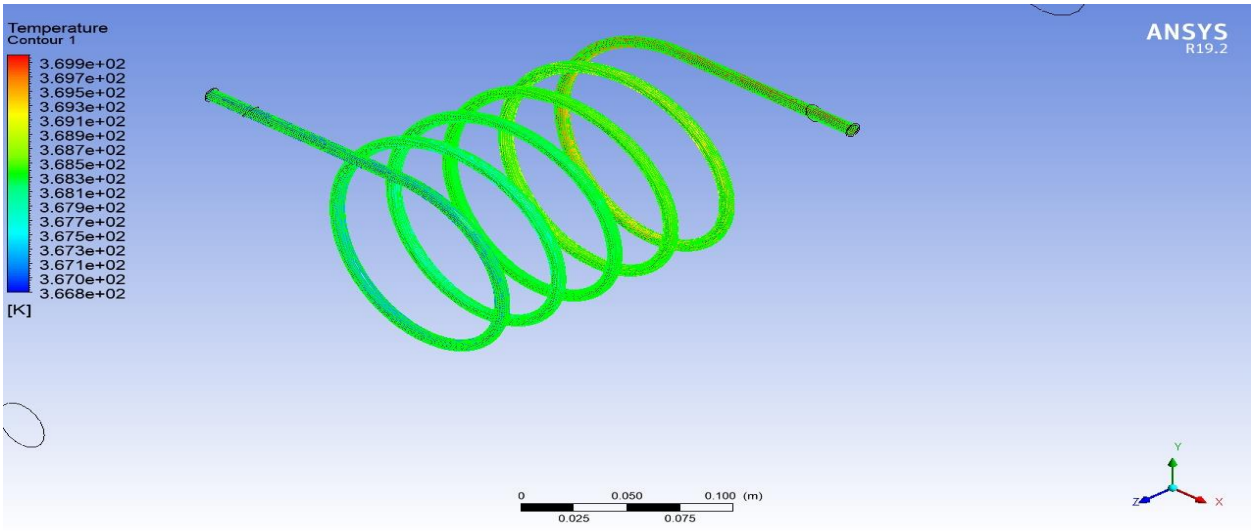

Figure5.14: Temperature contour all domain and water fluid location

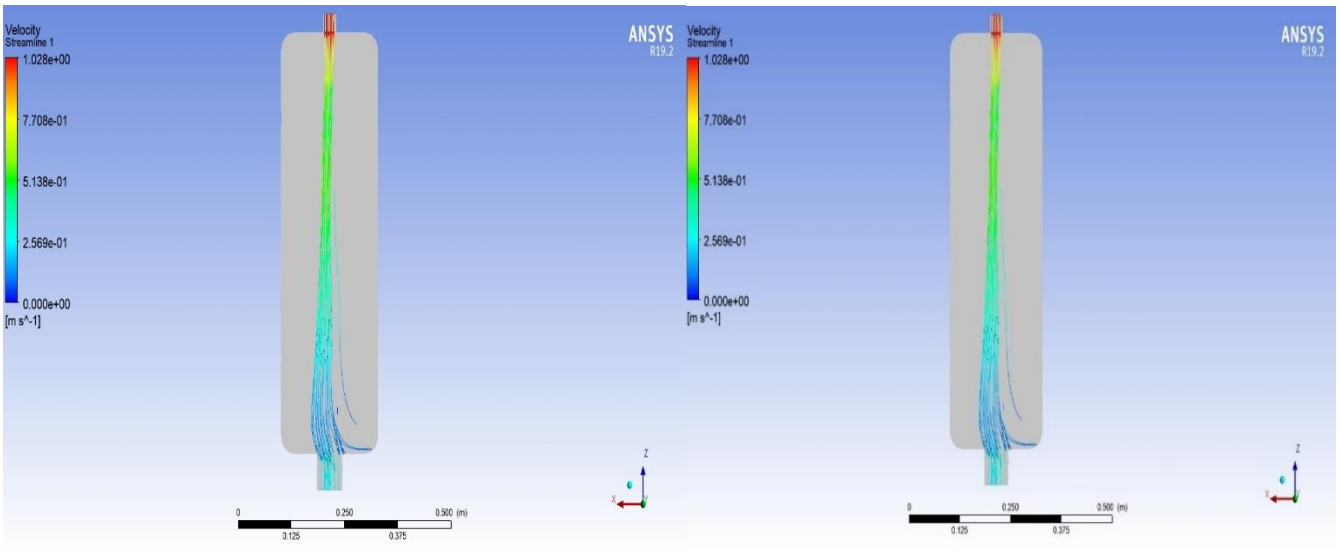

Figure a: Velocity streamlines all domains start from milk inlet velocity Figure b: Velocity streamline milk fluid domain start from milk inlet velocity

Figure5.15: Velocity streamline all domain and milk fluid domain and starts inlet velocity

Figures a and b both show the same information. The fluid flow is shown in the figure above, the velocity of the entrance is greater than the velocity of the outlet because the inlet diameter is smaller than the outlet. Then, to increase the smoothness of the fluid flow, increase the diameter of the milk outflow and the pitch length of the helical tube.

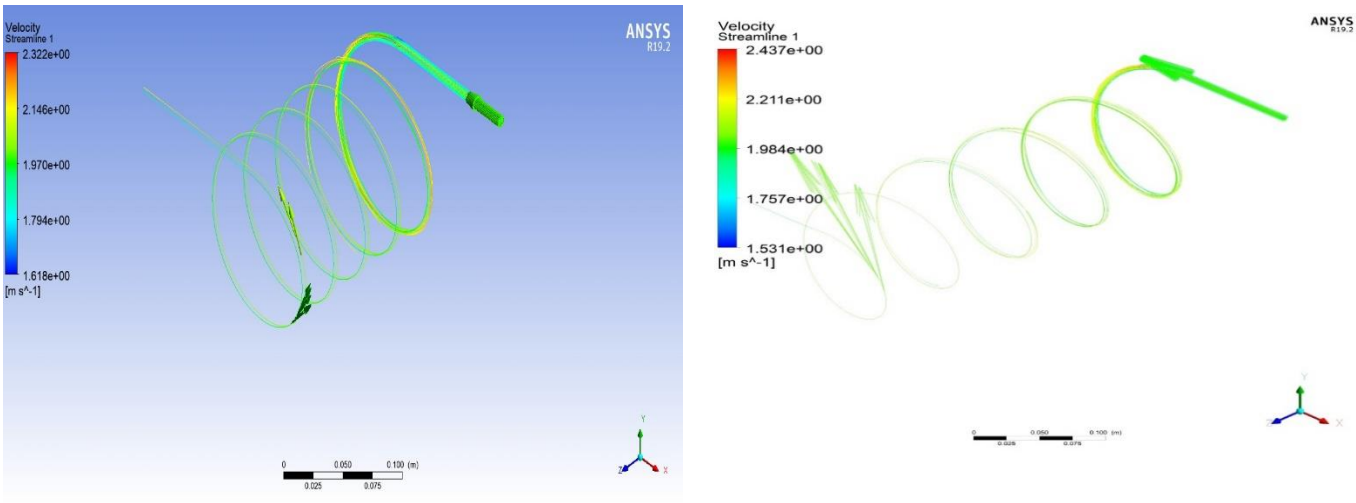

a.Velocity streamline for pitch length 187mm b. Velocity streamline for pitch length 374mm

Figure5.16: Velocity streamline water fluid domain start from water inlet velocity

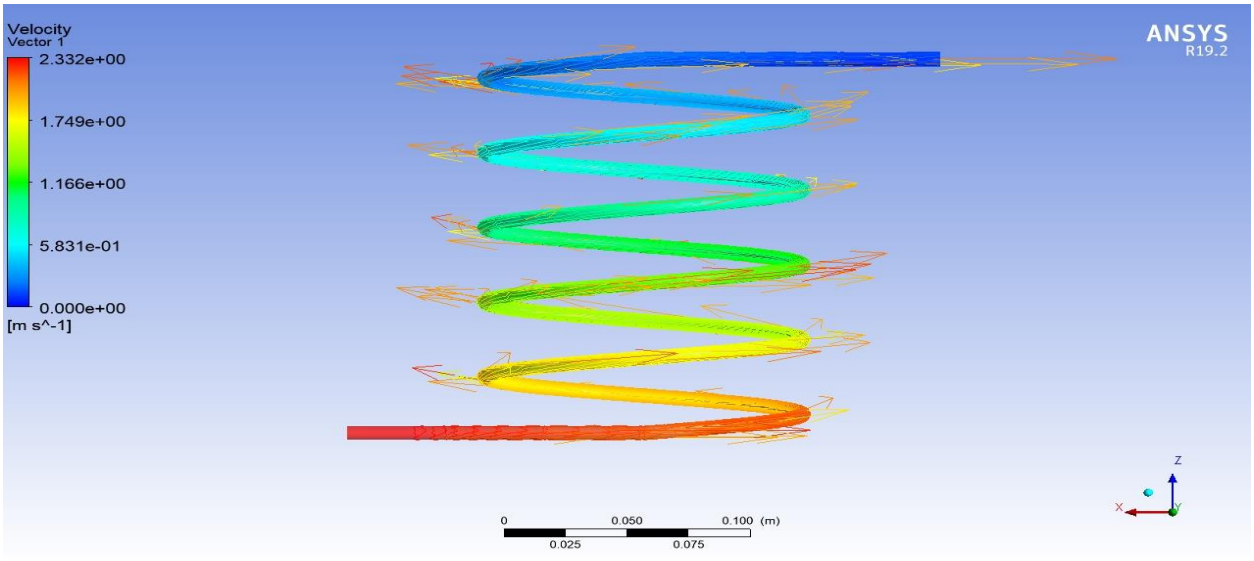

Figure5.17: Velocity vector all domain and water fluid location

This demonstrates how the temperature of a fluid impacts its velocity. The velocity is higher in hotter areas than in colder areas. Because of the helical tube, there is a slight fluctuation in vector line flow. The diameter of the helical tube should be added as a recommendation to make vector lines flow smoothly.

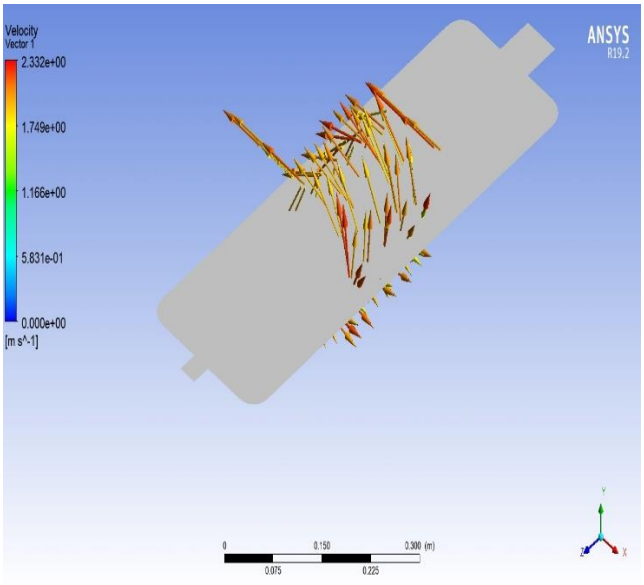

a. Velocity vector for pitch length 187mm

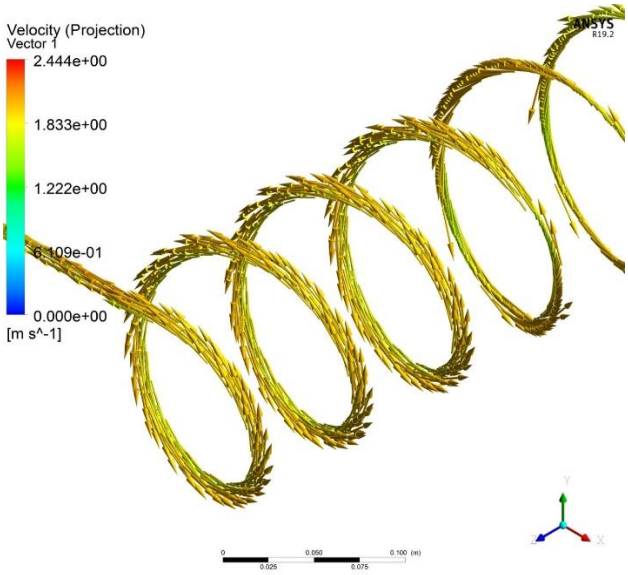

b. Velocity vector for pitch length 374mm

Figure5.18: Velocity vector water fluid domain and water fluid and plane location

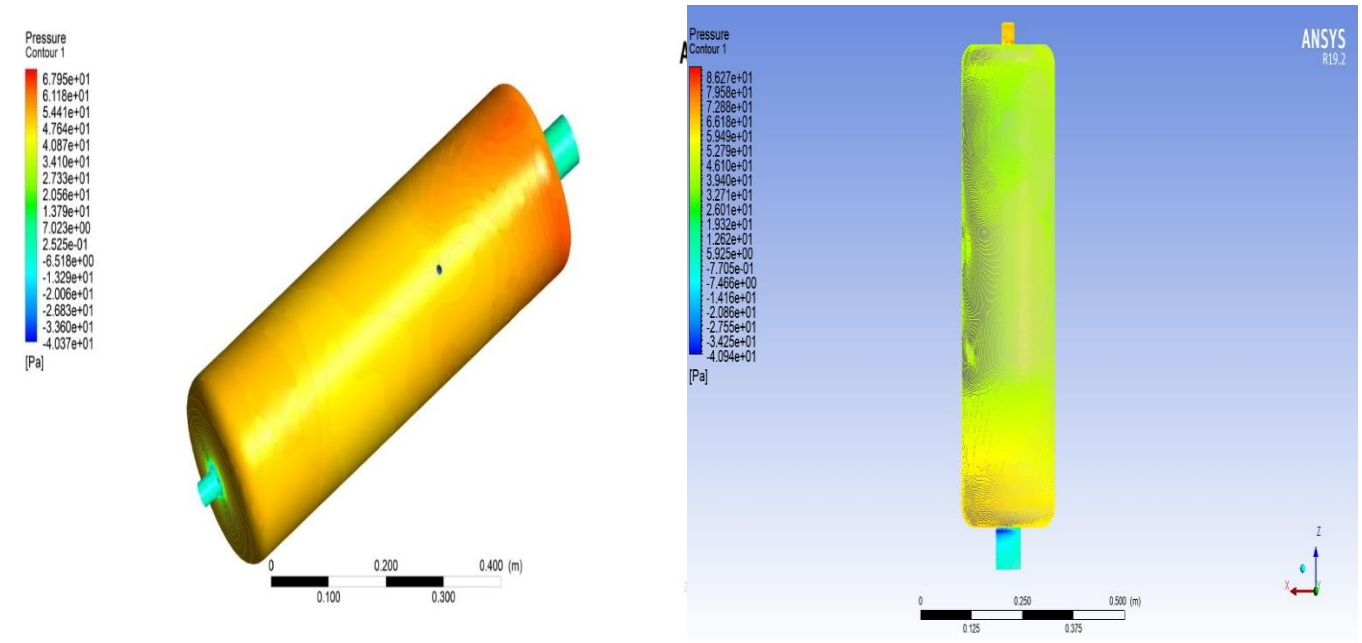

Figure5.19: Pressure contour all domain and wall milk fluid location

From the above two figures, figure b shows smooth flow because the pitch length is greater than the figure a. Because the inlet diameter is less than the outlet, the pressure in the inlet is higher than the pressure in the outlet, which means smaller diameter higher pressure and because there is free space between the internal storage and the helical tube, milk fluid flows easily through the wall. Increase the helical tube pitch length for a smoother flow.

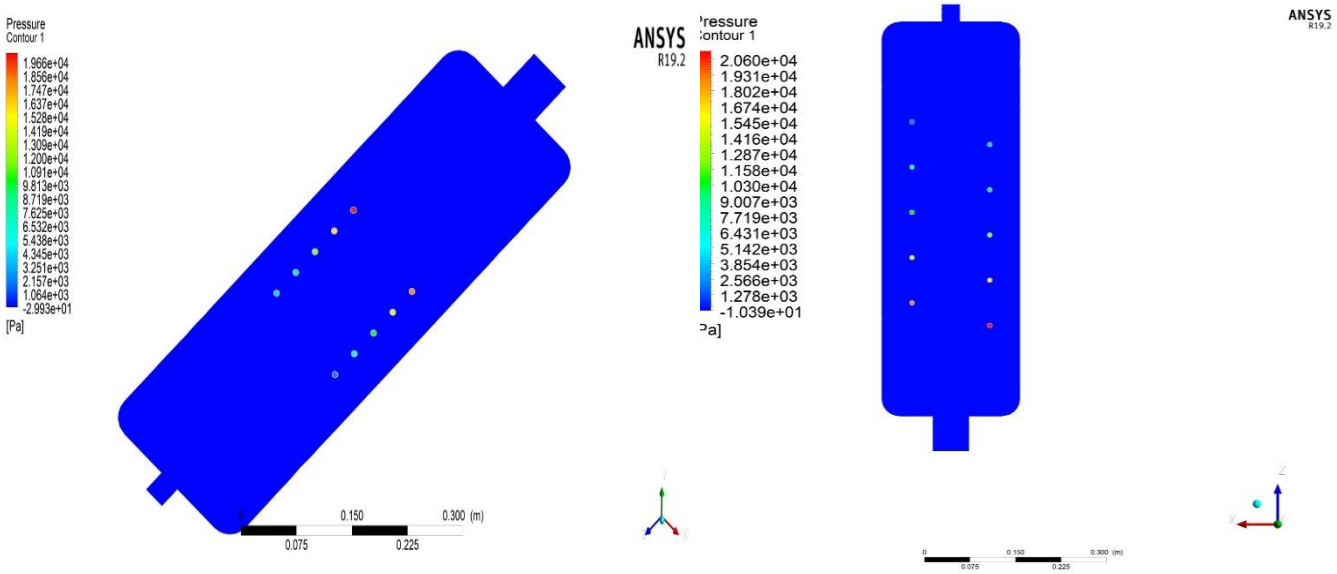

a. Pressure contour for pitch length 187mm b. Pressure contour for pitch length 374mm

Figure5.20: Pressure contour all domain and plane1 location

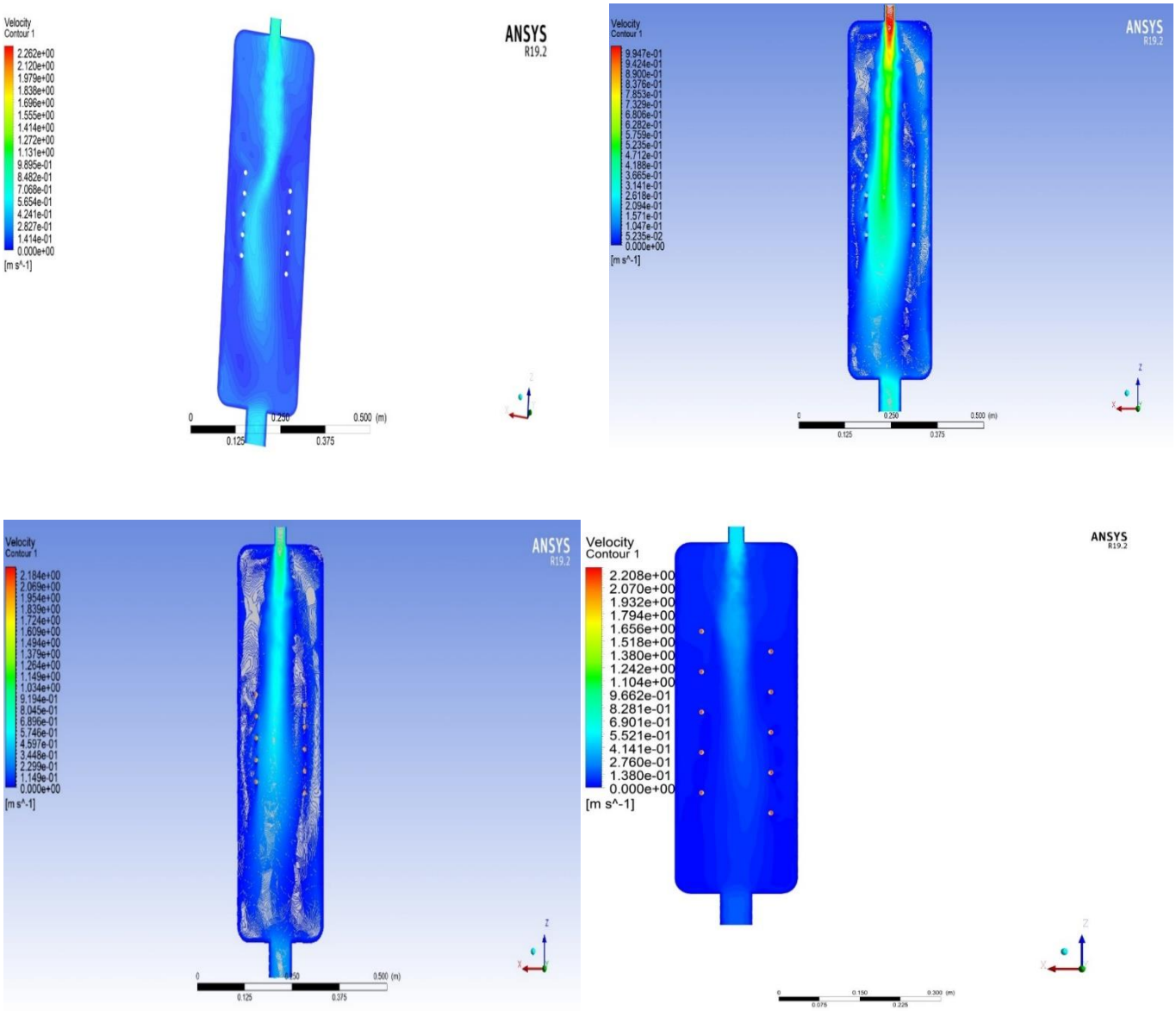

a.For helical tube axial length 187mm b. For helical tube axial length 374mm

Figure5.21: Velocity contour domain milk fluid and plane location

a. Velocity contour domain milk fluid for 187mm b. Velocity contour domain milk fluid for 374 mm

Figure5.22: Velocity contour all domain and location plane

The fluid flows smoothly on the top surface, but the flow is not smooth on the middle surface due to heat exchanges between the heated coil tube and the cold milk fluid, resulting in some fluctuation. Increasing the pitch length of a helical tube heat exchanger solves this type of problem.

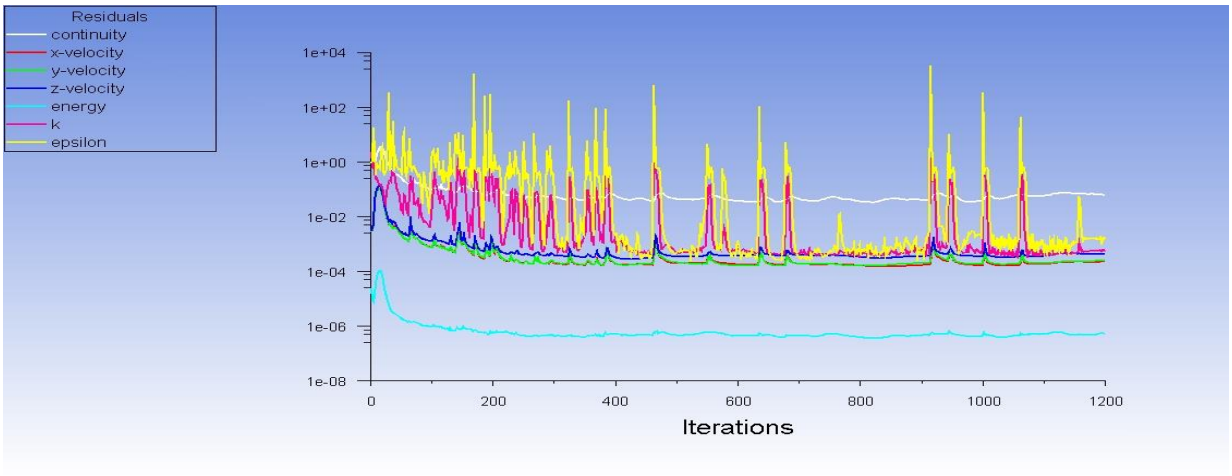

Figure5.23: Residuals for 1200 iteration and residual number 10^{-6}

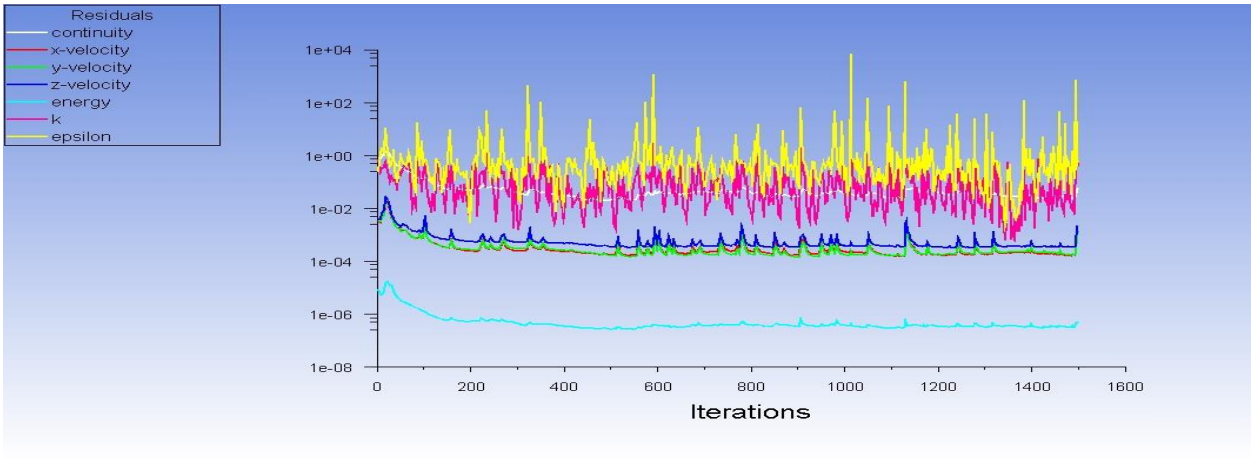

Figure5.24: Residual graph for1500 iteration and 10^{-6}*residual number*

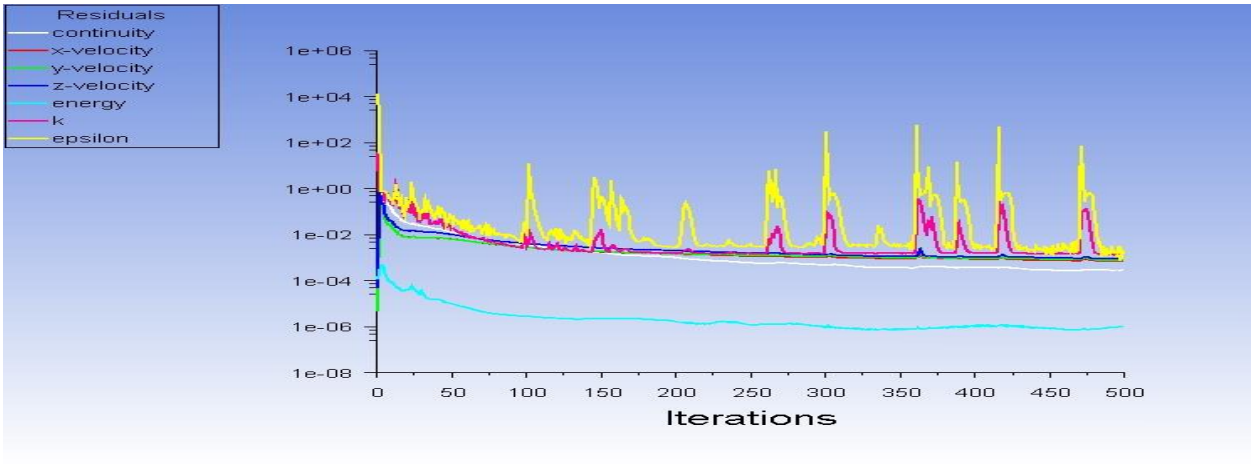

Figure5.25: Residual graph for iteration 500 and 0.001 residual number

We can see from the figures above that reducing the number of iterations speeds up convergence, but increasing the number of iterations results in smoother and more reliable outcomes.

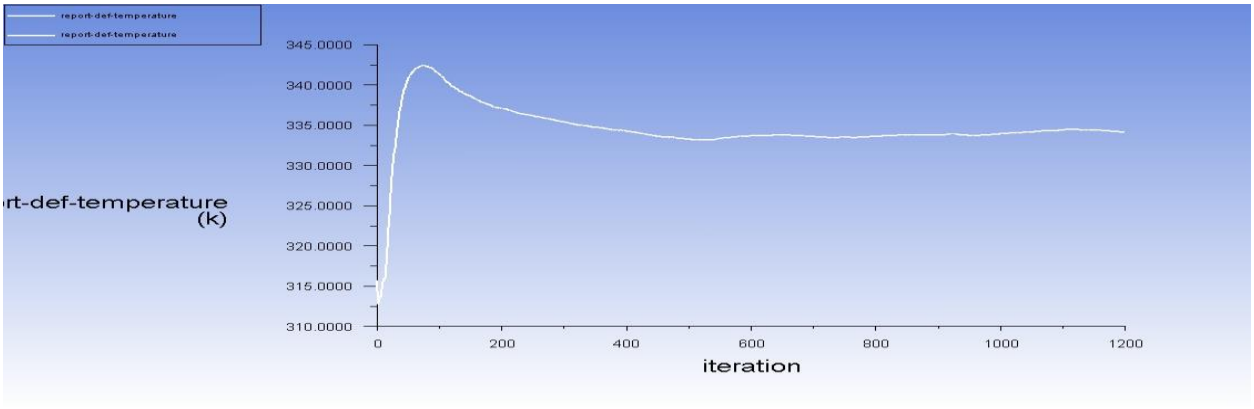

Figure 5.26a: Output report temperature versus iteration number 1200 and 10^{-6}

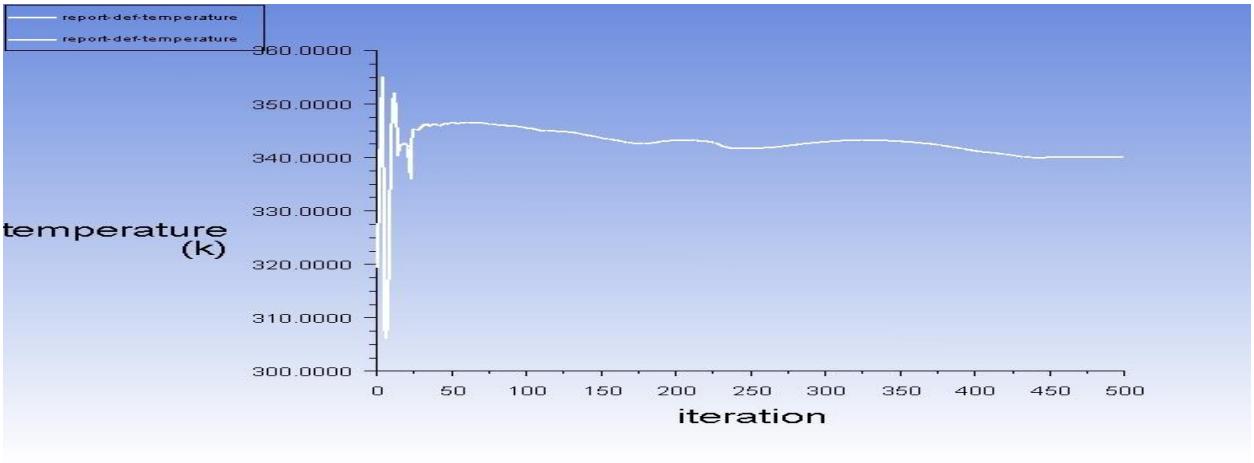

Figure5.26 b: Temperature graph for 500 iterations and 0.001 residual number

The graph above shows the temperature gradually rising until the point when the milk is pasteurized, then gradually lowering. This is a fantastic result, indicating that my designed temperature is nearly identical to the output temperature. We compare Figure 5.25a and 5.25 b, Figure 5.25a is clear information about pasteurization than Figure5.25 b.

5.2.3b: For transient analysis

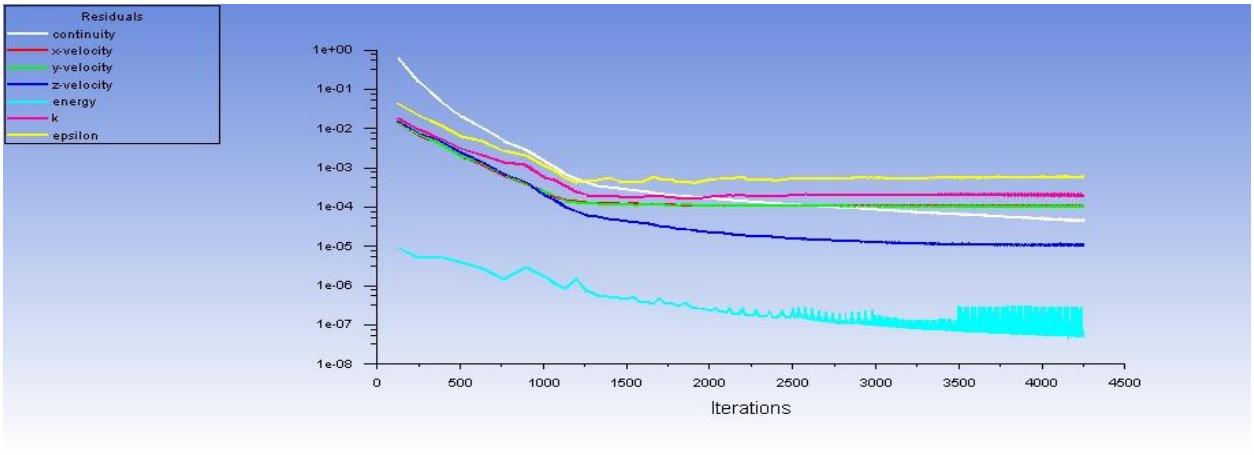

Figure5.27: Transient analysis residual graphs

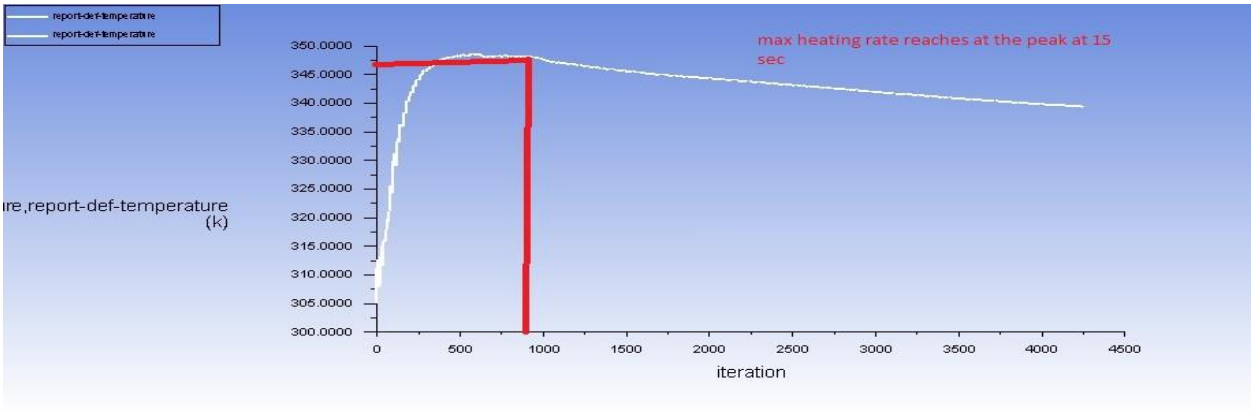

Figure5.28a: Transient analysis temp versus iteration graphs

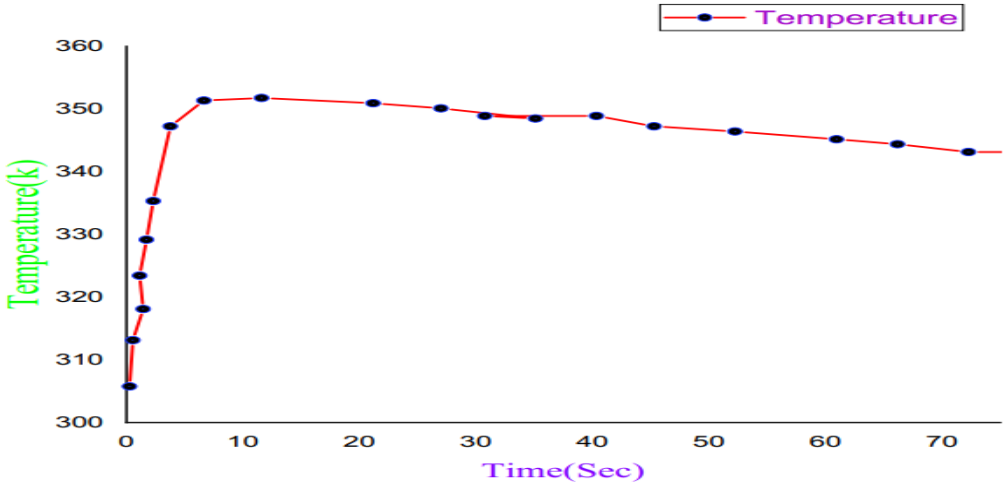

Figure5.28b: Transient analysis temp versus time graphs

The fluid reaches its maximal heating rate peak at 15 seconds, as shown in the graph above. In addition, this graph demonstrates that the pasteurization procedure takes 15 seconds. The temperature of the fluid milk is consistently spread after it has been pasteurized.

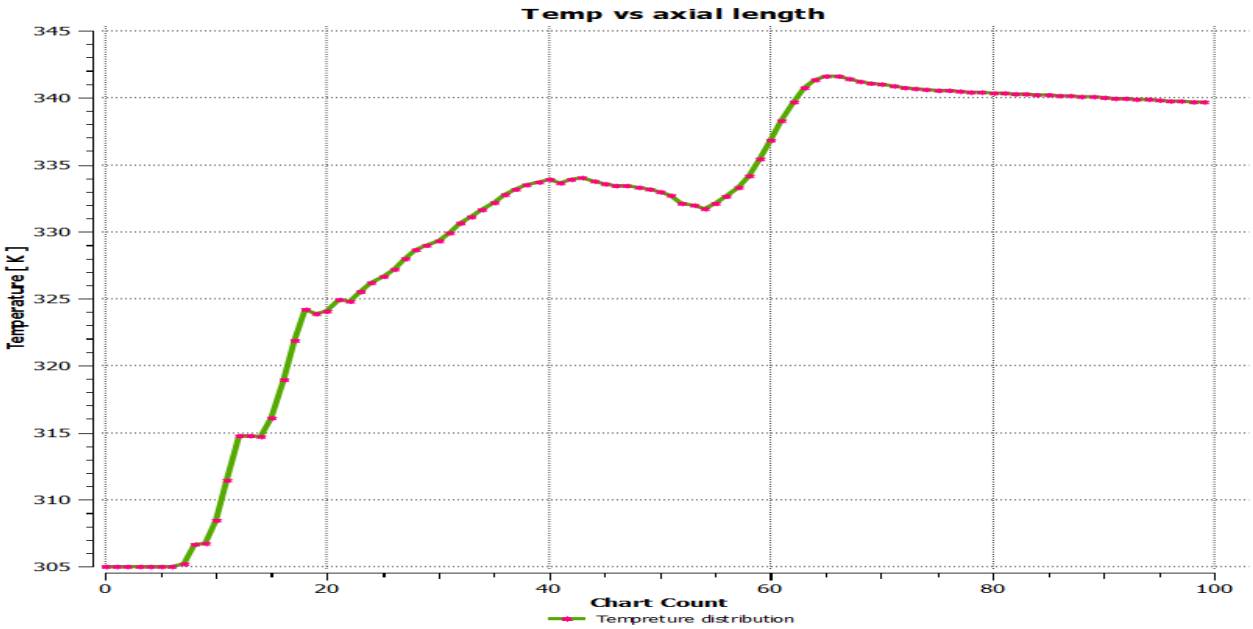

Figure5.29a: Temperature versus chart count for 187mm axial helical tube length

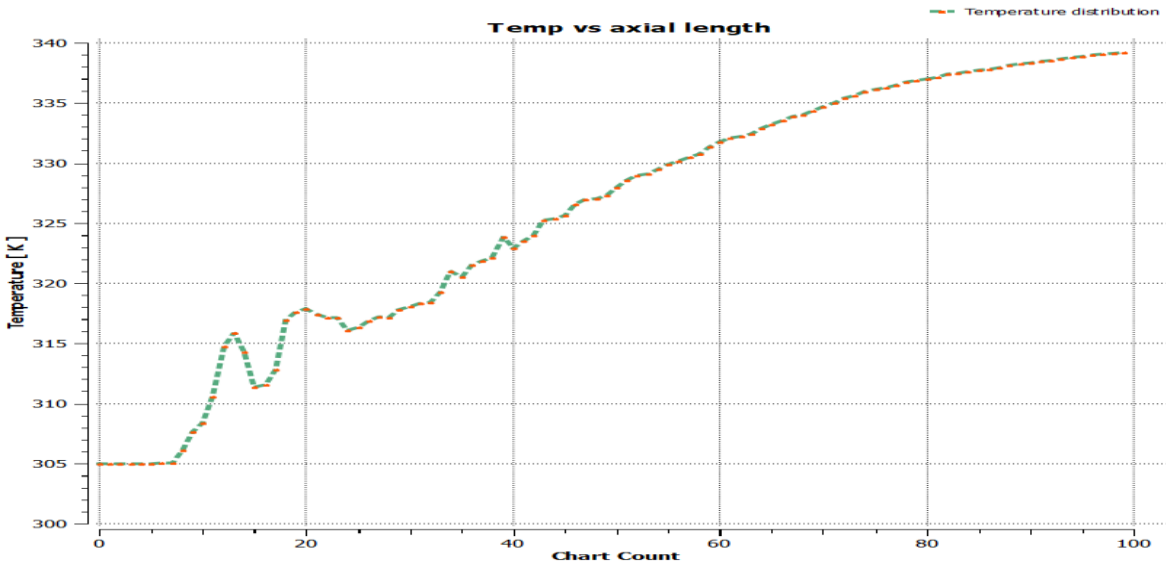

Figure5.29 b: Temperature versus chart count for 374mm axial helical tube length

The above graphs shows,the cold milk fluid is continually heated by hot helical tubes, and when the temperature of the milk fluid rises while the helical tube loses heat, the desired outlet pasteurization temperature is obtained.

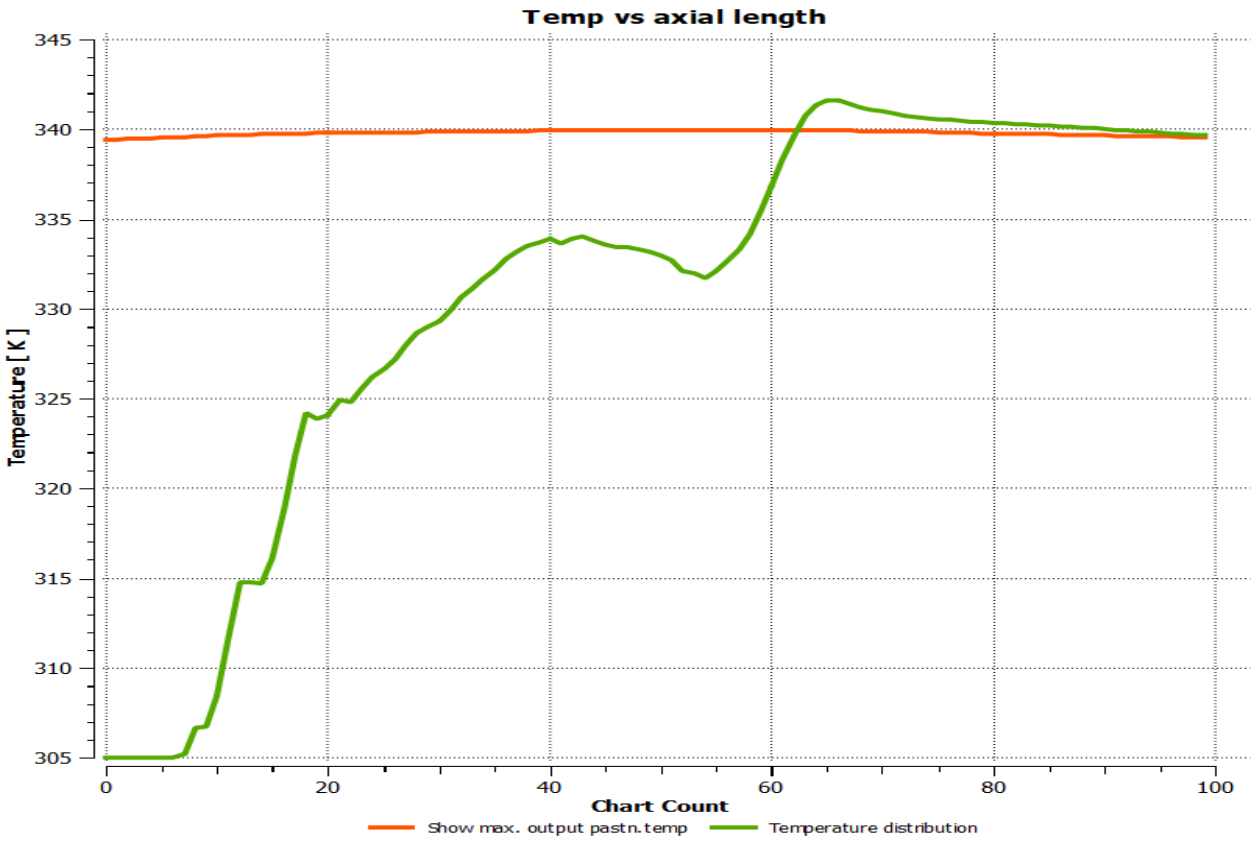

Figure5.30: Temperature versus axial HT length and to show peak pasteurization point

The Pea Green color graphs show the temperature of milk fluid steadily increasing until pasteurization, then remaining constant, whereas the orange color indicates the milk's output pasteurization temperature.

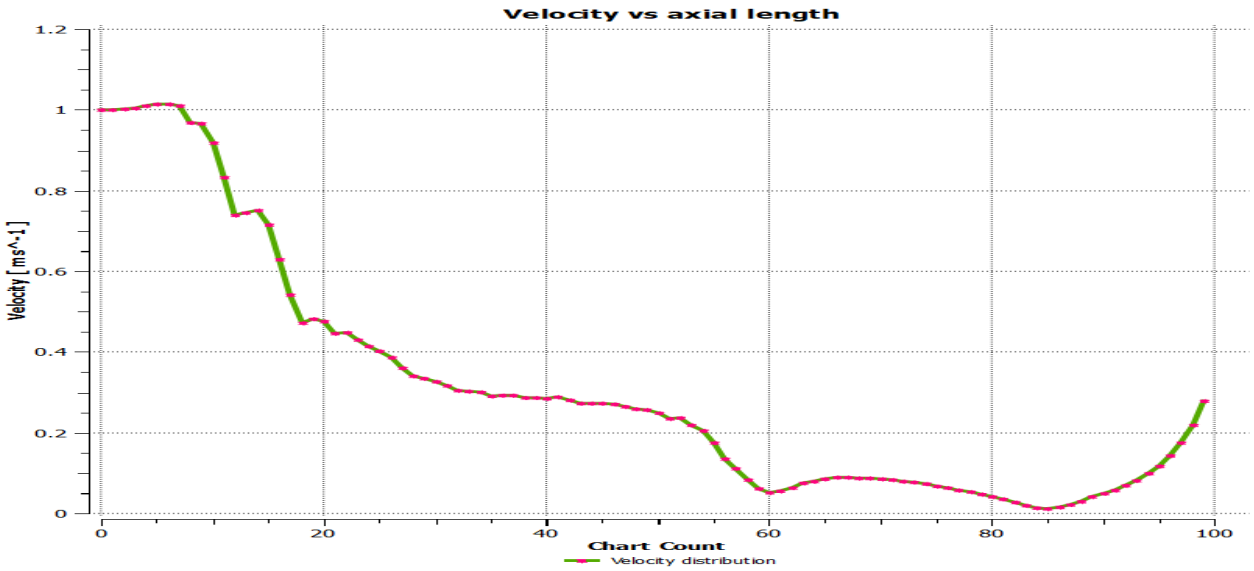

Figure5.31 a: Velocity versus chart count for 187mm axial helical tube length

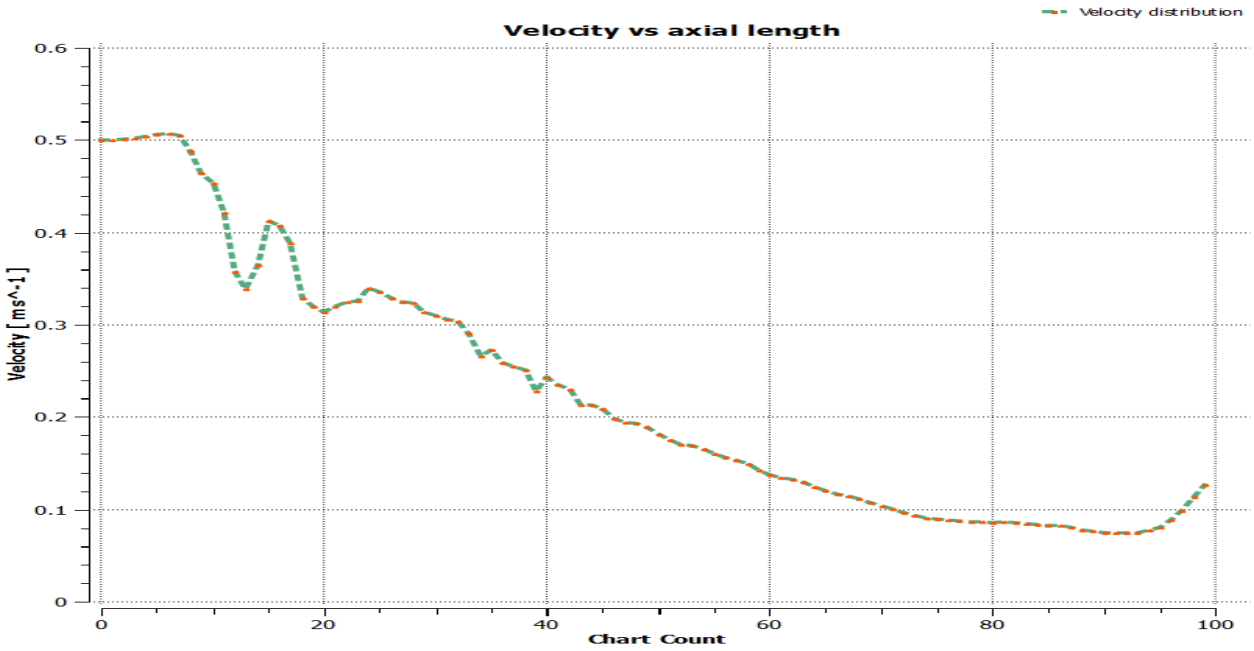

Figure5.31 b: Velocity versus chart count for 374mm axial helical tube length

As can be seen in the graph above, the velocity is steadily decreasing, and by lowering the inflow velocity, the fluid has more time to heat up and reach the desired pasteurization temperature.

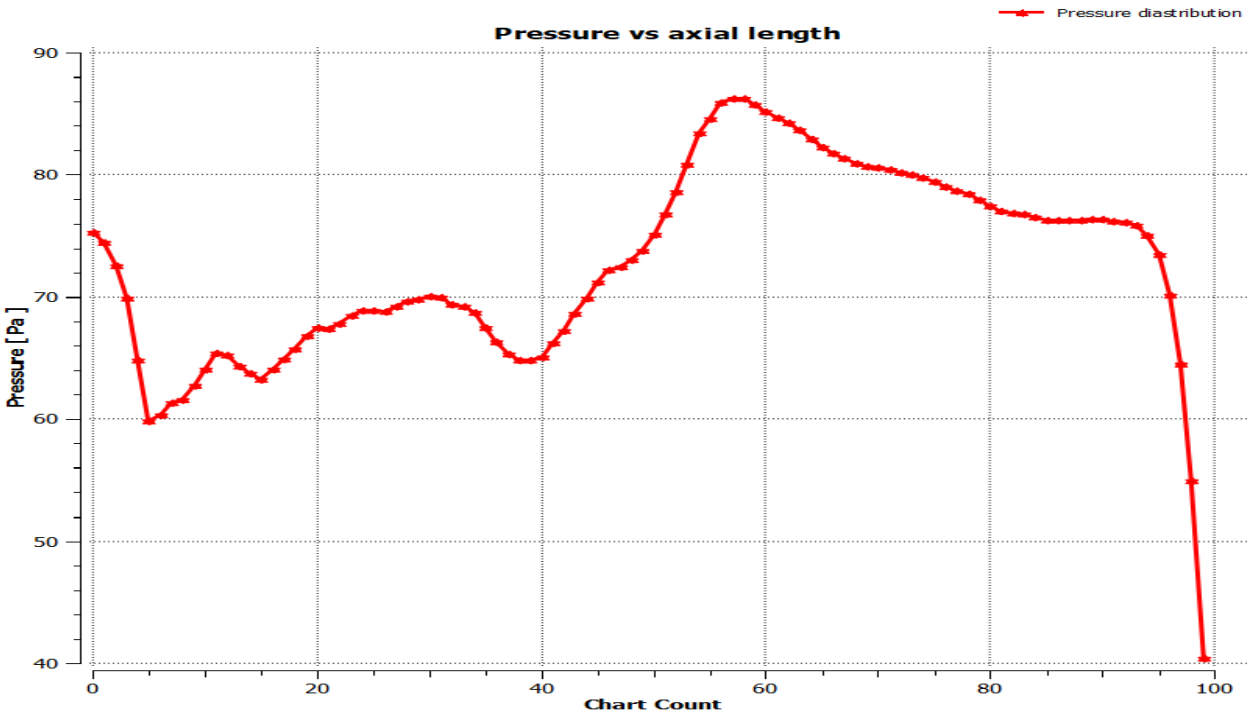

Figure5.32a: Pressure versus chart count for 187mm axial helical tube length

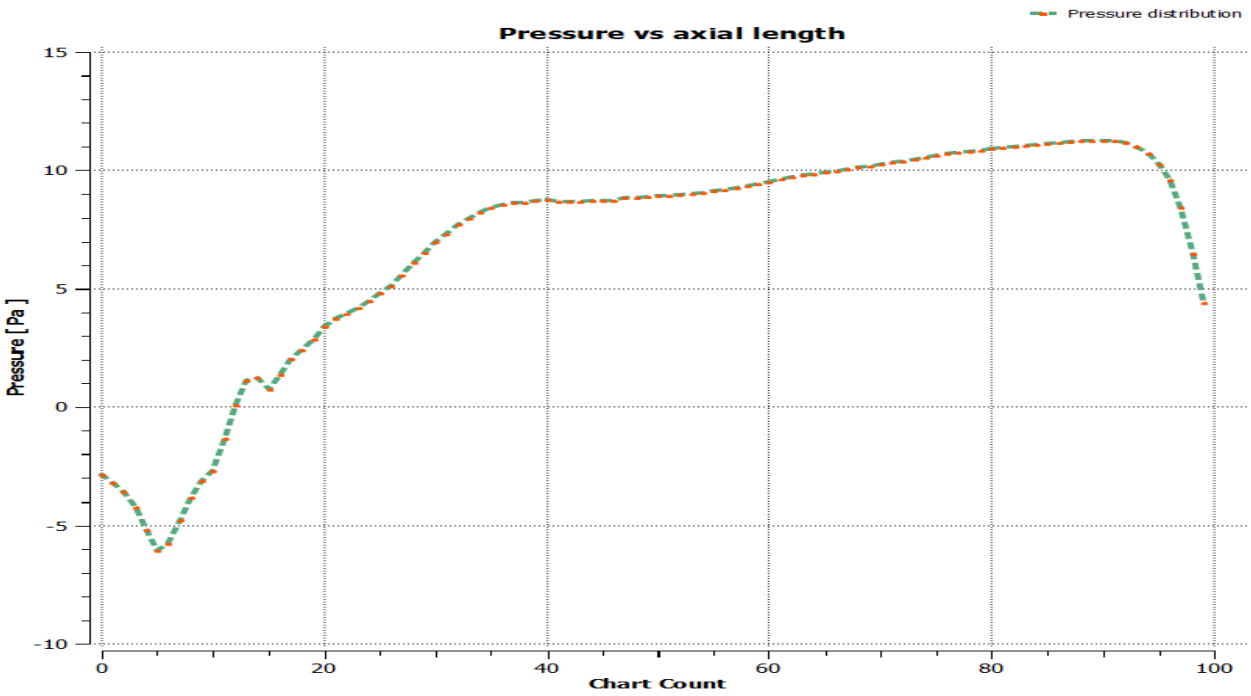

Figure5.32b: Pressure versus chart count for 374mm axial helical tube length

The above figure informs, because the cold milk fluid and hot helical tube exchange heat, the pressure lowers as the milk fluid approaches the helical tube, then increases as the milk fluid near pasteurization. After that, it's all downwards.

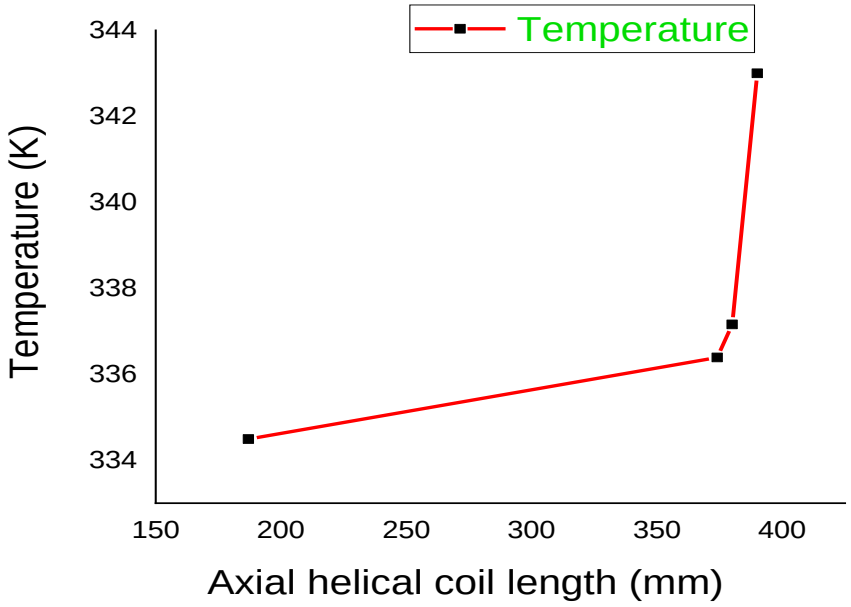

Figure5.33: Output temperature versus Axial helical tube length

The output temperature rises as the axial helical tube length increases shown in the graph above. Because the fluid gets more heating time and a more ideal pasteurization temperature when we lengthen the axial helical tubes.

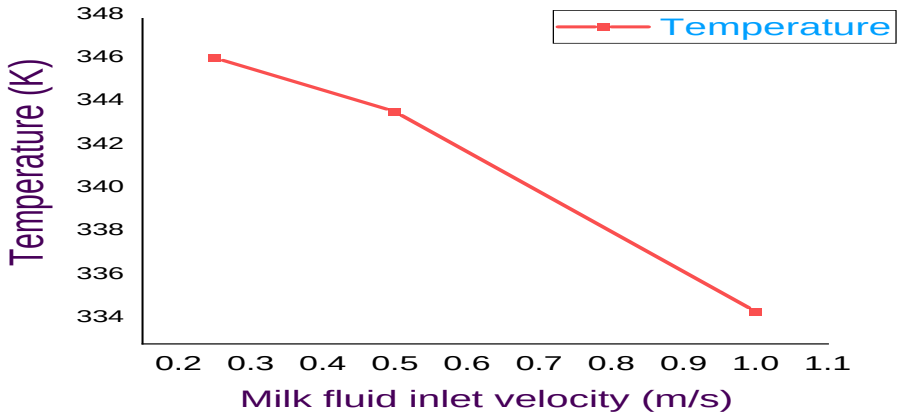

Figure5.34: Output temperature versus Milk fluid inlet velocity

The entrance velocity of milk fluid drops, resulting in higher output temperature because the fluids get more heating time, and vice versa. However, we receive a higher output temperature, which allows us to minimize the storage inlet diameter.

CHAPTER SIX

CONCLUSION AND RECOMMENDATION

6.1 CONCLUSION

A small-scale milk pasteurization system was constructed utilizing solar energy in this study, and performance was evaluated using CFD for 120 liters of milk at once.

The pasteurization process is then divided into two loops, one for solar energy water heating and the other for hot water milk heating, with a heat exchanger connecting the two loops.

The system makes use of a 22.3° inclined evacuated tube solar collector with a gross area of $2.42m^2$. The average temperature of the hot water that exited the collector and was kept in a thermal storage tank was 79°C to 82.32°C. However, following energy loss to the ambient, the hot water temperature intake to the helical tube heat exchanger was between 70°C and 78°C. Furthermore, the pasteurized milk temperature derived from the CFD study ranged from 65.5°C to 69°C and it takes 15seconds, which is within the permissible standard temperature range for pasteurized milk.

Using CFD data, increase the pitch length of the helical tube heat exchanger and the diameter of the milk outflow to smooth the fluid flow and decreasing the velocity, the flowing fluid gets more heating time and to achieve the required outputs. Increasing iteration numbers and lowering residual numbers for desired outcomes.

Finally, a solar-powered milk pasteurization system proved to be a feasible option in this case, since it reached the appropriate milk pasteurization temperature range while being heated to kill microorganisms that cause milk deterioration.

6.2 RECOMMENDATIONS

This research found that using solar thermal energy to pasteurize fresh liquid milk for Doyogena Town may achieve an appropriate milk pasteurization temperature.

The following points, on the other hand, should be looked into deeper.

- Cost estimation of the total system is strongly recommended for future inquiry.
- Use a technique like this to pasteurize fruit juice.
- Using an integrated collector storage system to optimize the system for large-scale milk pasteurization.
- Coduct the experiments to asses the performance of the moedled system

References

A Melese and W Tesfaye Bacteriological Quality and safety of Raw Cow's Milk in and around Jigiga city of Somali Region, Eastern Ethiopia [Journal]. - 2015. - Vol. 3. - pp. 48-55.

Farjana [et al.] "Solar process heat in industrial systems- A global review," [Journal] // Renewable and Sustainable Energy Reviews, - 2017. - pp. 1-17.

Paraene [et al.] "Dynamic Modelling and Elements of Validation of Solar Energy," [Journal] // in ninth International IBPSA Conference, Montreal, Canada, - 2005.

[CSA] Central Statistical Agency the Democratic Republic of Ethiopia.Agricultural Sample Survey [Journal] // Livestock and livestock characteristics (private peasant holdings), Addis Ababa, Ethiopia. - 2017. - Vol. II.

Aboulmagd A [et al.] "A New Model for the Analysis of Performance in Evacuated Tube Solar Collectors," [Journal] // International High-Performance Buildings Conference, Purdue University. - 2014.

Adisu [et al.] "Large Scale Solar Water Heating Systems Analysis in Ethiopia: A Case Study," [Journal] // International Journal of Sustainable Energy. - 2013. - pp. 1-41.

Allouhia [et al.] "Design Optimization of a multi-temperature solar thermal heating system for an industrial process," [Journal] // Applied Energy. - 2017. - Vol. 206. - pp. 382-392.

Amitkumar [et al.] "Design and Thermal Evaluation of Shell and Helical Coil Heat Exchanger," [Journal] // International Journal of Research in Engineering and Technology, - 2015. - 1: Vol. 4. - pp. 416-423.

Andrzjcryk [et al.] "Performance Analysis of Helical Coil Heat Exchangers. The effect of external coil surface modification on heat exchanger effectiveness," [Book Section] // Thermodynamics. - 2016. - Vol. 37: 4.

Angstrom A Solar and terrestrial radiation [Journal] // Quarterly Journal of Royal Meteorological Society. - 924. - Vol. 50. - pp. 121-125.

Arinc and U.D Solar collector design project [Journal] // Journal of Thermal Sciences and Technology. - 1986. - 4: Vol. 8. - pp. 51-58.

Atia [et al.] "Solar Energy Utilization for milk Pasteurization," [Journal] // Solar Energy Systems. - 2015. - pp. 1-15.

Beckman W and Duffie J Solar engineering of thermal processes [Journal] // 3rd Edition, New York: Wiley and Sons, - 1980.

Bereda A, Yilma Z and Nurfeta A "Handling, processing, and utilization of milk and milk products in Ezha district of the Gurage zone, southern Ethiopia," [Journal] // Journal of Agricultural and Biological sustainable development, - 2013. - pp. 91-98.

Chatterjee [et al.] Microbiological examination of milk in Tara keswar, India with special reference to coliforms [Journal] // African Journal of Biotechnology. - 2006. - Vol. 5. - pp. 1383-1385.

Chetan Solanki Singh Solar Photovoltaics second edition, IIT Bombay, PHI Publications. [Book].

Collares – Pereira, M and A. Rabl "The Average Distribution of Solar Radiation Correlations between Diffuse and Hemiaspherical and Between Daily and Hourly Insolation Values," [Journal] // Solar Energy. - 1979a. - Vol. 22. - p. 155.

Cuiping [et al.] "Design of Coil Heat Exchanger for Remote Storage Solar Water Heating System," [Journal] // Solar Energy and Human Settlement. - 2007. - pp. 2123-2127.

Demissu and H "Assessment on Peri-Urban Dairy Production System and Evaluation of Quality of Cows' Raw Milk: A case of Shambu, Fincha, and Kombolcha Towns of Horro Guduru Wellega Zone, Ethiopia, " [Journal] // Science, Technology and Arts Research Journal. - 2014. - Vol. 3. - pp. 37-43.

Dewangan [et al.] "Stainless Steel for Dairy and Food Industry: A Review," [Journal] // Journal of Material Sciences and Engineering. - 2015. - Vol. 4. - pp. 2169-0022.

Duffie [et al.] Solar Engineering of Thermal Processes, 4th ed., John Wiley and Sons, Inc., [Book]. - 2013.

Emana and B Cooperatives A path to Economic and Social Empowerment in Ethiopia. [Journal] // International Labor Organization (ILO). Coop AFRICA (Working Paper No. 9),. - Dares Salam: : [s.n.], 2009..

Emmett and W.L.R Apparatus for Utilizing Solar Heat. U.S. patent no [Journal]. - January 3, 1911. - p. 505.

Erbs [et al.] "Estimation of the Diffuse Radiation Fraction for Hourly, Daily, and Monthly-Average Global Radiation," [Journal] // Solar Energy. - 1982. - Vol. 28. - p. 293.

Fathima, A, Sreekala, P and Mathew, B "Performance Analysis of Solar Thermal Evacuated Tube Collector Using Different nanofluids," [Journal] // International Journal of Engineering Sciences and Research Technology, - 2016. - 7: Vol. 5. - pp. 367-373.

Fenoll [et al.] Fluor metric determination of alkaline phosphatase in solid and fluid dairy products. [Journal] // Elsevier Talanta. - 2002. - Vol. 56. - p. 1021.

Flores-Flores [et al.] "Presence of mycotoxins I animal milk: A review, " [Journal] // Food control, - 2015. - Vol. 53. - pp. 163-176.

Frank, M and White Fluid Mechanics, Fourth Edition, University of Rhode Island: McGraw Hill Series in Mechanical Engineering. [Book].

Gao Y [et al.] "Effects of thermal mass and flow rate on the forced-circulation solar hot-water system: Comparison of water-in-glass and U-pipe evacuated-tube solar collectors," [Journal] // Solar Energy, - 2013. - Vol. 98. - pp. 290 - 301.

Gao Y [et al.] "Thermal performance and parameter analysis of a U-pipe evacuated solar tube collector," [Journal] // SolarEnergy. - 2014. - Vol. 104. - p. 714.

Ghoneim A "Optimization of Evacuated Tube Collector Parameters for Solar Industrial Process Heat," [Journal] // International Journal of Energy and Environmental Research, - 2017. - 2: Vol. 5. - pp. 55-73.

Goswami D [et al.] Principles of solar engineering, Taylor and Francis Group [Book]. - 2000. - Vol. 6.

Habtamu [et al.] "Determinants of supply chain coordination of milk and dairy industries in Ethiopia: A case of Addis Ababa and its surroundings," [Journal] // Springer Open Journal. - 2015. - 498: Vol. 4. - pp. 1287-1299.

Hafez [et al.] "Tilt and azimuth angles in solar energy applications-A review," [Journal] // Renewable and Sustainable Energy Reviews, - 2017. - Vol. 77. - pp. 147-168.

Hailemeskel Deginet Production, Handling, Traditional Processing Practices and Quality of Milk in Kembata Tembaro Zone Milk Shed Area, Southern Ethiopia. [Journal] // International Journal of Animal Science and Technology. - 2020. - 2: Vol. 4. - p. 33.

Harding GL, Zhiqiang Y and Mackey DW Heat extraction efficiency of a concentric glass tubular evacuated collector [Journal] // International Journal of Solar Energy. - 1985. - Vol. 35. - pp. 71-79.

Huang [et al.] "Influence of fluid milk product composition on fouling and cleaning of Ni-PTFE modified stainless steel heat exchanger surfaces," [Journal] // Journal of Food Engineering. - 2015. - Vol. 158. - pp. 22-29.

Incropera FP [et al.] Fundamentals of Heat and Mass Transfer, 6th ed. John Wiley and Sons: Hoboken [Book]. - 2007.

J. Razavi, M. R. Riazi and M. Mohamoodi Solar Energy [Journal]. - 2003. - Vol. 74. - p. 441.

Jafar Kazemi F, Ahmadifard E and Abdi H "Energy and Exergy Efficiency of Heat Pipe Evacuated Tube Solar Collectors," [Journal] // Thermal Science: - 2016. - 1: Vol. 20. - pp. 327-335.

Jamar A [et al.] "A review of water heating system for solar energy applications," [Journal] // International communications in Heat and Mass Transfer, - 2016. - Vol. 76. - pp. 178-187.

K Pihtili Flat plate solar collectors [Journal] // Journal of Thermal Sciences and Technology. - 1980. - Vol. 2. - pp. 21-24.

Kalb [et al.] "Fully Developed Viscous-Flow Heat Transfer in Curved Circular Tube with Uniform Wall Temperature," [Journal] // AICHE Journal. - 1974. - 2: Vol. 20. - pp. 340-346.

Kalogiroun and S A Solar thermal collectors and applications, Progress in energy and combustion science, [Journal]. - 2004. - 3: Vol. 30. - pp. 231-295.

Kalogiroun S The potential of solar industrial process heat applications. [Journal] // Appl Energy. - 2000. - Vol. 76. - pp. 337-361.

Kalogiroun SA Solar Energy Engineering: Processes and Systems. [Journal] // Academic Press: Oxford. - 2009.

Karunasree P "Review-A Brief Study on Milk," [Journal] // Journal of Food and Dairy Technology, - 2016.. - 3: Vol. 4. - pp. 2347-2359.

Kuppan and T Heat Exchanger Design Hand Books, Southern Railways Madras, India: Marcel Dekker, Inc. New York Basel [Book]. - 2000.

Lavan Z and T. Thomson “Experimental study of Thermally Stratified Hot Water Storage Tanks," [Journal] // Solar Energy. - 1977. - Vol. 19. - p. 519.

Lazova [et al.] "Performance Evaluation of a Helical Coil Heat Exchanger Working under Supercritical Conditions in a Solar Organic Rankine Cycle Installation," [Journal] // Energies. - 2016. - Vol. 9. - p. 432.

M Chikh Energy Procedia [Journal]. - 2012. - Vol. 18. - pp. 1068-1075.

M. Smyth, P. C. Eames and B. Norton Renewable Sustainable Energy Rev [Journal]. - 2006. - Vol. 10. - p. 503.

Makita K [et al.] "Risk assessment of staphylococcal poisoning due to consumption of informally marketed milk and homemade yogurt in Debre Zeit, " [Journal] // International journal of Food Microbial.,. - 2012. - 2: Vol. 1. - pp. 135-153.

Melese A and Tesfaye W Bacteriological Quality and safety of Raw Cow's Milk in and around Jigiga city of Somali Region, Eastern Ethiopia [Journal]. - 2015. - Vol. 3. - pp. 48-55.

Michael g [et al.] The first two Water systems piping experts, the sec of projects Raytheon engineers and Liberator Supervising discipline engineer Raytheon engineers and Constructors [Book Section].

Modi. A and Prajapat "Pasteurization Process Energy Optimization for a Milk Dairy Plant by Energy Audit Approach," [Journal] // International Journal of Scientific and Technology Research. - 2014. - 6: Vol. 3. - pp. 181-188.

Mohapatra [et al.] "Performance analysis of three fluid heat exchanger used in solar flat plate collector system," [Journal] // Energy Procedia. - 2017. - Vol. 109. - pp. 322-330.

Nahar N M Renewable Energy 26, [Journal]. - 2002. - p. 623.

Panchal H, Pateland R and Parmar D "Application of Solar Energy for Milk Pasteurization: A Comprehensive Review for Sustainable Development," [Journal] // Internationa Journal of Ambient Energy. - 2018. - pp. 1-5.

Parton WJ and Logan JA A model for diurnal variation in soil and air temperature [Journal] // Agric Meteoral, HTTPS:// doi. Org/10.1016/0002-1571(81)-90105-9. - Vol. 23. - pp. 205-216.

Patel [et al.] "Use of Renewable Energy in Dairy Industry," [Journal] // International Journal of Advance Research and Innovation, - 2016. - 2: Vol. 4. - pp. 433-437.

Pihtili K Flat plate solar collectors [Journal] // Journal of Thermal Sciences and Technology. - 1980. - Vol. 2. - pp. 21-24.

Pluta Z evacuated tubular or classical flat plate solar collectors [Journal] // Journal of Power Technologies. - 2011. - 91: Vol. 3. - pp. 158-164.

Prabhanjan [et al.] Natural Convection Heat Transfer from Helical Coiled Tubes [Journal]. - 2004. - Vol. 43. - pp. 359-365.

Prescott JA Evaporation from the water surface about solar radiation [Journal] // Transactions of the Royal Society of Australia. - 1940. - Vol. 46. - pp. 114-118.

Purandare [et al.] "Investigation on thermal analysis of conical coil heat exchanger," [Journal] // International Journal of Heat and Mass Transfer. - 2015. - Vol. 90. - pp. 1188-1196.

R Winston Solar concentrators of novel design [Journal] // Solar Energy. - 1974. - Vol. 16. - pp. 89-95.

R.S Soin [et al.] Sol. Energy [Journal]. - 1979.. - Vol. 23. - p. 69.

Ramachandra K, Shende B. W and Prasanta K. G Designing a helical-coil heat exchanger, Chemical Engineering [Book]. - 1982.

Rodriguez [et al.] "Solar thermal networks operating with evacuated-tube collectors," [Journal] // Energy. - 2017. - Vol. 3. - pp. 1-8.

Rodriguez-Hidgalo MC [et al.] Domestic hot water consumption vs. solar thermal energy storage: the optimum size of the storage tank [Journal] // Int. J. Appl. Energy. - 2012. - Vol. 97. - pp. 897-906.

Ruangwittayanusorna K, Promketa D and Chantiratikula A "Monitoring the Hygiene of Raw Milk from Farms to Milk Retailers," [Journal] // Agriculture and Agricultural Science Procedia, - 2016.. - Vol. 11. - pp. 95-99.

Sabiha [et al.] "Progress and latest developments of evacuated tube solar collectors," [Journal] // Renewable and Sustainable Energy Reviews, - 2015. - Vol. 15. - pp. 1038-1054.

Sadic, K and Hongtan Liu Heat exchangers, Selection, Rating, and Thermal Design, Second Edition, Department of Mechanical Engineering, University of Miami, Florida: CRC Press LLC [Book]. - 2002.

Seban [et al.] "Heat Transfer in Tube Coils with Laminar and Turbulent Flow," [Journal] // International Journal of Heat and Mass Transfer. - 1963. - 5: Vol. 6. - pp. 387-395.

Sharma A [et al.] "Solar industrial process heating: A review," [Journal] // Renewable and Sustainable Energy Reviews, - 2017. - Vol. 78. - pp. 124-137.

Shuhong [et al.] "Study on performance of storage tanks in solar water heater system in charge and discharge progress," [Journal] // Energy Procedia. - 2014. - Vol. 48. - pp. 384-393.

Sinnott and R.K Chemical Engineering Design, Fourth ed, Department in Oxford, UK: Elsevier [Book]. - 2005.

Siva Kumara S [et al.] "Design of Evacuated Tube Solar Collector with Heat Pipe," [Journal] // Materials Today, - 2017. - Vol. 4. - pp. 12641–12646.

Smith E.M Advances in Thermal Design of Heat Exchangers. John Wiley and Sons Ltd [Book]. - 2005.

Steen M and Meijer W "Inclusiveness of the small-Holder Farmer Key Success Factors for Ethiopian Agribusiness Development, " [Journal] // International Food and. - 2014. - Vol. 17. - pp. 83-88.

Suresh [et al.] "Solar energy for process heating: A case study of select Indian," [Journal] // Journal of Cleaner Production. - 2017. - Vol. 151. - pp. 439-451.

Tadesse M, Fentahun M and Tadesse G "Dairy Farming and its Importance in Ethiopia: A Review," [Journal] // World Journal Dairy and Food Sciences. - 2017. - 1: Vol. 12. - pp. 42-51.

Taylor P. B. "Energy and thermal performance in the residential sector," [Journal] // Ph.D. thesis, Potchefstroom University, - 2001.

Tegegne A [et al.] " Smallholder dairy production and marketing systems in Ethiopia: IPMS experiences opportunities for market-oriented development," [Journal] // in Project Working Paper 31,. - 2013.

Tsadkan Z and Gurga B Handling and utilization pattern of cattle milk and milk products in Northern Ethiopia [Journal] // Africa Journal of Agricultural Research. - 2018. - Vol. 13. - p. 34.

Verechshagin [et al.] "Methodology to calculate Design Parameters of Screw Heat Exchanger for Vat Pasteurizer," [Journal] // Journal of Engineering and Applied Science. - 2016. - 1: Vol. 11. - pp. 2955-2961.

Vishvakarma [et al.] "A Review on Heat Transfer through Helical Coil Heat Exchangers," [Journal] // International Journal of Engineering Science and Research. - 2016. - 5: Vol. 8. - pp. 607-612.

W. Chun [et al.] Appl. Therm. Eng. [Journal]. - 1999. - Vol. 19. - p. 807.

Wang Z [et al.] "Solar water heating: From theory, application, marketing and research," [Journal] // Renewable and Sustainable Energy Reviews, - 2015. - Vol. 41. - pp. 68-84.

Watts Simran "A mini-review on technique of milk pasteurization," [Journal] // Journal of Pharmacognosy and Phytochemistry, - 2016. - 5: Vol. 5. - pp. 99-101.

Wayua [et al.] "Design and Performance Assessment of a Flat Plate Solar Milk Pasteurizer for Arod Pastoral Areas of Kenya," [Journal] // Journal of Food Processing and Preservation. - 2012. - pp. 1-6.

Werner Vogel and Henry Kalb "Large-Scale Solar Thermal Power Technologies, Costs and Development", [Journal] // The Physics Institute at the University of Karlsruhe, Germany, Sandia National Laboratories, National Renewable Energy Laboratory U.S. Department of Energy. - 2010.

Winston R Solar concentrators of novel design [Journal] // Solar Energy. - 1974. - Vol. 16. - pp. 89-95.

Yadav [et al.] "Simulation Modeling for the Performance of Evacuated Tube Solar Collector," [Journal] // International Journal of Innovative Research in Science, Engineering and Technology, - 2017. - 4: Vol. 6. - pp. 5634-5642.

Yildirim N and Genc S "Thermodynamic analysis of a milk pasteurization process by geothermal energy," [Journal] // Energy. - 2015. - pp. 987-996.

Yildirim N., Genc, S Energy and exergy analysis of a milk powder production system," Energy Conversion and Management [Journal]. - 2017. - Vol. 149. - pp. 698-705.

Yilma Z, Guernebleich E and Ameha S " A Review of the Ethiopian Dairy sector," [Journal] // Food and Agriculture Organization of the United Nations, sub Regional office for Eastern Africa, - 2011. - p. 81.

Yodit A [et al.] "Assessment of staphylococcus aureus along the milk value chain and its public health importance in sebeta, central Oromia, Ethiopia," [Journal] // BMC Microbiology, - 2017. - Vol. 17. - p. 141.

Zahira [et al.] Fabrication and performance study of a solar milk pasteurizer [Journal] // J. Agri. Sci., Pakistan. - 2009. - 2: Vol. 46.

Zekai Sen "Solar Energy Fundamentals and Modeling Techniques, Atmosphere, Environment, Climate Change and Renewable Energy," [Journal] // Istanbul Technical University, Faculty of Aeronautics and Astronautics, Dept. Meteorology, Campus Ayazaga, Istanbul, Turkey, . - 2008.

Zorraquino [et al.] Effect of thermal treatments on the activity of quinolones in milk [Journal]. - 2008. - Vol. 63. - pp. 192-195.

APPENDIXES

Appendix A: Properties of various materials

Table A.1: ***Evacuated Tube Solar Collector Heat Transfer Coefficients***

Coefficients	Value (W/m^2 K)	Source
$h_{r-g,rad}$	0.43	$h_{r-g,rad} = \frac{\sigma(T_r^2+T_g^2)(T_r+T_g)}{1/\varepsilon_r+1/\varepsilon_g-1}$
h_{r-g}	0.43	$h_{r-g} = h_{r-g,rad} + h_{r-g,cond}$
$h_{g-a,rad}$	0	Neglectable
$h_{g-a,conv}$	12.4	$h_{wind} = 5.7V + 3.8$
h_{g-a}	12.4	$h_{g-a} = h_{g-a,rad} + h_{g-a,conv}$
h_{r-a}	0.6	Experimental results
h_f	$h_f = \frac{\lambda_f}{D}Nu$	$Nu = 1.75\left[Gz + 5.6\times10^{-4}\left(Gr_f\ Pr_f\frac{L}{D}\right)^{0.70}\right]^{1/3}\left(\frac{V_{av}}{V_{wall}}\right)$

Continued

Coefficients	Value (W/m^2 K)	Source
$h_{r-Al,rad}$	0.35	$h_{r-Al,rad} = \frac{\sigma(T_r^2+T_{Al}^2)(T_r+T_{Al})}{1/\varepsilon_r+1/\varepsilon_{Al}-1}$
$h_{r-Al,cond}$	26.7	$h_{r-Al,cond} = \lambda_{air1}/\delta_{air1}$
h_{r-Al}	27.05	$h_{r-Al} = h_{r-Al,rad} + h_{r-Al,cond}$
$h_{Al-Cu,rad}$	0.58	$h_{Al-Cu,rad} = \frac{\sigma(T_{Al}^2+T_{Cu}^2)(T_{Al}+T_{Cu})}{1/\varepsilon_{Al}+1/\varepsilon_{Cu}-1}$
$h_{Al-Cu,cond}$	26.7	$h_{r-Al,cond} = \lambda_{air2}/\delta_{air2}$
h_{Al-Cu}	27.28	$h_{Al-Cu} = h_{Al-Cu,rad} + h_{Al-Cu,cond}$

Table A.2: ***Physical properties of manifold header construction materials***

Parameters	Symbol	Value	Unit
Material of internal cover of the manifold header (Stainless steel cover)			
Thermal conductivity of the internal cover	K_1	15	W/m k

The thickness of the internal cover	e_1	1.2	mm
Insulating material (Polyurethane foam)			
Thermal conductivity of Insulating material	K_2	0.06	W/m k
The thickness of Insulating material Material of internal cover (Stainless steel)	e_2	15	mm
Thermal conductivity of the internal cover	K_3	15	W/m k
The thickness of the internal cover	e_3	1.2	mm

Table A.3: Properties of Insulation Materials

Materials	**Density, ρ Kg/m3**	**Thermal Conductivity, W/m.K**
Glass fiber	56–72	0.032–0.039
Polyurethane foam	24–40	0.023–0.026
Foamed Glass	144	0.058
Calcium Silicate	240	0.54
Phenolic Foam	35-120	0.018 - 0.022
Polystyrene Foam	30 -60	0.033 -0.045
polystyrene	15 -30	0.033 -0.038

Appendix B-1: Moody Chart

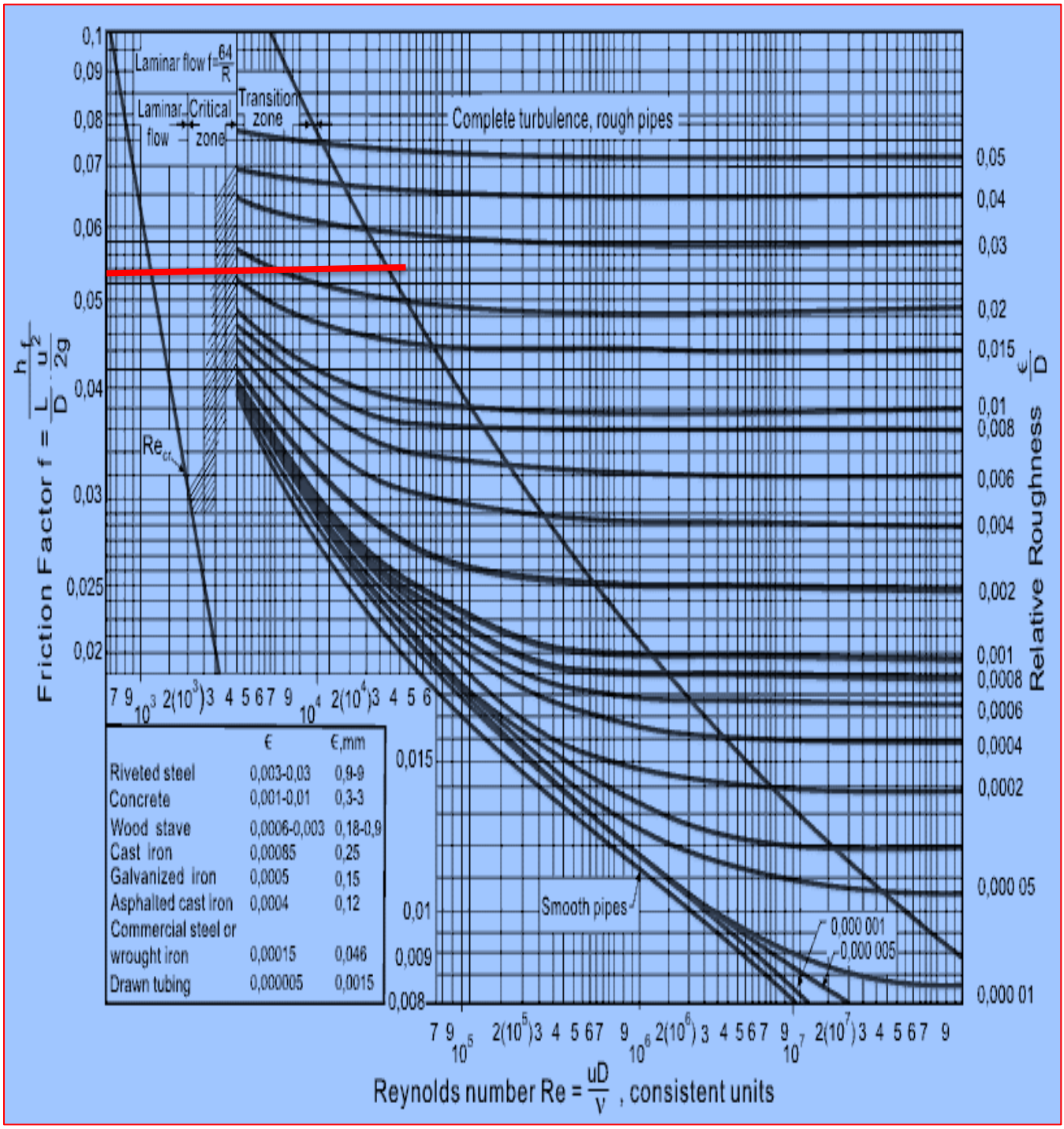

Figure B.1: ***Moody Chart***

Appendix B-2: Economic Thickness of Insulation

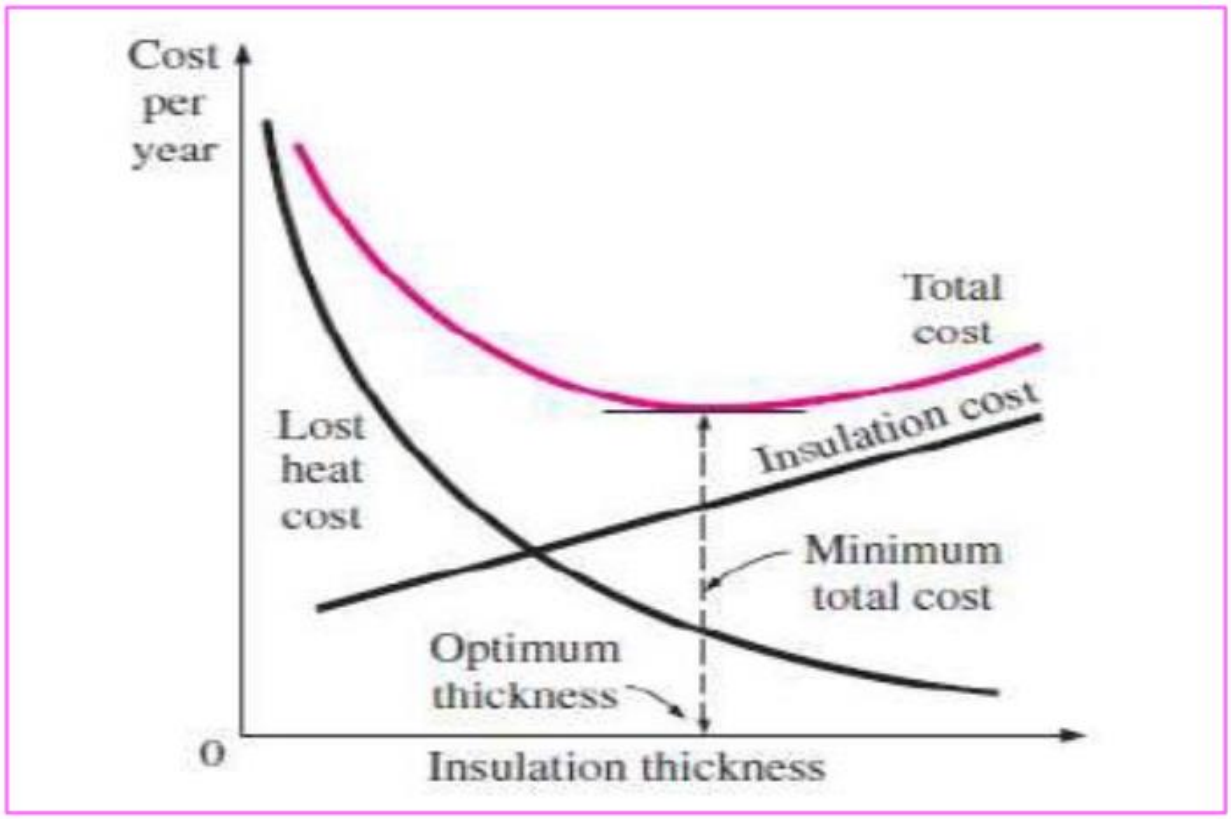

Appendix B-3: Solar Water Pump Selection Chart

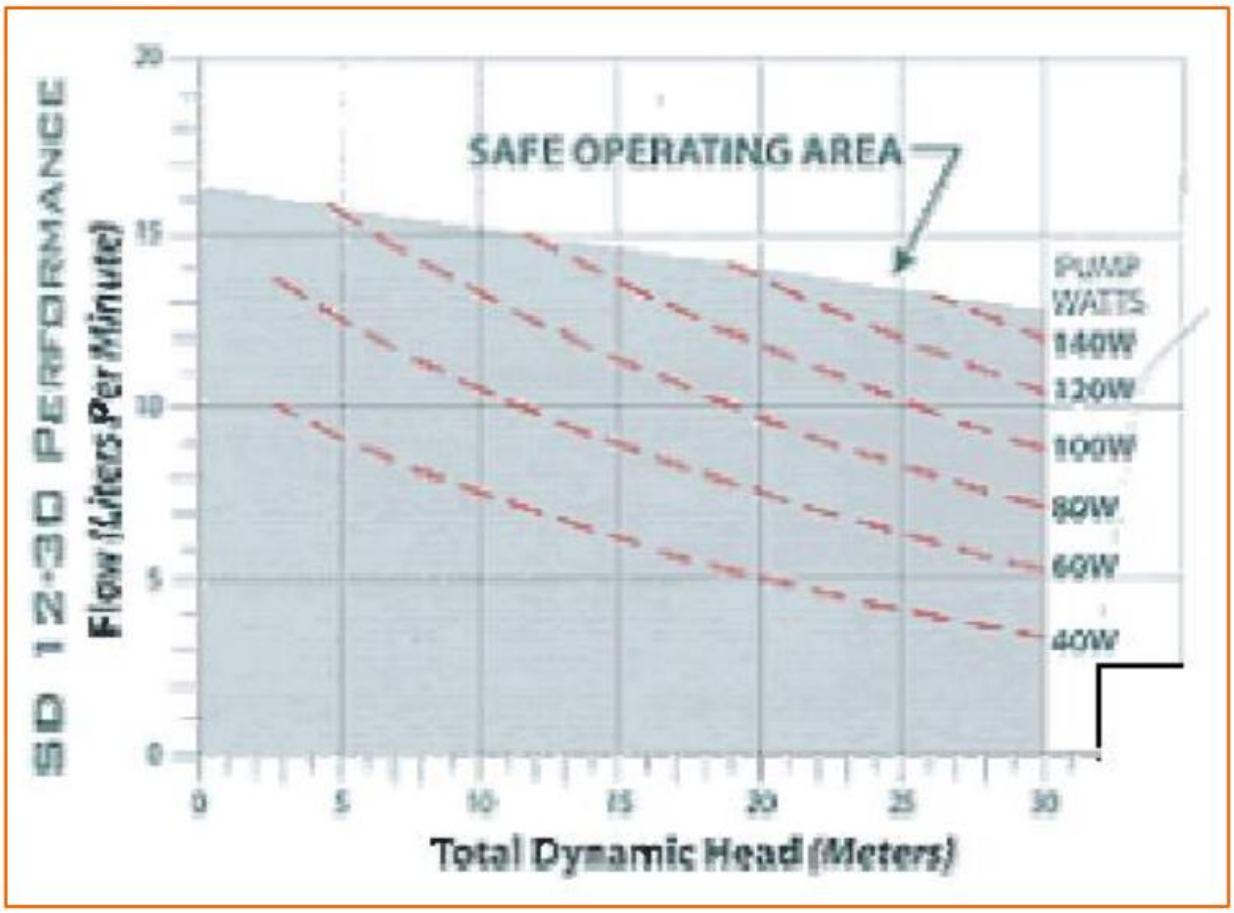

Figure B.3: A graph used to size a pump (from Kyocera Solar)